



Calhoun: The NPS Institutional Archive
DSpace Repository

Theses and Dissertations

1. Thesis and Dissertation Collection, all items

2013-06

Non-intrusive vibration monitoring in US Naval and US Coast Guard ships

Gerhard, Katherine Leigh

Monterey California. Naval Postgraduate School

<https://hdl.handle.net/10945/40221>

This publication is a work of the U.S. Government as defined in Title 17, United States Code, Section 101. Copyright protection is not available for this work in the United States.

Downloaded from NPS Archive: Calhoun



Calhoun is the Naval Postgraduate School's public access digital repository for research materials and institutional publications created by the NPS community. Calhoun is named for Professor of Mathematics Guy K. Calhoun, NPS's first appointed -- and published -- scholarly author.

Dudley Knox Library / Naval Postgraduate School
411 Dyer Road / 1 University Circle
Monterey, California USA 93943

<http://www.nps.edu/library>

Non-Intrusive Vibration Monitoring in US Naval and US Coast Guard Ships

By
Katherine Leigh Gerhard

Bachelor of Science in Electrical Engineering
United State Naval Academy, 2006

Submitted to the Department of Mechanical Engineering and Department of System Design and Management in Partial Fulfillment of the Requirements for the Degrees of

of
Naval Engineer
and
Master of Science in Engineering and Management
at the
Massachusetts Institute of Technology
June 2013

© 2013 Katherine Leigh Gerhard. All rights reserved.

The author hereby grants to MIT and the US Government permission to reproduce and to distribute publicly paper and electronic copies of this thesis document in whole or in part in any medium now known or hereafter created.

Signature of Author



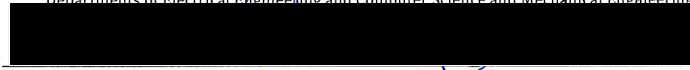
Department of Mechanical Engineering
System Design and Management Program
May 10, 2013

Certified by



Steven B. Leeb
Professor of Electrical Engineering and Computer Science and Mechanical Engineering
Departments of Electrical Engineering and Computer Science and Mechanical Engineering

Accepted by



Patrick Hale, Director, System Design and Management Fellows Program
Engineering Systems Division
Thesis Advisor

Certified by



Chris Schantz
Department of Mechanical Engineering
-Supervisor

Accepted by



David Hardt
Chairman, Department Committee on Graduate Students
Department of Mechanical Engineering

Non-Intrusive Vibration Monitoring in US Naval and US Coast Guard Ships

By
Katherine Leigh Gerhard

Bachelor of Science in Electrical Engineering
United State Naval Academy, 2006

Submitted to the Department of Mechanical Engineering and Department of System Design and Management in Partial Fulfillment of the Requirements for the Degrees of

Naval Engineer
and
Master of Science in Engineering and Management
at the
Massachusetts Institute of Technology
June 2013

© 2013 Katherine Leigh Gerhard. All rights reserved.

The author hereby grants to MIT and the US Government permission to reproduce and to distribute publicly paper and electronic copies of this thesis document in whole or in part in any medium now known or hereafter created.

Signature of Author _____
Department of Mechanical Engineering
System Design and Management Program
May 10, 2013

Certified by _____
Steven B. Leeb
Professor of Electrical Engineering and Computer Science and Mechanical Engineering
Departments of Electrical Engineering and Computer Science and Mechanical Engineering
Thesis Advisor

Accepted by _____
Patrick Hale, Director, System Design and Management Fellows Program
Engineering Systems Division
Thesis Advisor

Certified by _____
Chris Schantz
Department of Mechanical Engineering
Co-Supervisor

Accepted by _____
David Hardt
Chairman, Department Committee on Graduate Students
Department of Mechanical Engineering

This Page Intentionally Left Blank

Non-Intrusive Vibration Monitoring in US Naval and US Coast Guard Ships

by

Katherine Leigh Gerhard

Submitted to the Department of Mechanical Engineering and Department of System Design and Management in Partial Fulfillment of the Requirements for the Degrees of

Engineer in Naval Architecture and Marine Engineering
and
Master of Science in Engineering and Management

Abstract

In 2011, the Laboratory for Electromagnetic and Electronic Systems proposed a new type of vibration monitoring system, entitled vibration assessment monitoring point with integrated recovery of energy or VAMPRIE, in their work entitled *VAMPIRE: Accessing a Life-Blood of Information for Maintenance and Damage Assessment* [1]. The proposed monitoring system includes a self-power harvesting accelerometer installed in motors on US Navy and US Coast Guard vessels used to monitor equipment vibration and diagnose the source of the high vibrations.

Utilizing the observations and tools designed by the VAMPIRE project as a foundation, this thesis takes the LEES lab-designed CAPTCHA accelerometers to the US Navy and US Coast Guard fleets to test the lab-designed tool, collect ship equipment data, and verify the VAMPIRE concepts. The CAPTCHA's ability to monitor the vibrations of these systems could be used to immediately diagnose system casualties, aid in parts repair, and ultimately, become a tool to promote Condition-Based Maintenance (CBM). Measurements and experimentation were conducted on two USCG ventilation fans in the lab as well as onboard the USCGC SENECA (WMEC-906), USCGC BERTHOLF (WMSL 750), USCGC STRATTON (WMSL 752), USS MICHAEL MURPHY (DDG 112), USS INDEPENDENCE (LCS 2), and USS SAN DIEGO (LPD 22).

Data was collected and analyzed using a MATLAB program developed to diagnose the types of vibrations seen in various experiments and observe high vibrations in the commissioned ships. The combined results of the CAPTCHA-recorded lab tests and ship testing corroborate the theories proposed in the VAMPIRE paper; however, additional studies could make the VAMPIRE proposal a robust solution to a fleet-wide vibration-induced maintenance problem.

Thesis Advisor: Steven Leeb

Title: Professor of Electrical Engineering and Computer Science

This Page Intentionally Left Blank

Acknowledgements

“Rest and be thankful” – William Wordsworth

I would like to thank the following people for their assistance, encouragement, and most importantly patience throughout this project. First and foremost, I would like to thank Dr. Steve Leeb who guided and advised me during throughout this project. I would also like to thank Pat Hale, who not only read my thesis, but made the SDM Program much more enjoyable. I would like to thank Bart Sievenpiper, Travis Anderson, Chris Schantz, John Donnal for assistance, patience, and adventures over the past year to keep this research moving forward. For the hours of distraction, laughter, and office push-ups, I would like to thank the 2N class of 2013.

“A dream doesn’t become reality through magic; it takes sweat, determination, and hard work”- Colin Powell

I would like to thank my wonderful family and friends for all the support, phone calls, and words of encouragement along the way. This three year journey would not have been possible without you guys!

“It is not the critic who counts; not the man who points out how the strong man stumbles, or where the doer of deeds could have done them better. The credit belongs to the man who is actually in the arena, whose face is marred by dust and sweat and blood; who strives valiantly; who errs, who comes short again and again, because there is no effort without error and shortcoming; but who does actually strive to do the deeds; who knows great enthusiasms, the great devotions; who spends himself in a worthy cause; who at the best knows in the end the triumph of high achievement, and who at the worst, if he fails, at least fails while daring greatly, so that his place shall never be with those cold and timid souls who neither know victory nor defeat.”- Theodore Roosevelt

And so, I present my sweat and blood.

Table of Contents

Abstract	4
List of Figures	9
List of Tables	12
List of Equations	13
1.0 Motivation for Research	15
1.1 Why Monitor Vibrations?	15
1.1.1 Predictive or Condition-Based Maintenance.....	16
1.1.2 Acoustic Interference	17
1.1.3 Scheduling and Operational Requirements	18
1.1.4 Longer Life Expectancy of Ships	20
1.1.5 Historical Navy Vibration Problems	21
1.2 VAMPIRE	23
1.2.1 VAMPIRE Concepts.....	24
1.2.2 Disruptive Technology.....	25
1.2.3 Ultimate Goals of VAMPIRE	27
1.2.4 Current State of VAMPIRE.....	28
2.0 Sources of Study Data	29
2.1 ICAS/MCMAS	29
2.1.1 Data Available from ICAS/MCMAS	30
2.1.2 Need More Than ICAS.....	31
2.2 LEES Lab Testing (USCG Fan)	32
2.2.1 Rotor Imbalance.....	33
2.2.2 Loose Mounting.....	34
2.3 Ship Visits	35
2.3.1 US Navy Ship Visits	35
2.3.2 US Coast Guard Ship Visits	41
3.0 Experiment Equipment & Analysis Tools	44
3.1 Commercial-Off-The-Shelf	44
3.2 CAPTCHA: Accelerometers Developed in the LEES Lab	45
3.3 MATLAB Whisker Diagnostic Tool	46
4.0 Diagnostic Lab Tests	54
4.1 Rotor Imbalance	54
4.2 Loose Mounts	57
4.3 Comparison	62
5.0 Diagnostic Validation on a USCGC SENECA	65
5.1 Rotor Imbalance	66
5.2 Loose Mounts	68
5.3 Comparison	71
6.0 USN and USCG Fleet Vibration Testing	75
6.1 WMSL 750- USCGC BERTHOLF & WMSL 752- USCGC STRATTON	75
6.2 USS MICHAEL MURPHY (DDG 112)	80
6.3 USS INDEPENDENCE (LCS 2)	84
7.0 Future Work	87

7.1 Continued Diagnostic Testing on Equipment	87
7.2 Diagnostic Signatures of Vibrations	87
7.3 Vibration Standards	88
7.4 Future Platform Tests.....	88
7.5 Steady State Analysis	89
7.5 Hardware & Software Capabilities	90
8.0 Conclusions and Recommendations	91
9.0 Appendices	92
9.1 Background of Vibration Mounts.....	92
9.2 Data Summary	94
9.2.1 Experimental Summary.....	95
9.2.2 Whisker Diagnostic Tool.....	100
9.2.3 VAMPIRE MATLAB Code.....	104
9.2.4 Lab MATLAB Code	110
9.2.5 USGC SENECA MATLAB Code.....	116
9.2.6 National Security Cutters MATLAB Code.....	123
9.2.7 USS MICHAEL MURPHY MATLAB Code.....	127
9.2.8 LCS MATLAB Code	132
9.3 Gulf Coast Instructions	133
9.4 Acronyms	134
10.0 Bibliography	135

List of Figures

FIGURE 1: FAULT DETECTION AND DIAGNOSIS PROCESS [2].....	15
FIGURE 2: EQUIPMENT FAILURE MAINTENANCE PATH [5].....	16
FIGURE 3: ACOUSTIC MINE IN GOSPORT [9].....	17
FIGURE 4: USS BATAAN (LHD 5) ASSISTING IN HAITIAN RECOVERY [10].....	19
FIGURE 5: MAINTENANCE AND MODIFICATION COST PER SHIP VS OPTEMPO [12].....	19
FIGURE 6: DOD BUDGE FY11-17 PER FYDP IN FY 13 [14].....	20
FIGURE 7: VARIETY OF FAULTS THAT CAUSE VIBRATIONS IN MACHINES [8].....	21
FIGURE 8: MILITARY VIBRATION STANDARD MIL-STD-167-I [17].....	22
FIGURE 9: GENERAL GUIDELINES FOR IMBALANCED EQUIPMENT [17].....	22
FIGURE 10: VIBRATION LEVELS BASED ON EQUIPMENT SIZE [17].....	23
FIGURE 11: STEAD STATE CONDITION OF THE LAB-TESTED COAST GUARD FAN [18].....	24
FIGURE 12: LAB-TESTED COAST GUARD FAN SPIN-DOWN IN LOWER FREQUENCIES [18].....	25
FIGURE 13: REPAIR SEVERITY FOR EG&G [19].....	26
FIGURE 14: EXAMPLE RESULT FROM AN EG&G VIBRATION ANALYSIS [19].....	26
FIGURE 15: UTTERBACK'S DEPICTION OF DISRUPTIVE TECHNOLOGY IN THE MARKETPLACE [20].....	26
FIGURE 16: A PHYSICAL MODEL OF VAMPIRE UNDER CONSTRUCTION IN THE LEES LABORATORY [18].....	27
FIGURE 17: CONDITION BASED MAINTENANCE SYSTEM EMPLOYED BY THE US NAVY [21].....	29
FIGURE 18: RESULTS READ IN IPARS REPORT BASED UPON ICAS DATA [23].....	30
FIGURE 19: STATE AND VIBRATIONS FOR GTG #1 ON USS HALSEY IN MCMAS.....	30
FIGURE 20: TRANSFER OF ICAS DATA OFF SHIP [21].....	31
FIGURE 21: SPIN-DOWN OF GTG #1 FROM MCMAS DATA.....	32
FIGURE 22: US COAST GUARD VENTILATION FANS TESTED IN THE LEES LAB [18].....	33
FIGURE 23: USCG VENTILATION FAN WITHOUT EXTRA WEIGHT [18].....	33
FIGURE 24: USCG VENTILATION FAN WITH ADDED WEIGHT [18].....	34
FIGURE 25: TIGHTENED MOUNT ON USCG VENTILATION FAN [18].....	34
FIGURE 26: LOOSENED SCREW ON USCG VENTILATION MOUNT [18].....	34
FIGURE 27: USS INDEPENDENCE (LCS 2) MOORED PIERSIDE IN SAN DIEGO.....	35
FIGURE 28: HARD-MOUNTED SEA WATER SERVICE PUMP ON USS INDEPENDENCE.....	37
FIGURE 29: USS SAN DIEGO (LPD 22) OFF THE COAST OF SAN DIEGO, CA [25].....	37
FIGURE 30: SAN CLEMENTE ISLAND, CA THE US NAVY'S BASE FOR ACOUSTIC TRIALS AND TESTING [26].....	38
FIGURE 31: VIBRATION ISOLATION MOUNTS ON FIRE PUMP 1 ON USS SAN DIEGO.....	39
FIGURE 32: ANGLED DISCHARGE PIPING ON A USS SAN DIEGO FIRE PUMP.....	39
FIGURE 33: USS MICHAEL MURPHY (DDG 112) AT SEA DURING HER "SUPER TRIAL" COMPLETED ON MARCH 9, 2012 [27].....	40
FIGURE 34: ROBUST VIBRATION MOUNTS ON FIRE PUMP #1 ON USS MICHAEL MURPHY.....	40
FIGURE 35: ALL THREE NATIONAL SECURITY CUTTERS IN ALAMEDA, CA.....	41
FIGURE 36: USCGC SENECA PIERSIDE IN BOSTON, MA [29].....	42
FIGURE 37: FORWARD VENTILATION FAN UNDER THE BRIDGE ON THE USCGC SENECA.....	43
FIGURE 38: AFT HVAC SUPPLY FAN ON USCGC SENECA.....	43
FIGURE 39: GULF COAST DATA CONCEPT, LLC USB ACCELEROMETER X6-1A [30].....	44
FIGURE 40: EXPLODED VIEW OF GCDC ACCELEROMETER [30].....	45
FIGURE 41: CAPTCHA ACCELEROMETER WITH TRIPLE BATTERY POWER.....	46
FIGURE 42: INTERNAL CIRCUIT BOARD OF A CAPTCHA ACCELEROMETER.....	46
FIGURE 43: BASELINE LAB TEST (APPENDIX 9.2.4).....	47
FIGURE 44: WIRE WRAPPED AROUND FAN BLADE IN LAB (APPENDIX 9.2.4).....	47
FIGURE 45: LAB COMPARISON BETWEEN A BASELINE RUN AND A WIRE WRAPPED AROUND ROTOR BLADE ON Z-AXIS (APPENDIX 9.2.4).....	49
FIGURE 46: LAB COMPARISON OF IMBALANCE ON A SMALLER FREQUENCY SCALE ON Z-AXIS (APPENDIX 9.2.4).....	49
FIGURE 47: OPERATIONAL PROFILE OF MOTOR (APPENDIX 9.2.2).....	50
FIGURE 48: SELECTING POINTS ALONG THE SPIN-DOWN (SELECTION MADE BY INDICATION OF BLUE DOTS) (APPENDIX 9.2.2).....	51
FIGURE 49: WHISKER TRACING FOR SPIN-DOWN WITH PLUS OR MINUS THREE TIMES THE SAMPLING FREQUENCY (APPENDIX 9.2.2).....	52

FIGURE 50: FUNDAMENTAL SPIN-DOWN DIAGNOSTIC GRAPH COMPARING A BASELINE RUN TO LOOSE AND CLAMPED MOUNT SCENARIOS (APPENDIX 9.2.2).....	53
FIGURE 51: CAPTCHA ATTACHED TO SIDE OF FAN WITH COMMAND STRIPS.....	54
FIGURE 52: CAPTCHA ATTACHES TO EQUIPMENT VIA COMMAND STRIPS.....	55
FIGURE 53: AXIS ORIENTATION ON THE CAPTCHA FOR THE LAB TESTS (SIDE VIEW OF FAN).....	55
FIGURE 54: WIRE WRAPPED AROUND SINGLE FAN BLADE (SEE RED ARROW).	56
FIGURE 55: BASELINE RUN COMPARED TO A WIRE WRAPPED AROUND A SINGLE ROTOR BLADE- 29 MARCH 2013 (APPENDIX 9.2.4).....	57
FIGURE 56: CORNER MOUNTING BOLT ON A LAB TEST FAN.	58
FIGURE 57: LAB FANS CONFIGURED WITH ALL FOUR BOLTS REMOVED ON MOTOR 1.....	59
FIGURE 58: TIME- SERIES LAB COMPARISON OF BASELINE FAN AND LOOSE MOUNTING IN X DIRECTION (APPENDIX 9.2.4).....	59
FIGURE 59: TIME- SERIES LAB COMPARISON OF BASELINE FAN AND LOOSE MOUNTING IN Z DIRECTION (APPENDIX 9.2.4).....	60
FIGURE 60: LAB COMPARISON BETWEEN BASELINE RUN AND FOUR LOOSE MOUNTS (APPENDIX 9.2.4).	61
FIGURE 61: LAB COMPARISON BETWEEN BASELINE RUN AND FOUR LOOSE MOUNTS TRUNCATED BY A LOW PASS FILTER (APPENDIX 9.2.4).....	61
FIGURE 62: LAB TEST SPIN-DOWN FOR LOOSE MOUNTS AND COMPLETELY REMOVED MOUNTS- 5 APRIL 2013 (APPENDIX 9.2.4).....	62
FIGURE 63: BASELINE COMPARISON TO MOTOR WITH LOOSE MOUNTS IN THE LAB- 29 MARCH 2013 (APPENDIX 9.2.4).....	63
FIGURE 64: BASELINE COMPARISONS TO AN IMBALANCED FAN (RIGHT)-29 MARCH 2013 (APPENDIX 9.2.4).....	64
FIGURE 65: AXIS ORIENTATION FOR THE CAPTCHAS DURING MARCH 20, 2013 TESTS.....	66
FIGURE 66: AXIS ORIENTATION FOR CAPTCHAS DURING MARCH 29, 2013 TESTS.....	66
FIGURE 67: IMBALANCE INDUCED ON SENECA FAN VIA WIRE WRAPPED ON ROTOR BLADE (LEFT) THROUGH FAN ACCESS (RIGHT).....	67
FIGURE 68: BASELINE RUN VS WIRE WRAPPED AROUND ROTOR BLADE ON USCGC SENECA (APPENDIX 9.2.5). ..	67
FIGURE 69: VIBRATION MOUNTS FOR VENTILATION FAN ON SENECA.	68
FIGURE 70: SIDE VIEW OF VIBRATION MOUNTS ON SENECA.....	68
FIGURE 71: SENECA MOUNTS CLAMPED.	69
FIGURE 72: CLAMPED MOUNTS ON SENECA FANS WITH C-CLAMPS AND WOODEN BLOCKS.....	69
FIGURE 73: FUNDAMENTAL SPIN-DOWN OF SENECA FAN BASELINE VS SEQUENTIAL LOOSENING OF THE MOUNTS (APPENDIX 9.2.5).....	70
FIGURE 74: FUNDAMENTAL SPIN-DOWN OF SENECA FAN BASELINE VS LOOSE MOUNTS AND CLAMPED MOUNTS (APPENDIX 9.2.5).....	71
FIGURE 75: FUNDAMENTAL SPIN-DOWN OF SENECA FAN BASELINE VS LOOSE MOUNTS AND WIRE WRAPPED ROTOR BLADE.	72
FIGURE 76: FUNDAMENTAL SPIN-DOWN OF SENECA FAN- BASELINE VS VARIOUS VIBRATION SOURCES (APPENDIX 9.2.5).....	73
FIGURE 77: FUNDAMENTAL SPIN-DOWN OF SENECA FAN- CLAMPED AND LOOSE MOUNTS VS WIRE WRAPPED AROUND ROTOR BLADE (APPENDIX 9.2.5).	74
FIGURE 78: USCGC BERTHOLF FORWARD VENTILATION FANS.....	76
FIGURE 79: CAPTCHA AXIS ORIENTATION ON BERTHOLF VENTILATION FANS. BOTTOM FAN (LEFT), TOP FAN (RIGHT).....	76
FIGURE 80: USCGC STRATTON VENTILATION FANS.....	77
FIGURE 81: USCGC STRATTON VENTILATION FAN CAPTCHA ORIENTATION. BOTTOM FAN (LEFT), TOP FAN (RIGHT).....	77
FIGURE 82: TOP VENTILATION FANS COMPARED ON THE TWO NATIONAL SECURITY CUTTERS (APPENDIX 9.2.6)....	78
FIGURE 83: BOTTOM VENTILATION FANS COMPARED ON THE TWO NATIONAL SECURITY CUTTERS (APPENDIX 9.2.6).	79
FIGURE 84: ALL FOUR VENTILATION FANS COMPARED FOR VIBRATIONS DURING SPIN-DOWN (APPENDIX 9.2.6). ...	80
FIGURE 85: FIRE PUMP #2 ON THE MICHAEL MURPHY.....	81
FIGURE 86: FIRE PUMP #3 ON THE MICHAEL MURPHY.....	81
FIGURE 87: FIRE PUMP #5 ON MICHAEL MURPHY (Z DIRECTION UP, OUT OF THE CAPTCHA; X DIRECTION PERPENDICULAR TO Y DIRECTION).....	82

FIGURE 88: COMPARISON OF THE THREE FIRE PUMPS ON DDG 112 (APPENDIX 9.2.7).....	83
FIGURE 89: FIRE PUMPS ON DDG 112 COMPARED TO MIL-STD 167-1 (APPENDIX 9.2.7).....	84
FIGURE 90: AXIS ORIENTATION ON LCS 2'S FIRE PUMP #1.	85
FIGURE 91: AXIS ORIENTATION ON LCS 2'S FIRE PUMP #3.	85
FIGURE 92: POWER SPECTRAL DENSITY FOR FIRE PUMPS #1 AND #3 ON LCS 2 (APPENDIX 9.2.8).	86
FIGURE 93: STEADY STATE COMPARISON BETWEEN TWO BERTHOLF VENTILATION FANS. GOOD FAN (TOP) VS BAD FAN (BOTTOM) (APPENDIX 9.2.6).	90
FIGURE 94: RIGIDLY MOUNTED ROTATING SYSTEM (EX. FAN).	92
FIGURE 95: CUT AWAY OF THE FAN RIGIDLY MOUNTED FAN.	92
FIGURE 96: SPRING MOUNTED ROTATING SYSTEM (EX. VIBRATION MOUNTED FAN).....	93
FIGURE 97: CUT AWAY OF THE SPRING MOUNTED FAN.....	93

List of Tables

TABLE 1: EXPERIMENTS CONDUCTED ON LAB FAN TO INDUCE A LOOSE MOUNT SCENARIO-29 MARCH 2013.	58
TABLE 2: SECOND SET OF TESTS RUN ON COAST GUARD LAB FAN- 5 APRIL 2013.	58
TABLE 3: TESTS RUN ON THE USCGC SENECA ON MARCH 20, 2013.	65
TABLE 4: TESTS RUN ON THE USCGC SENECA ON MARCH 29, 2013.	65
TABLE 5: DATA COLLECTED FROM THE USCGC BERTHOLF ON JANUARY 8, 2013.	75
TABLE 6: DATA COLLECTED FROM THE USCGC STRATTON ON JANUARY 9, 2013.	75
TABLE 7: FIRE PUMPS TESTED ON USS MICHAEL MURPHY.	81
TABLE 8: GENERIC OUTLINE OF FUTURE DIAGNOSTIC TESTING.	87

List of Equations

EQUATION 1.....	48
EQUATION 2.....	51
EQUATION 3.....	52
EQUATION 4.....	95
EQUATION 5.....	95
EQUATION 6.....	96

This Page Intentionally Left Blank

1.0 Motivation for Research

Vibration monitoring involves the measurement and analysis of vibrations associated with machinery operations and is specifically aimed at the detection and identification of machinery faults. Machinery vibrations are common to any rotating or moving piece of equipment and can be seen anywhere from land-based industrial businesses to sea-faring vessels.

Vibrations, rated higher than normal, are the telltale sign of irregular operations, due to either malfunction or impending failure. Understanding how to detect and diagnose the cause of these vibrations is one of the first steps towards preserving and maintaining an efficient, working machinery environment. In conjunction with the Laboratory for Electromagnetic and Electronic Systems, this thesis discusses research done to forward vibration detection and diagnosis onboard US Navy (USN) and US Coast Guard (USCG) vessels.

1.1 Why Monitor Vibrations?

Machinery vibrations aboard ships can result in fatigue failure of structural members or major machinery components, can adversely affect the performance of vital shipboard equipment, and can increase maintenance costs. A ship is an extremely complex assembly of structural and mechanical components, which are, in turn, stimulated by a large number of dynamic forces both transient and periodic in nature, which may be significantly increased in severity by sea and operating conditions. Although limited vibration studies are normally conducted during the design and construction of most ships, the complexity of the many potential problems can result in serious shipboard vibration problems [1].

The response of shipboard equipment may be related to its own exciting forces or to those transmitted through the ship's structure [1]

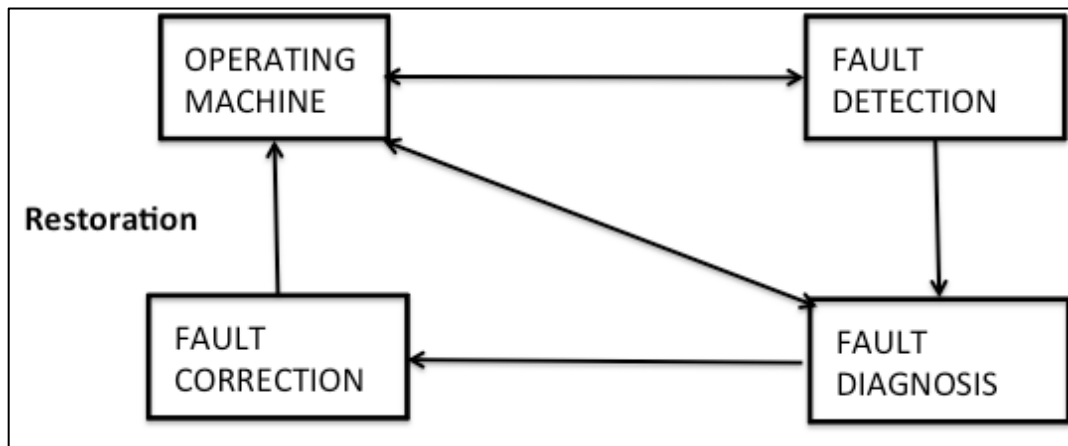


Figure 1: Fault Detection and Diagnosis Process [2].

Understanding the vibration profiles for USN and USCG equipment provides critical information for operations and maintenance. Real-time monitoring of system components allows early detection of degradation, allowing early repair of equipment before failure could occur. Additionally, the vibrations caused by

equipment vibrations can be transferred to hull structures, contributing to radiated acoustic noise.

1.1.1 Predictive or Condition-Based Maintenance

Many ship inspections, due to budgetary pressure, such as zone inspections, have been eliminated [3]. Having the capability to monitor shipboard vibrations for equipment degradation allow sailors to practice predictive maintenance. According to RADM Dave Lewis, head of the Program Executive Office for Surface Ships, the purpose of predictive maintenance is to “fix it before it breaks [3].” An example is the new Littoral Combat Ship (LCS) class combatants in the USN. “Because of its small core crew of 40 Sailors, plus 10 more temporarily assigned for the deployment... much of the maintenance during the [LCS 1] deployment will be accomplished by Navy and contractor support personnel in ports, and governed by condition-based monitoring of the ship’s systems by the Navy. Monitoring technology will be key to determining the health of the ship and be used to aid in predictive maintenance [4].”

As seen in Figure 2, there are three main types of shipboard maintenance, predictive, preventative, and corrective or crisis maintenance. Preventative and corrective maintenance are conducted when a machine is periodically (according to a time schedule) maintained or a fault is discovered by either the sailor or by a complete failure in the system; no monitoring equipment is required for either of these maintenance styles.

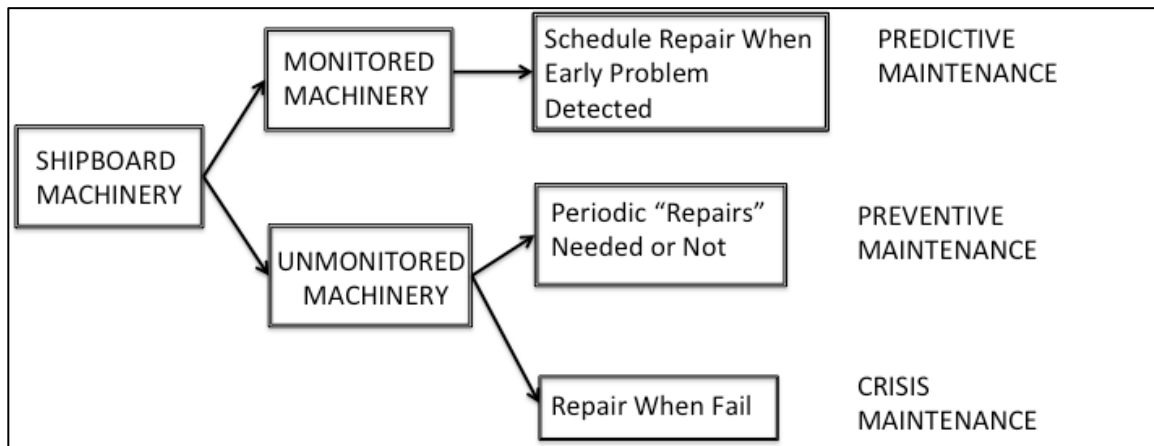


Figure 2: Equipment Failure Maintenance Path [5].

Predictive maintenance, also known as Condition Based Maintenance (CBM) in the USN and USCG, is maintenance based on objective evidence of actual or predictable failure of ship’s installed systems or components [6]. It basically means conducting maintenance when the need is detected by one or more indicators. These indicators or monitors highlight when equipment is going to fail or performance is deteriorating [7]. This concept is applicable to mission critical systems that incorporate fault reporting and active redundancy.

Historically, CBM was introduced into the USN and USCG to maintain mission critical equipment during critical time periods such as deployments and underway times. Utilizing real-time data collected from the equipment, maintenance and resources can be optimized to maintain mission readiness. Condition monitoring systems determine the equipment's current "health" and alert the operator only when maintenance is required. In accordance with the Navy's maintenance policy, diagnostics, inspections, non-intrusive monitoring for trending/analyses and tests shall be utilized to the maximum extent possible to determine performance and material condition of, and to predict and schedule required corrective maintenance action on, ships systems and equipment [6]. Ideally, condition-based maintenance allows the maintenance personnel to do only the right things, minimizing spare parts cost, system downtime and time spent on maintenance.

1.1.2 Acoustic Interference

Although not discussed in detail in this thesis due to classification level, the study of marine machinery vibrations is extremely applicable to acoustic sensitivity. Vibratory motion is a phenomenon inherent to all machinery regardless of material condition and is measured in terms of the physical motion of the machine or the sound produced by the motion. Measurements of mechanical vibration are favored for machinery condition monitoring purposes, whereas acoustic vibration measurements have greater importance and use in noise control and reduction analyses [8].

Vibrations can propagate directly from shipboard structure into the ocean and pose problems particularly for mine warfare and underwater ship signature detection. By understanding the vibrations of shipboard equipment, a ship's captain can opt not to operate certain equipment in certain conditions or areas of operation.



Figure 3: Acoustic Mine in Gosport [9].

For instance, there are acoustic mines as seen in Figure 3 which can passively and actively monitor audio activity in its vicinity. Depending on its design, it will either actively send out audio pulses, not unlike a sonar, listening via hydrophone to the speed at which the echo returns to it or passively listen to its environment, depending only on the noise that is made without its interference. This hydrophone listens for particular noises made by a vessel's machinery.

Passive listening modes in an acoustic mine can be sensitized to the sound of specific engines or other characteristic acoustic signatures, while active modes can send out acoustic pulses to seek out and identify targets. With vibration monitoring equipment installed, a commanding officer can make informed decisions for the safety of the crew and the criticality of the mission. Real-time vibration data could mean the difference between not only functionality and loss of equipment, but possibly life or death.

1.1.3 Scheduling and Operational Requirements

The operational tempo (OPTEMPO) of the USN and USCG is at such a high level today that events such as emergency availabilities or repairs can disrupt and even compromise critical missions. High operational tempo has long been a problem. It limits the amount of time the Navy has to conduct assessments, wears down the ship, and puts added strain on the crew, who may not have enough time to do maintenance [3]. In order to align maintenance needs with these operational demands, CBM policies are being implemented across the fleet to detect problems early and keep assets on station.

For example, in 2010 when a massive earthquake shook Haiti, US ships and assets were sent down to the badly damaged country to provide relief and medical attention. However, the USS BATAAN, a large-deck amphibious ship sent down in support of these missions in Figure 4, failed to complete the mission in a timely manner; the operational requirement- in this case emergency medical care- was not initially met. The ship was unable to accept and treat wounded Haitians in a timely manner due to water-producing equipment failure. Instead of arriving on station and immediately treating patients, the BATAAN had to wait for a support vessel to arrive and provide them with the much-needed water.



Figure 4: USS BATAAN (LHD 5) Assisting in Haitian Recovery [10].

As US Navy LT Hooper noted, “With short-notice surge deployments becoming the norm, the Navy has got to start doing some serious thinking about how it manages ship maintenance and surge availability [11].” The USS BATAAN was surged during an emergency situation and due to maintenance and equipment failure, could not meet the operational requirements. With continuous vibration monitoring and fault notification, the engineering equipment responsible for this failure could have been fixed prior to deploying. Proper planning for replacement and repair could have been made.

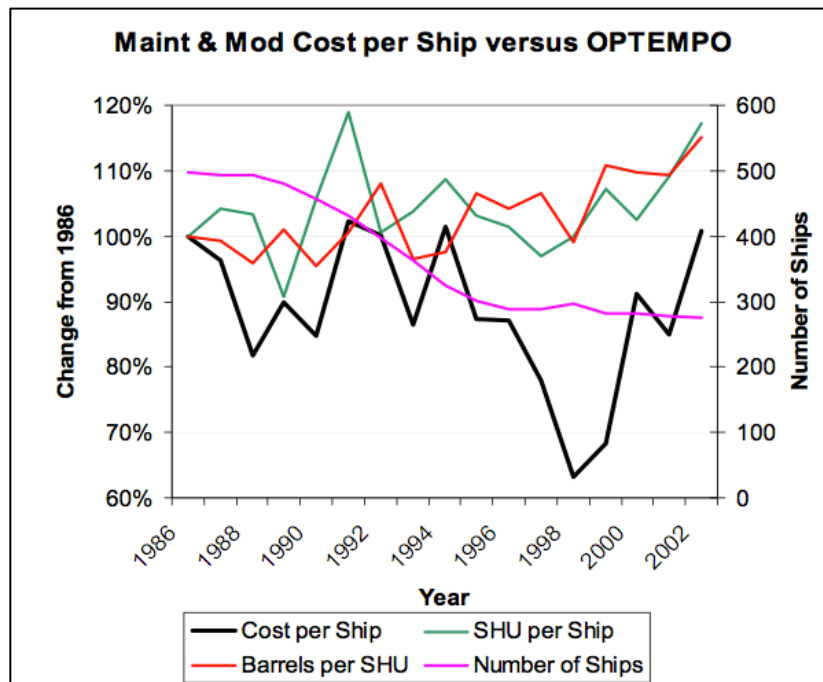


Figure 5: Maintenance and Modification Cost per Ship VS OPTEMPO [12].

In a study conducted for the Department of Defense, maintenance and modernization costs were compared to the OPTEMPO of US Navy ships. As seen in Figure 5, the OPTEMPO or Steaming Underway Hours (SUH) of the fleet is increasing, as compared to the base year of 1986 in this graph, and the maintenance and modernization dollars have either stayed the same or dropped drastically [12]. With higher OPTEMPO and lower repair dollars available, precise maintenance planning is key for effective use of the maintenance budget allocated to each ship. Vibration monitoring could provide one avenue to plan and predict maintenance repair during one of the few downtimes a ship experiences without interfering with its mission requirements.

1.1.4 Longer Life Expectancy of Ships

Due to procurement budget cuts and reductions in maintenance funding as seen in Figure 6, USN and USCG ships are being forced to endure longer operational life cycles beyond their originally designed-for life cycle. With these extensions, vibration monitoring plays a critical role in ensuring good material condition of these older ships. For example, two of the oldest ships in the Navy’s fleet, the USS BLUE RIDGE and USS MOUNT WHITNEY, were recently extended to almost 70 years of service life to provide the Navy with two command ships that have proved to be vital assets in recent years. According to the report, “With the service lives of USS BLUE RIDGE and USS MOUNT WHITNEY being extended to 2039 and possibly beyond, it is critical that adequate resources are provided to maintain, sustain, and retain these platforms [13].”

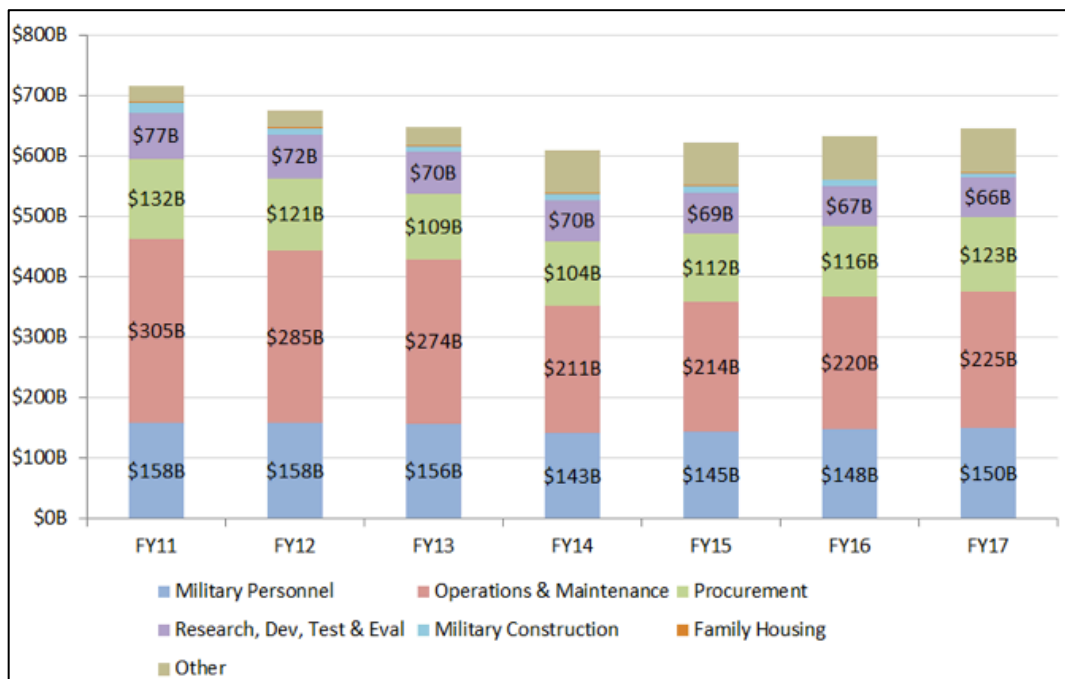


Figure 6: DoD Budge FY11-17 per FYDP in FY 13 [14].

1.1.5 Historical Navy Vibration Problems

Equipment vibrations are not new to the USN or USCG. Since the first installation of rotating equipment on ocean-going vessels, vibrations have caused maintenance and operational problems. In hydraulic ship systems, the major equipment sources of vibrations are pumps, which are predominantly of the centrifugal, piston or screw type and fans.

High pressure pumps can be either the reciprocating or the rotary vane, gear, or screw type. The reciprocating piston or plunger pumps are complex, have many moving parts, experience valve and seal wear, and normally produce high structure borne and fluid noise levels. Rotary screw pumps are the most common positive displacement pumps in naval service. The two types used are the twin-screw pump (surface ship Lube Oil (L/O) and Fuel Oil (F/O)) and the triple-screw pump (surface ship F/O Service and sub L/O and Hydraulic system). These pump designs have high stresses in the screws and rotors at high pressure, and have extensive rolling and rubbing contact area.

Fans are a major source of vibration in a ship's ventilation system. A fan's vibration spectrum normally consists of both wide-band and discrete components. The wide-band part of the spectrum originates from the rotation of the fan and drive bearings, while the discrete components are caused by the imbalance of rotating parts and interaction between fan rotor blades [1]. In addition to the aforementioned vibration sources, aerodynamic forces acting upon the air duct also as a result of turbulent air flow also provide a vibration source in these systems [15].

There are two main sources of shipboard equipment vibrations: internal and external vibrations. A variety of these vibrations can be seen in Figure 7. The most common are imbalance or "unbalance" in the rotor and failure in the vibration isolation mounts. Imbalance has long been recognized as the fundamental source of vibration in rotating machinery [16]. Likewise, it is common for mounts to become loosened during underway operations as the equipment shakes and rattles with the moving of the ship and other equipment operations.

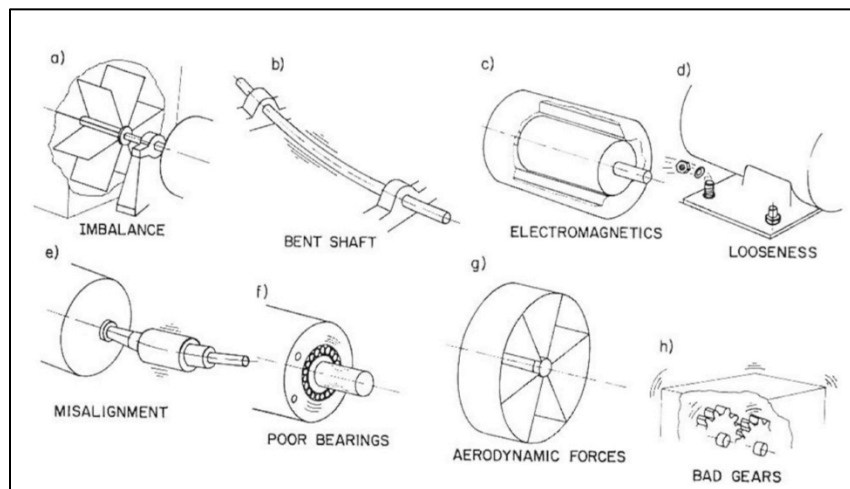


Figure 7: Variety of Faults that Cause Vibrations in Machines [8].

Imbalance:

Machines are subject to several types of imbalance conditions, the most common of which is called a static imbalance. A static imbalance is a condition where the center of rotation of a rotor does not correspond to its center of mass, or in other words, its center of gravity does not lie on its axis of rotation [17].

The simplest type of imbalance is equivalent to a “heavy spot” or added weight at a single point in the rotor and is known as a static imbalance. With each rotation, this extra weight causes the body of the motor to displace which leads to vibration. This situation occurs in the field when fan blades are damaged or fouled or when bearings wear[1]. A static imbalance can be modeled as a weight attached to the rotor blade.

To measure imbalances, the USN currently utilizes MIL-STD-167 as the standard for acceptable vibration levels seen in Figure 8. This limit is used if no average data is available for expert system analysis and sets the alarm level at 107 VdB above a frequency of 1000 RPM.

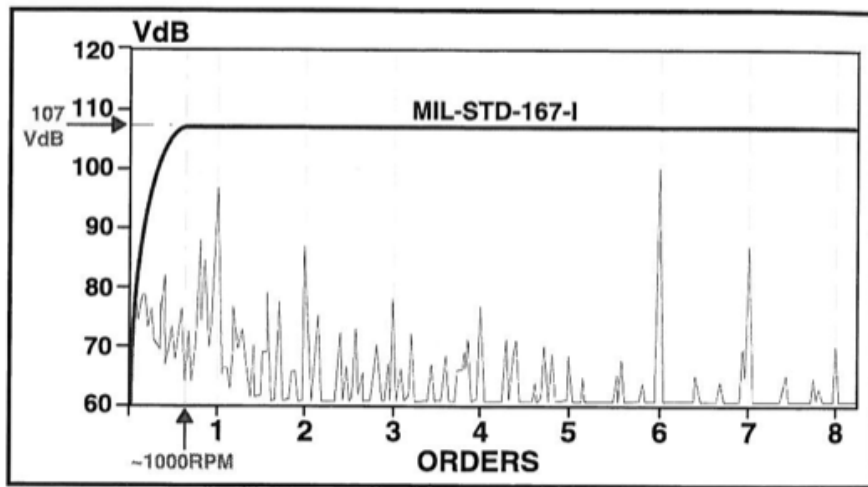


Figure 8: Military Vibration Standard MIL-STD-167-I [17].

However, as this standard was developed in 1974 and a bit outdated, the generic guidelines for general use in diagnosing imbalance for machines running at 1800 or 3600 RPM are seen in Figure 9. Figure 10 depicts the impact of equipment size on vibration levels.

1X Vibration Level, VdB	Diagnosis	Repair Priority
Less than 108 VdB	Slight Imbalance	No Recommendation
108 VdB-114 VdB	Moderate Imbalance	Desirable
115 VdB- 124 VdB	Severe Imbalance	Important
More than 125 VdB	Extreme Imbalance	Mandatory

Figure 9: General Guidelines for Imbalanced Equipment [17].

1X Vibration Level, VdB	Machine Type	Repair Priority
109 VdB	Small Single-Stage Pump	Desirable
118 VdB	Large Hydraulic Pump	Desirable
116 VdB	Medium Sized Fan	Desirable

Figure 10: Vibration Levels Based on Equipment Size [17].

Loose Mounts:

If a mounting or frame loosens over time, the mount can no longer dampen vibrations. This results in an increase in the radial vibration of the body of the machine. An improperly mounted machine can damage parts of the moving machine as well as add noise to the ship, which can be a source of acoustic signature in the water. Mechanically, loose mounting also causes fatigue in the structure of the motor which can reduce the lifetime of the machine.

Others:

Imbalance and loose mounts are the traditional causes of vibration in machinery on ships; however, there are other causes which can also result in vibrations.

A shaft can bend or sag between two bearings causing vibrations. As it rotates, the stress pattern alternates. If it rotates fast enough, it is in danger of whirling, a situation which may be compared with the action of a skip-rope and one in which the fiber in tension remains in tension. This condition is likely to be destructive and obviously would transfer large unbalanced forces to the rest of the structure [16].

Additionally, machines can internally experience coupling misalignment, bearing defects, and worn components. Externally, vibrations can be induced from load variations on the equipment, vibrations from adjacent equipment not associated with defects in the monitored machinery, and changes in flow conditions [2].

1.2 VAMPIRE

In *VAMPIRE: Accessing a Life-Blood of Information for Maintenance and Damage Assessment*, a team of MIT students, professors, and military personnel proposed a prototype and method for harvesting power from the magnetic field of the power supply to a given pump or piece of equipment in an effort to provide operators and maintainers real-time vibration data on the ship's engineering equipment [18]. This paper demonstrates a work-in-progress for in situ vibration monitoring called vibration assessment monitoring point with integrated recovery of energy (VAMPIRE).

This VAMPIRE prototype and the preliminary signal processing experiments establish the foundation for the research conducted in this thesis. It explores features that may be demanded in future vibration sensors: nonintrusive installation requiring no custom power or data wiring; maintenance-free, self-powered sensors; and scalable access to information, ranging in flexibility from a

“reduced” figure-of-merit to detailed time-series information permitting cross-correlation study with power consumption and operating condition.

The future of the proposed VAMPIRE is to supply more detailed information that can diagnose types of imbalances as well as inform a real-time signature assessment as part of a tactical decision aide (TDA).

1.2.1 VAMPIRE Concepts

Utilizing a commercial-off-the-shelf (COTS) accelerometer and two single phase coast guard ventilation fans installed in the lab, the VAMPIRE team proposed two main concepts. First, it would be possible to create a wireless, self-power harvesting accelerometer, installed the terminal box of motor-driven equipment on USN and USCGC vessels, which would measure and diagnose high vibrations. Second, with preliminary testing conducted on USCG ventilation lab fans, high vibrations can be recognized in the time-series analysis of the steady state condition of the fans and vibration diagnostics may be discernable in the spin-down frequencies.

During the normal, steady state condition of a piece of equipment, high vibrations, regardless of source, can be seen. As seen in Figure 11, in the steady state condition of the 60Hz Coast Guard fan, imbalancing the fan (internal vibrations) and loosening the mounting system (external vibrations) are both seen as an increase in acceleration. There is very little difference between the two sources of vibrations other than the higher amplitude of vibrations during steady state.

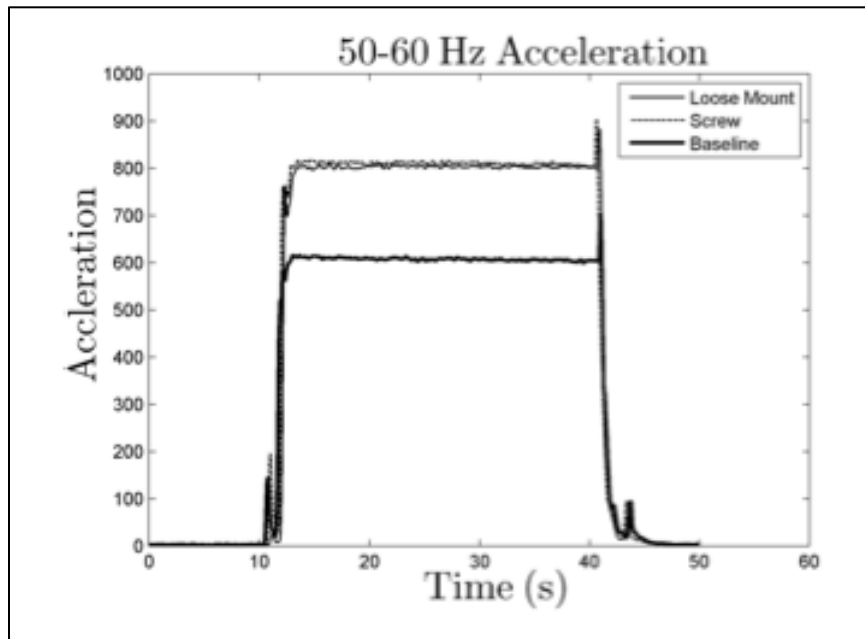


Figure 11: Stead State Condition of the Lab-Tested Coast Guard Fan [18].

However, during the spin-down, the various sources of vibrations excite the motor at various frequencies and amplitude allowing for the identification of cause of vibration. Figure 12 depicts the spin-down of the 60 Hz Coast Guard lab fan. In it, the imbalanced fan remains “excited” throughout the frequency spectrum as it spins

down. The loosened mounts, though, are less excited in the “sub-operational” frequencies- ie- below the 30-40 Hz range.

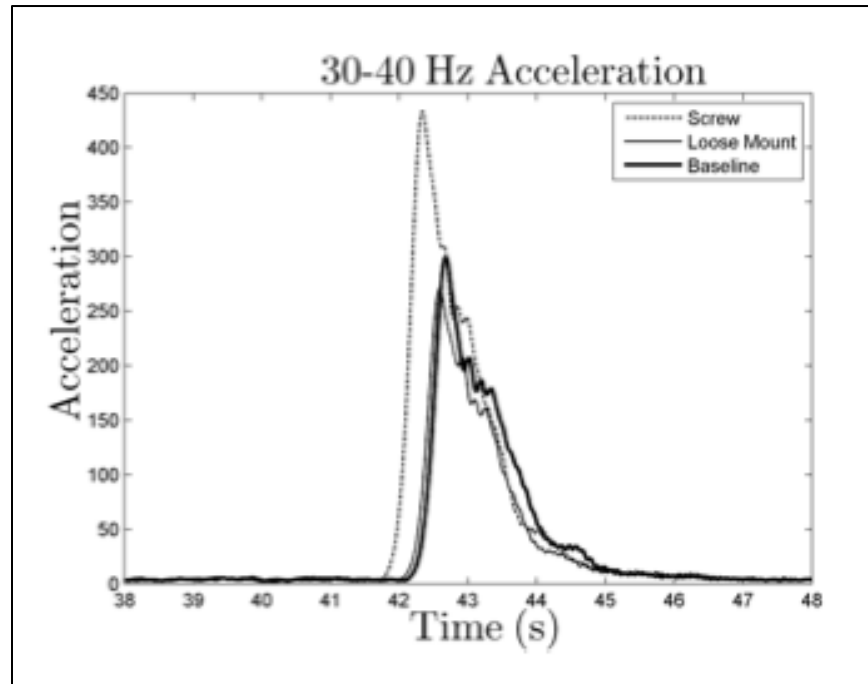


Figure 12: Lab-Tested Coast Guard Fan Spin-down in Lower Frequencies [18].

The research in this thesis seeks to corroborate these theories with real USN and USCG fleet diagnostic tests and data analysis.

1.2.2 Disruptive Technology

The VAMPIRE concept would provide a low-cost, disruptive technology to the USN and USCG, which could displace repetitive, expensive contractor visits. Both the USN and USCG hire contractors to visit individual ships several times a year to take vibration readings, process the data, diagnose the problem, and eventually report back to the ship potential problems and solutions.

Each year, the USCG hires United Research Services- Edgerton, Germeshausen, and Grier Technical Services Division (URS- EG&G TSD) to monitor vibrations and provide technical support services to the cutters. The EG&G Technical Service team uses a FLI WATCHMAN® vibration data collector fitted with a triaxial vibration sensor to take vibration measurements [19]. They temporarily attach these data collectors to the machinery at selected locations, usually at or near the machine’s bearing housings. Vibration measurements are made automatically over two frequency ranges, often at 10 times and 100 times the rotational rate of the machine being tested. As the data is collected, it is stored in the memory of the portable data collector. When the data collection has been completed, the data is processed and is stored into an ExpertALERT database. The ExpertALERT system contains an automated diagnostic system that has been set up to identify which machines have abnormally high vibration (as compared to the machine’s baseline signature), and to diagnose the nature and severity of the faults seen in Figure 13. Diagnostic results

are reviewed by a facility vibration expert and edited as necessary for inclusion into the Vibration Analysis Report [19] for example Figure 14. Each visit and subsequent report costs the USCG on the order of hundreds of thousands of dollars for the entire fleet.

Repair Priority Definitions

- Mandatory:** Machine failure is certain within days to weeks. Repair should be accomplished as soon as possible. Meanwhile, the machine should be secured or tested daily.
- Important:** Machine problems or failure are probable within weeks to months. Repair should be accomplished at the next convenient downtime, or in the next two to six months. Meanwhile, the machine should be tested weekly.
- Desirable:** Machine problems are probable within months to years. Repair can be deferred and scheduled based on changing fault severity over time. Meanwhile, the machine should be tested monthly.

Figure 13: Repair Severity for EG&G [19].

#5 FIRE PUMP

IMPORTANT: BALANCE UNIT.

Acquired: 9/15/2009 9:14:10 PM Speed: 1X = 3589
 Maximum Level is 121 (+14) VdB [2R] at 1.00x

SERIOUS MOTOR IMBALANCE

Figure 14: Example Result from an EG&G Vibration Analysis [19].

The VAMPIRE technology, wirelessly installed in the terminal boxes of shipboard equipment, could reduce if not completely eliminate the need for these inspections and thus provide a potential technological disruption similar to James Utterback’s depiction of a disruptive technology in Figure 15.

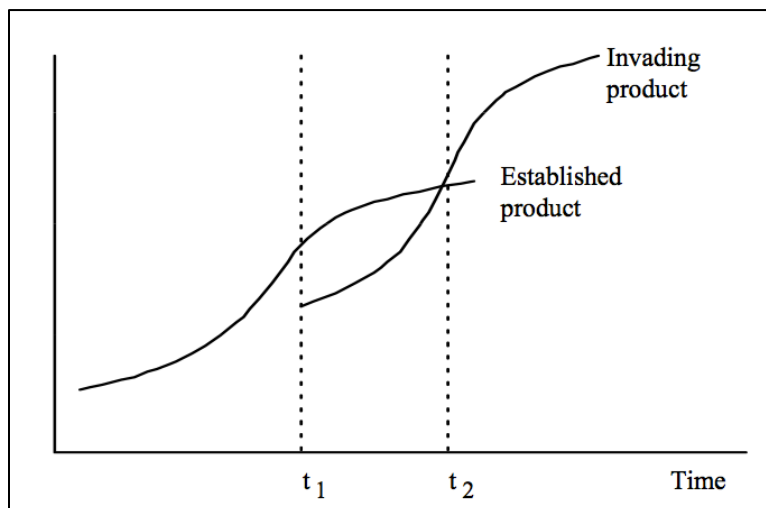


Figure 15: Utterback’s Depiction of Disruptive Technology in the Marketplace [20].

The real-time VAMPIRE vibration analysis provides a simple solution to the need for immediate maintenance feedback at a fraction of the current cost, a characteristic of a disruptive technology [20]. Unlike the repetitive contractor costs, the VAMPIRE technology would only incur the initial installation cost and minor system upgrade costs.

1.2.3 Ultimate Goals of VAMPIRE

In an effort to monitor and diagnose vibrations in marine machinery, the Office of Naval Research (ONR) initiated this study to develop VAMPIRE. Much like submarine vibration monitoring systems, ONR hopes to integrate this technology into surface ships to promote CBM and assist in monitoring acoustic noise signals originating from machine vibrations. The ultimate goals proposed were to create a device that could gather vibration data, analyze the data for detection of faults, perform diagnosis for faults detected, predict remaining life for failing components, and make or recommend maintenance actions.

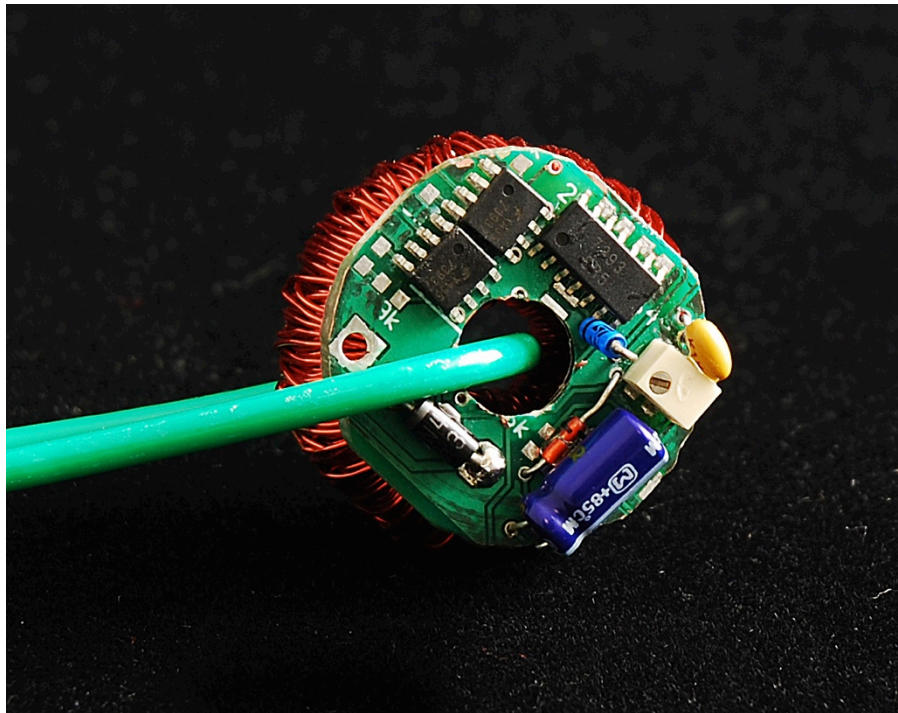


Figure 16: A physical model of VAMPIRE Under Construction in the LEES Laboratory [18].

The VAMPIRE acceleration monitor could be designed into the equipment to be monitored. The design will be a nonintrusive vibration monitor that requires no electrical connections. This new vibration monitor is a small toroidal transformer that self-powers from the magnetic fields around a wire feeding an electromechanical load of interest, e.g., a motor as seen in Figure 16. This monitor could store data for later retrieval, or communicate wirelessly, or potentially communicate with a nonintrusive load monitor (NILM) collating data via a power line carrier modem. The system is maintenance free and easily installed as part of a new or retrofit motor enclosure cover. It could also measure temperature and other important diagnostic indicators. VAMPIRE could provide in-situ monitoring for a

load while powering itself from the magnetic fields around the wires energizing the load [18].

The wireless aspect of VAMPIRE supports user mobility, a necessary requirement on naval vessels, allowing network connectivity in locations without wired ports. This option also supports a cheaper installation price without the cost of wires running in every engineering space.

1.2.4 Current State of VAMPIRE

The current iteration of the VAMPIRE research is two-fold. First, the VAMPIRE accelerometer itself is in the form of a battery-powered device sampled at a rate of 3.2 kHz as discussed in Section 3.2 in order to gather diagnostic data on USN and USCG ships. This device has been tested against the latest commercial-of-the-shelf (COTS) accelerometer and proven to be superior in data collection and analytical results. The self-power harvesting portion of the device is under construction in the LEES laboratory.

Second, the VAMPIRE program is in the process of gathering diagnostic data from the USN and USCG fleets to aid in software architecture and validation. Initial tests in the laboratory were conducted to demonstrate the data capturing ability of the VAMPIRE accelerometers and possibilities of the VAMPIRE idea. To validate the closely controlled laboratory results, the VAMPIRE accelerometers were taken to the two fleets, USN and USCG, to measure machine vibrations, induce vibrations in a realistic setting, and validate the findings in the lab. This thesis discusses those experiments and validates the laboratory testing using the CAPTCHA accelerometers, the current VAMPIRE technology.

2.0 Sources of Study Data

The primary sources of data for this thesis were the Navy's Integrated Condition Based Assessment System (ICAS) [21], LEES laboratory fan experiments, three USN ship visits including USS INDEPENDENCE, USS SAN DIEGO, and USS MICHAEL MURPHY and three USCG ship visits including USCGC SENECA, USCGC BERTHOLF, and USCGC STRATTON.

2.1 ICAS/MCMAS

The US Navy currently employs a COTS software system called ICAS or Integrated Condition Based Assessment System in order to accomplish its Condition Based Maintenance (CBM) objectives as seen in Figure 17. An online monitoring and condition assessment system, ICAS is currently installed on over 100 Navy ships and provides CBM coverage on over 15 mission critical Hull, Mechanical, and Electrical (HM&E) systems including Main Propulsion, Ships Service Gas Turbine Generators, Air Conditioning, High and Low Pressure Lube Oil, and the Main Reduction Gear[22]. ICAS relies on the aggregation of applicable sensor data available from the Machinery Control Message Acquisition System (MCMAS). The ICAS vibration-monitoring program utilizes the vibration signal from machinery to produce a measurement of the overall level of vibration that the machinery is experiencing. This overall or broadband vibration level is the root mean square (rms) level of the vibration signal. The equipment used for measuring this level is much like a voltmeter, which indicates the rms level of an electrical voltage signal.

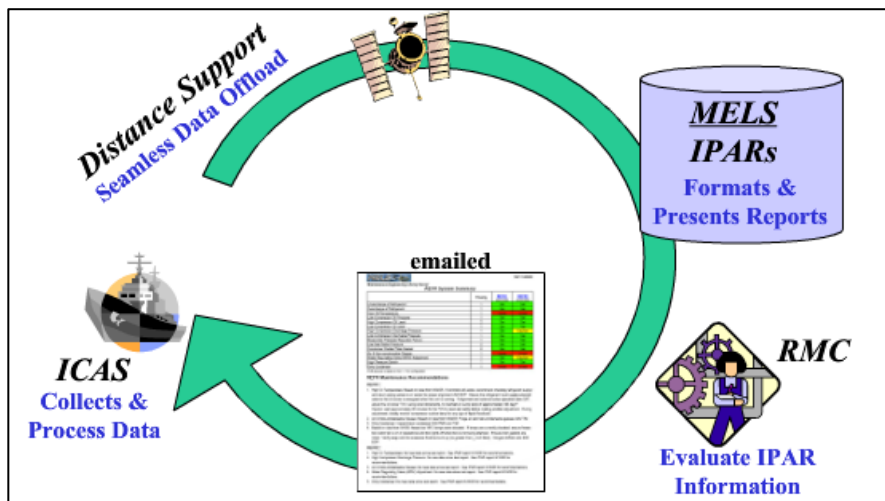


Figure 17: Condition Based Maintenance System Employed by the US Navy [21].

Through workstations in every major machinery compartment, ICAS detects and processes equipment failures. Data is collected from these workstations and sent shoreside to the Maintenance Engineering Library Server (MELS) for distance support and analysis. Integrated Performance Analysis Reports (IPARS) are then generated and sent to the regional maintenance centers (RMC) for maintenance action. Figure 18 depicts the standard output as seen in the IPARS by the ship and RMC.

GTG System Summary				
	Priority	GTG1 08/26/2009	GTG2 04/11/2009	GTG3 04/10/2009
Engine Over Temp	1	Sat	Sat	Sat
Engine Over Speed	1	Sat	Sat	Sat
Engine Under Speed	2	Sat	Sat	Sat
Gen Lube Oil Press Low	1		Sat	Sat
Fail To Fire	1	Sat	Sat	Sat
Out of Spec Start	3	Sat	Sat	Sat
Start Over Temp	1	Sat	Sat	Sat
Start Reliability	3	Sat	Unsat	Sat
Start Vibrations High (Hot)	3	Sat	Sat	Sat
Start Vibrations High (Cold)	3	Sat	Sat	Sat

Figure 18: Results Read in IPARS Report Based Upon ICAS Data [23].

The IPARS results, garnered from ICAS data, are governed by the NAVSEA Technical Specification S9073-AX-SPN-010/MVA Vibration Analysis, Machinery. MIL-STD-167-1 covers internally excited vibration of all rotating equipment except reciprocating machinery, and MIL-STD-167-2 cover reciprocating machinery, propulsion systems and shafting. They are based on a displacement (mils peak) spectrum which is actually equivalent to a constant velocity of 0.13 inches per second (170VdB) above 1200 RPM.

2.1.1 Data Available from ICAS/MCMAS

In order to analyze operational vibration collection systems, data from ICAS was analyzed to determine the extent of capability and possible outputs. The data from ICAS/MCMAS can only be accessed by an entity with processing capabilities- ie- either the ship or NAVSESS Philadelphia. However, if data is procured, operations, frequencies, power, current, and vibrations can be analyzed for major engineering equipment in one-second increments as seen in the example in Figure 19.

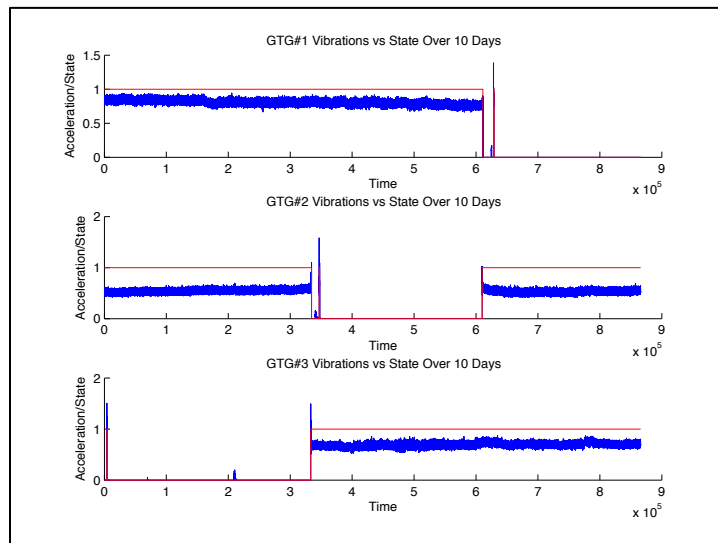


Figure 19: State and Vibrations for GTG #1 on USS HALSEY in MCMAS.

2.1.2 Need More Than ICAS

This system can be utilized to see operating profiles of major engineering equipment, trend analysis, and even simple vibration analysis, but it still falls short of aptly providing the ship with the needed information for successful vibration monitoring.

The biggest fault of MCMAS is access to the actual data. If a ship does not save the data, then the data is lost. Trend analyses are the biggest advantage of MCMAS, yet without data saved over time, no analyses can be done. In addition to actually obtaining the data, processing and analyzing the data takes a considerable amount of time as seen in Figure 20. If conducted by the ship, it can be done on station; however, if a subject matter expert is not present, then the data must be sent off ship for analysis. Valuable time could be wasted waiting on a diagnosis pending all required data is available.

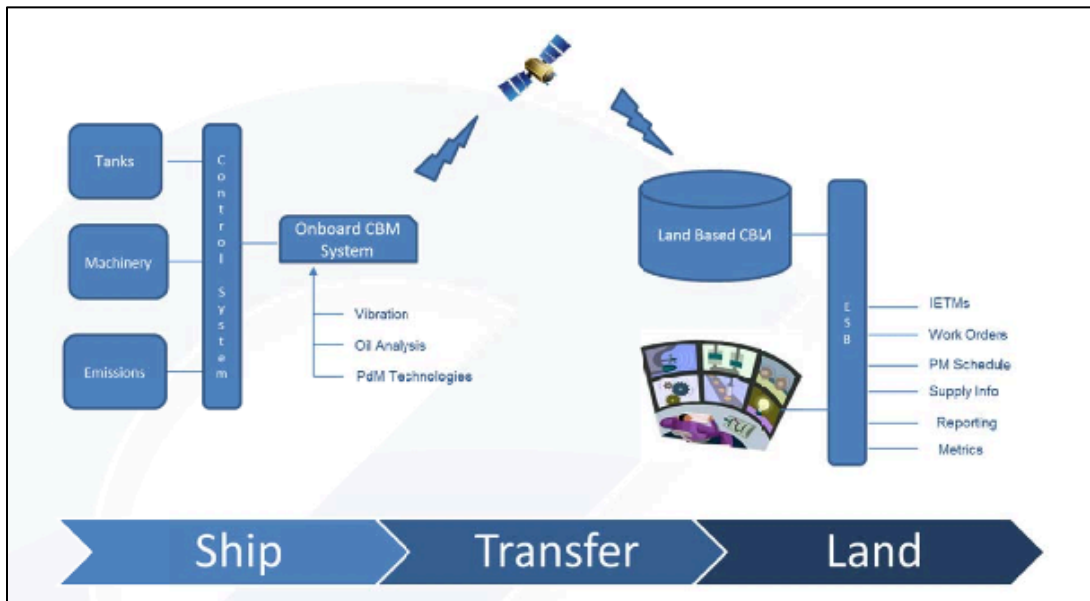


Figure 20: Transfer of ICAS Data Off Ship [21].

If MCMAS data is sent off-ship for analysis, the returned report is vague and typically includes a one-line result. Figure 18 reports the status of the major engineering equipment as “UNSAT” or “SAT”. However, with these results, no explanation is made as to what “Sat” actually means and the “Unsat” result explanation provides little instruction for the operator or even the repair facility. The Unsat Start Reliability comment reads, “No new data available for IPAR review. If this unit has operated in the last six months, please have your ICAS administrator verify operation by reviewing applicable trend and event data. Contact your local RMC if you need further assistance[23].” The grey indicates that an analysis was not available. With these results, the ship is left with an “UNSAT” result but no direction on how to treat or remedy the fault.

As mentioned earlier, the highest fidelity of MCMAS data comes in one-second increments. For example, examining the spin down of Gas Turbine Generator #1

from Figure 19, the fidelity of the data is not good enough to draw clear conclusions about the state of the generator. Figure 21 depicts the spin-down of the generator in as much detail as possible. No clear diagnosis can be made from these graphs.

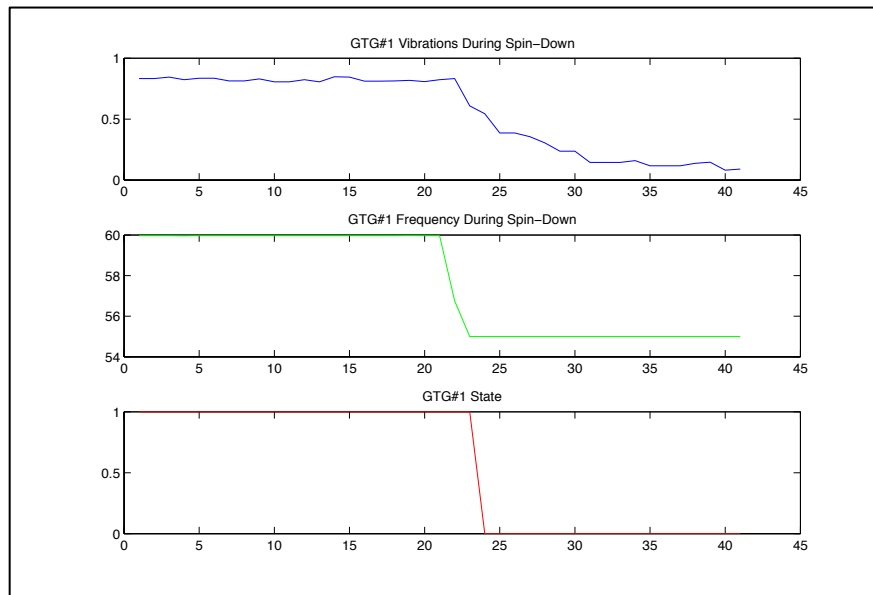


Figure 21: Spin-Down of GTG #1 From MCMAS Data.

Finally, ICAS and MCMAS are underutilized. A US Navy Port Engineer responsible for repair naval vessels stated that ICAS has great potential, but it is extremely underutilized. Until data is actually sent off the ship to be processed, ICAS will not be beneficial to the fleet [24].

2.2 LEES Lab Testing (USCG Fan)

During the initiation of the VAMPIRE research, a lab study was conducted on two USCG single-phase ventilation fans, which were mounted to a steel frame and tested as seen in Figure 22. The two motors were mechanically coupled through the steel frame. The motor on the left is the intake fan while the motor on the right is the exhaust. The VAMPIRE team ran experiments on the fans with the initial VAMPIRE accelerometers to test the effect of certain faults on radial vibration. The first experiment produced vibrations due to a rotor imbalance and the second experiment produced vibrations due to a loose mount. The resultant data was used to supplement baseline diagnostic data in the research presented in this thesis and can be seen in Appendix 9.2. Once the next iteration of accelerometers was developed, the CAPTCHA, these tests were run again. Experimental summaries and results of these tests can also be seen in Section 4.0.

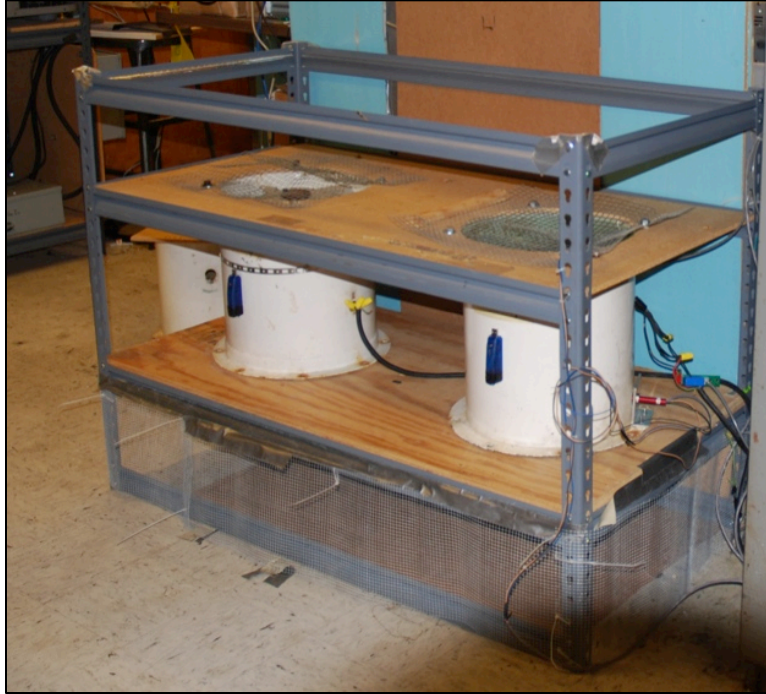


Figure 22: US Coast Guard Ventilation Fans Tested in the LEES Lab [18].

2.2.1 Rotor Imbalance

In the lab during the original VAMPIRE testing, weights of different sizes were added to the hub of the fan to induce an imbalance in the rotor. With each rotation, the extra weight caused the body of the motor to displace and incur vibrations. The radial acceleration was measured prior to the addition of the weights as well as with the added weight. Figure 23 and Figure 24 depict the two experimental conditions of the fan. The first picture does not have the added weight of a screw while the second pictures clearly does.



Figure 23: USCG Ventilation Fan Without Extra Weight [18].

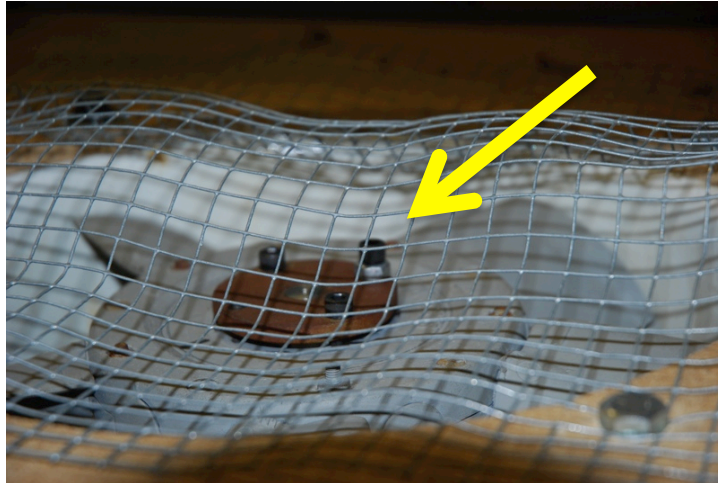


Figure 24: USCG Ventilation Fan with Added Weight [18].

2.2.2 Loose Mounting

The second set of experiments run in the LEES lab was to induce vibrations due to loose mounting on the ventilation fans. To simulate a loose mount in the lab, the mounting screws attached to the motor were loosened. Figure 25 depicts a properly tightened screw, which mounts the intake motor to the steel cage, while Figure 26 shows a loosened screw. As the mounting screw is loosened, the radial vibration increases, as expected.

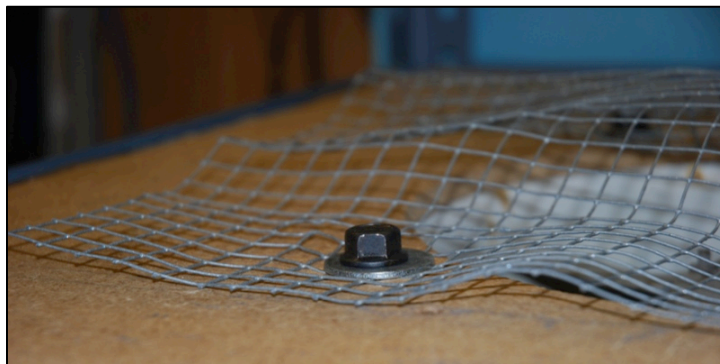


Figure 25: Tightened Mount on USCG Ventilation Fan [18].

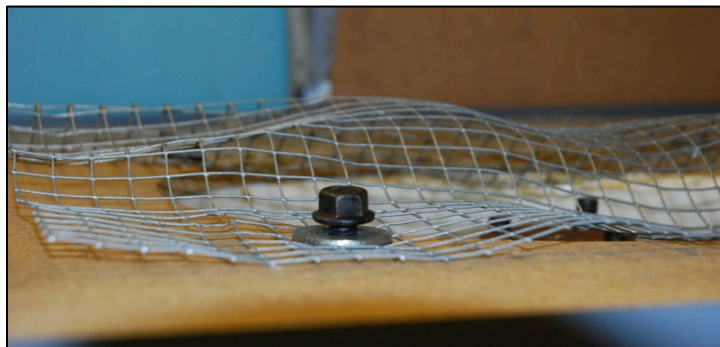


Figure 26: Loosened Screw on USCG Ventilation Mount [18].

2.3 Ship Visits

The majority of the data collected for this thesis was gathered through six ship visits over the past year, three to US Naval ships and three to US Coast Guard ships. Each ship visit harbored a different goal and objective for data gathering depending on ship type and visit environment. The Famous Class visit to the USCGC SENECA was to gather diagnostic data for known vibration problems on fans still installed on a ship. The focus of the National Security Cutters visit was to garner a comparative study between equipment from two similar hulls. The focus of the Naval ship visits was to collect overall vibration data from the ships. The data was gathered with the help of John Donnal, Bart Sievenpiper, Chris Schantz and the coordination assistance of Bob Weaver from NAVSEA. The crews of these ships coupled with the acoustic team from NSWC Carderock was exceedingly helpful in gathering the required data.

2.3.1 US Navy Ship Visits

Three USN ships were visited during this thesis and included the USS INDEPENDENCE, USS SAN DIEGO, and USS MICHAEL MURPHY. Measurements were made and data collected from equipment including fire pumps, ventilation fans, seawater service pumps and chill water pumps as detailed in Appendix 9.1. These ship visits were warranted to gather data on each piece of machinery in their operational environment.

2.3.1.1 USS INDEPENDENCE (LCS 2)



Figure 27: USS INDEPENDENCE (LCS 2) Moored Pierside in San Diego.

The first ship visit was to USS INDEPENDENCE (LCS 2) stationed in San Diego, California. The original plan with this ship visit was to ride the ship during her acoustic trials, but due to the failure of several big pieces of engineering equipment,

the acoustic trials were cancelled. However, the ship still got underway and was able to accommodate us for the accelerometer testing both inport and underway.

Accelerometers were installed on Friday, July 6, 2012 while the ship was pierside. They were turned on to get a baseline reading of the pumps inport. They were then shut off until Monday, July 9, 2012. Before getting underway on Monday, July 9, 2012, each of these accelerometers were turned on and left on for the duration of the underway time. On Wednesday, July 11, 2012, they were shut off and removed from the fire pumps and structural mounts. Data was then processed and analyzed from the accelerometers.

USS INDEPENDENCE is the second littoral combat (LCS) ship to be constructed by the US Navy and the first trimaran LCS to join the US Navy Fleet. The primary operational objective behind the design of this ship was speed; the faster, the better. The trimaran hull configuration exhibits low hydrodynamic drag, allowing efficient operation on two diesel powered water jets at low speeds, and high speed operations on two gas turbine powered water jets at speeds up to a sustainable 44 knots. The secondary objective was ship automation to reduce manning. Everything from the startup of the engines to the Roomba cleaning the pilot house is automated. The ship was initially designed for only 40 crew members with additional manpower for mission modules and air detachments.

Designed for fast speed and not necessarily quiet maneuvering, the LCS 2 platform primarily falls into ONR's concern for CBM. The INDEPENDENCE, being the first in it's class, has encountered numerous maintenance and equipment failures (mainly due to first-in-class issues however) which could be remedied in the future with an installed vibration detection device. This could prove particularly useful in future INDEPENDENCE class ships after the initial design problems have been solved and normal operational maintenance and equipment upkeep falls upon the shoulders of the few sailors manning the ship. In line with the automation theme, the accelerometers would be able to alert the two to four engineering department sailors to physically inspect the pumps and correct the problems in a timely, but not operationally-detrimental, timeframe.

LCS 2 has three fire pumps overall, with only one online during normal underway steaming. All three fire pumps are hard mounted to the deck close to the hull in engineering spaces and any noise from the pumps directly resonates to the sea. Each centrifugal pump is rated at 150 HP, 440 V, 3 phase power at 60 Hz and rotates at 3470 rotations per minute. Vibrations in these fire pumps are of particular interest since they are among the largest pump systems on board and interface directly with the ocean. There are no resilient mounts or any form of damping on the pumps or appendages of the pump leading to the sea similar to this sea water pump seen in Figure 28.

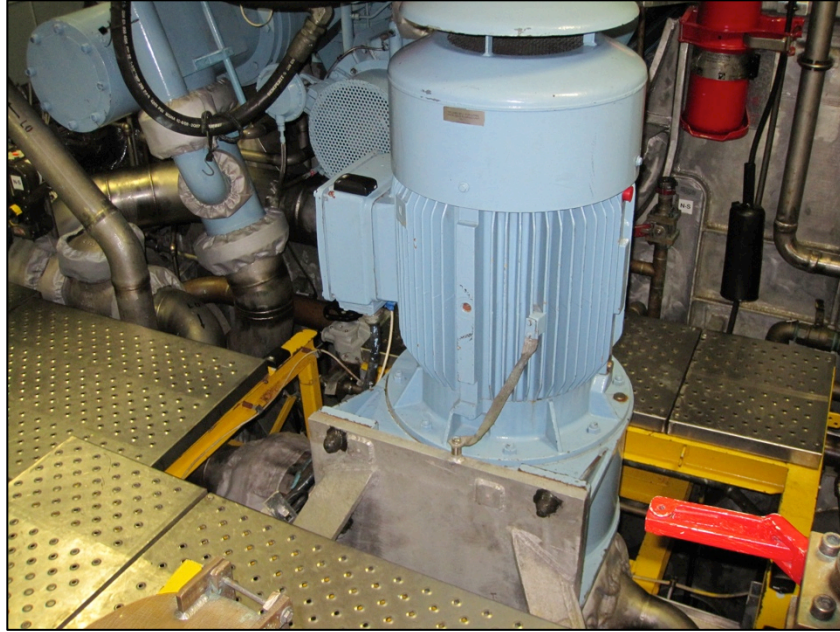


Figure 28: Hard-mounted Sea Water Service Pump on USS INDEPENDENCE.

2.3.1.2 USS SAN DIEGO (LPD 22)

The second ship visit conducted was to the USS SAN DIEGO stationed in San Diego, CA from October 1 through 3, 2012.



Figure 29: USS SAN DIEGO (LPD 22) Off the Coast of San Diego, CA [25].

Following the commissioning of each US Naval combatant, a series of tests and trials are conducted on the ship to verify sea worthiness and deployment ready. In October of 2012, the LEES research team traveled out to San Diego and San Clemente Island, California in Figure 30 to participate in the Acoustic Trials for the USS SAN DIEGO. During these trials, the team again tested the CAPTCHA accelerometers on the LPD 22's fire pumps for vibration and structure borne vibration. Prior to getting underway, the accelerometers were placed on board and turned on. Each day of the trials, the accelerometers were verified for functionality

or moved if a team member deemed one pump to be more interesting than the others.



Figure 30: San Clemente Island, CA the US Navy's Base for Acoustic Trials and Testing [26].

USS SAN DIEGO is the sixth amphibious transport dock in the SAN ANTONIO LPD 17 class of ships. With a ship's crew of roughly 340 sailors, the SAN DIEGO can transport equipment, up to 500 Marines, Marine Air detachments, and landing crafts. LPD 22 was designed to transport mass quantities of people and goods at slower speeds (up to 22 knots) from one place to the next for the US Navy and Marines [25]. She was commissioned in May 2012 to the US Navy Fleet. Due to the missions of the LPD 22, ONR should primarily be concerned with the CBM ramifications of vibration monitoring. The ship is not solely focused on being quiet, but rather operationally dependable for transporting troops. They do, however, have vibration isolation mounts on each fire pump the discharge piping is angled to disperse noise even more as seen in Figure 31 and Figure 32.

There are ten fire pumps onboard USS SAN DIEGO located in each Main Engine Room and Auxiliary Space. Each centrifugal fire pump is rated at 150 HP, 440 V, 175 Amps, and is 3 phase power at 60 Hz. The pumps rotate at 3570 rotations per minute with a minimum efficiency of 0.97.

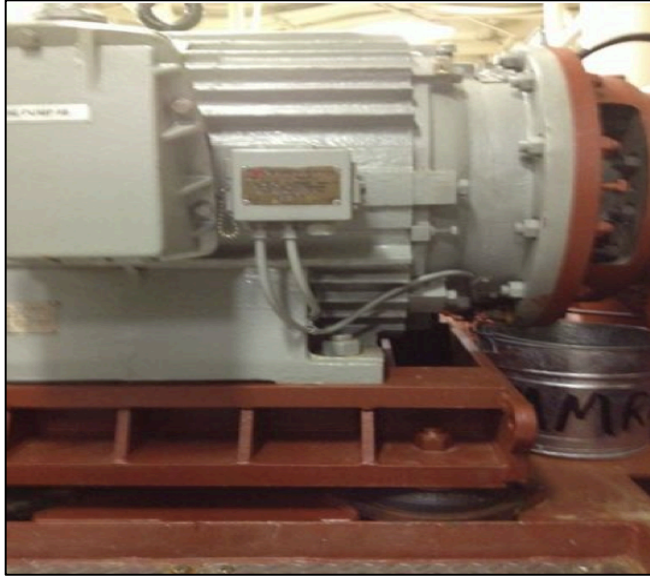


Figure 31: Vibration Isolation Mounts on Fire Pump 1 on USS SAN DIEGO.

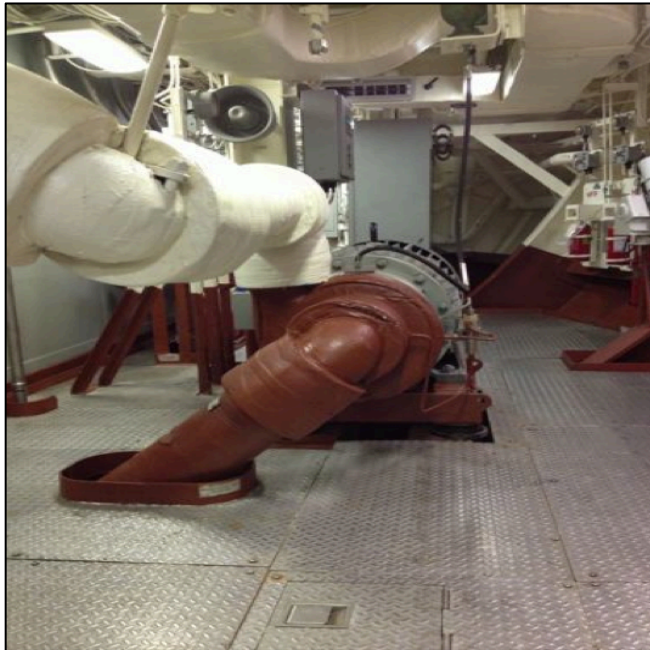


Figure 32: Angled Discharge Piping on a USS SAN DIEGO Fire Pump.

2.3.1.3 USS MICHAEL MURPHY (DDG 112)

The third and final US Navy ship visit was the USS MICHAEL MURPHY (DDG 112) seen in Figure 33 from November 11th through the 14th in 2012. Data was collected in port on November 11th and underway during the Acoustic Trials the following week.



Figure 33: USS MICHAEL MURPHY (DDG 112) at Sea During Her “Super Trial” Completed on March 9, 2012 [27].

USS MICHAEL MURPHY (DDG 112), named for the Medal of Honor recipient, is the 62nd ship in the DDG 51 ARLEIGH BURKE class of destroyers. The DDG 51 class of ships are multi-mission combatants designed to operate in multi-threat air, surface, and subsurface threat environments [27]. Utilizing a gas turbine propulsion system, USS Michael Murphy can operate independently or as part of carrier strike groups, surface action groups, amphibious ready groups, and underway replenishment groups [28]. With the latest in weapon systems, engineering, and technology, the MICHAEL MURPHY was designed for speed as well as combat effectiveness. Additionally, to meet the ship’s missions, it was enhanced with noise reduction gear through the ship such as more robust vibration isolation mounts as seen in Figure 34.



Figure 34: Robust Vibration Mounts on Fire Pump #1 on USS MICHAEL MURPHY.

Unlike the LCS 2 and LPD 22, ONR is particularly interested in the acoustic noise that radiates from equipment on the DDG 112 to the sea. The DDG 112 was built,

like all ARLEIGH BURKE Destroyers, to suppress as much noise as possible to dampen ambient sounds during vital operations.

There are six fire pumps on the MICHAEL MUPRHY located in the main engine and auxiliary spaces. The fire pumps are of the same model as the fire pumps seen on the LCS 2 and LPD 22 rated at 150 HP, 440 V, 175 Amps, and has 3 phase power at 60 Hz. The crew on DDG 112 cycled the pumps on November 11, 2012 while the ship was in port, allowing the accelerometers to pick up pump transients and analyze the pumps in a calm, steady state. The accelerometers were turned off following the inport testing and only turned on again the morning of November 13, 2012 when the ship got underway. Once underway, the accelerometers were left on until the Acoustic Trials were over on the afternoon of November 14, 2012.

2.3.2 US Coast Guard Ship Visits

Over the past year, three different USCG ships were visited to gather diagnostic and comparative measurements on various engineering equipment found in Appendix 9.1. Diagnostic data was gathered from the USCGC SENECA, while running and transient measurements were taken from two National Security Cutters, USCGC BERTHOLF and USCGC STRATTON.

2.3.2.1 USCGC BERTHOLF (WMSL-750) and USCGC STRATTON (WMSL-752)

The USCGC BERTHOLF is the first of the Legend Class National Security Cutters for the Coast Guard. She, along with the third vessel of its class the USCGC STRATTON, is stationed in Alameda, CA.



Figure 35: All Three National Security Cutters in Alameda, CA.

The NSC is the largest of three new cutter classes in the Coast Guard fleet being introduced as part of the Coast Guard's modernization efforts. The NSC has the

capabilities for feeding, sleeping, berthing, and providing power for the crew, much like a small city or town. There is a gas turbine and two diesel engines that operate together to drive the cutter at a top speed of 28 knots. The cutter must be able to reach maximum speed to carry out its operational commitments including law enforcement, pollution response, search and rescue, and a host of other mission.

There are five fire pumps on the BERTHOLF located in the main engine and auxiliary spaces. The fire pumps are different from the US Navy fire pumps as each pump is dry started and can pump up to 1000 GPM. These pumps are rated at roughly 3600 RPM. On January 8 2013, engineering equipment on the BERTHOLF was tested for vibrations including Fire Pump #1, all three chill water pumps, a helo hangar exhaust fan (01-65-0), and two ventilation fans just forward of the wardroom. The following day, the same equipment was tested for vibrations and comparative analysis on the STRATTON, the third in the Legend Class Cutters.

2.3.2.2 USCGC SENECA (WMEC-906)

The final ship visit for this thesis was the USCGC SENECA, stationed in the Boston Harbor, MA as seen in Figure 36.



Figure 36: USCGC SENECA Pierside in Boston, MA [29].

The SENECA serves as a platform for Operation New Frontier, the Coast Guard's operation to employ armed helicopters and non-lethal use of force technology to stop drug laden, go- fast vessels. SENECA's actions contributed to the one hundred percent interdiction rate during Operation New Frontier, making it the most successful counter-drug operation in Coast Guard history. Additionally, the cutter's advanced technology and high speed capability identifies the SENECA as an effective Search and Rescue (SAR) and Maritime Law Enforcement (MLE) platform [29].

The SENECA was visited on March 20 and March 29, 2013. During the first visit, data was collected on induced imbalance vibrations on two supply fans while the ship was in port. The supply fans were the forward ventilation fan under the bridge, Figure 37, and the aft HVAC supply fan for the armory, Figure 38. The second trip to the SENECA included monitoring the same fans for vibrations incurred from loose mounts and clamping the mounts or “shorting” the mounts.



FWD Ventilation (02-53-1)
3450 RPM
60 Hz
Single Phase
115 V

Figure 37: Forward Ventilation Fan Under the Bridge on the USCGC SENECA.



AFT HVAC Supply Fan (2-208-1)
3600 RPM
60 Hz
Three Phase
440 V

Figure 38: Aft HVAC Supply Fan on USCGC SENECA.

3.0 Experiment Equipment & Analysis Tools

3.1 Commercial-Off-The-Shelf

In order to validate the accelerometers developed in the LEES laboratory, commercial-off-the-shelf (COTS) accelerometers were also used to measure the vibrations of the ships' equipment. The COTS accelerometers used were the Gulf Coast Data Concepts, LLC USB Accelerometer X6-1A (GCDC) seen in Figure 39. These accelerometers utilize low noise digital accelerometer sensor coupled with real-time data stamps to measure vibrations. They are capable of measuring 3 axis (X, Y, Z) vibrations at a sample rate of up to 200 Hertz. The Gulf Coast Accelerometers can have either 12 or 16 bit resolution. They are powered by standard "AA" alkaline or lithium batteries for longer recording time and write data to removable microSD cards. A simple pushbutton start signified by a blinking LED begins data collection and the same pushbutton is used to stop recording data. When connected via the USB to a personal computer, the accelerometer appears as a standard mass storage device containing the comma delimited data files and user setup files. Once downloaded, the data .CSV files are easily imported to other processing software, including MATLAB.

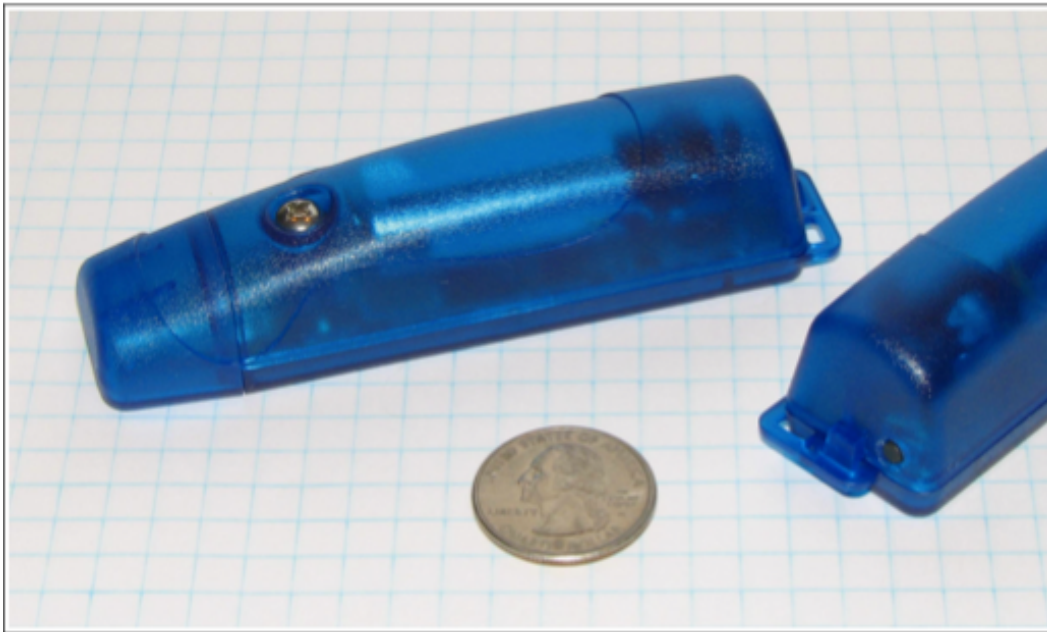


Figure 39: Gulf Coast Data Concept, LLC USB Accelerometer X6-1A [30].

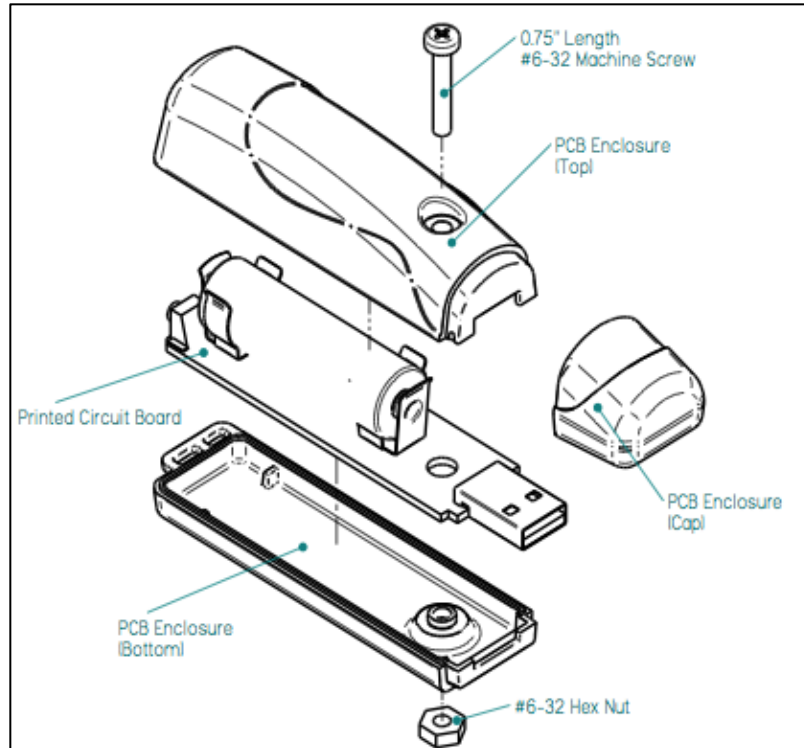


Figure 40: Exploded View of GCDC Accelerometer [30].

For these experiments, the GCDC accelerometers were affixed to the terminal box of the equipment via 3M double-sided foam tape. The point of contact was cleaned first with alcohol swabs, wiped dry, and then affixed with the GCDC Accelerometer with the tape.

3.2 CAPTCHA: Accelerometers Developed in the LEES Lab

The primary, lab-developed accelerometers or CAPTCHAs used during these experiments were designed to measure 3 axis (X, Y, and Z) vibrations. Vibrations are sampled at 3.2 KHz using these accelerometers, considerably more than the GCDC accelerometers. . The current iteration is a low power battery operated package seen in Figure 42 and Figure 42. With the self-power harvesting iteration still in the design phase, these accelerometers were custom designed for long-term vibration monitoring with triple the battery power as the GCDC accelerometers. Like the GCDC accelerometers, the CAPTCHA accelerometers record data via a microSD card. The data, however, can only be transferred to a personal computer via a python program developed by John Donnal and Jim Paris, which converts the data into .txt files. These files can then be easily read into processing software such as MATLAB.



Figure 41: CAPTCHA Accelerometer with Triple Battery Power.

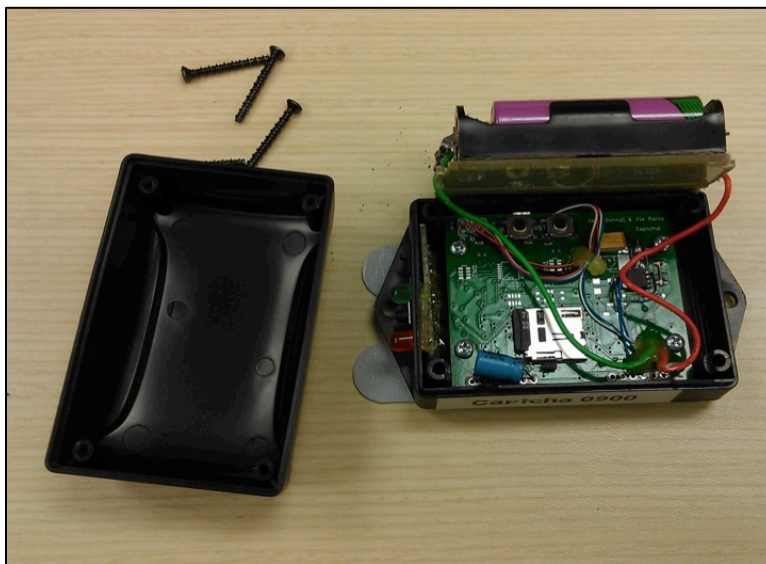


Figure 42: Internal Circuit Board of a CAPTCHA Accelerometer.

During the experiments, each CAPTCHA was adhesively taped on the top of the terminal box via command strips to simulate the location of the future self-power harvesting accelerometer, which will be mounted inside the terminal box of the equipment. CAPTCHAs were also foam mounted adhesively to structures connected to the equipment in order to collect any external or structural borne vibrations.

3.3 MATLAB Whisker Diagnostic Tool

Initially, raw time- series acceleration graphs were generated to depict the differences between testing scenarios. For example, Figure 43 and Figure 44 demonstrate the runs created in the Lab during a baseline run and an imbalance-induced run when a wire was wrapped around a single rotor blade. From these

graphs, it is clear to see that the maximum acceleration of the wire wrapped fan (612.8) is much greater than the baseline fan (232.5). However, beyond recognizing an increase in vibrations, these graphs do not convey much at the moment. The increases in accelerations and vibrations are expected, but do not correlate the vibrations to the known problem, the imbalance due to the wire.

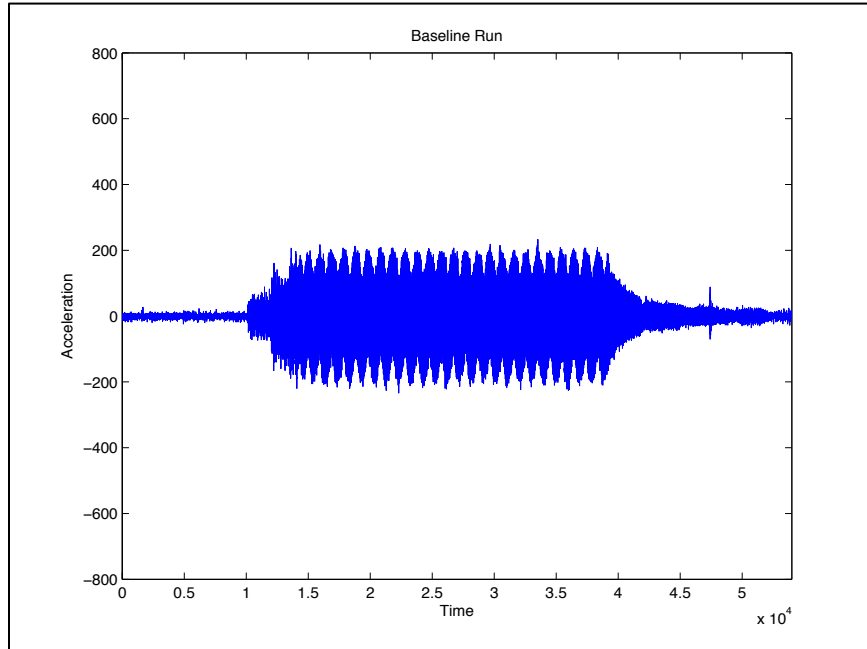


Figure 43: Baseline Lab Test (Appendix 9.2.4).

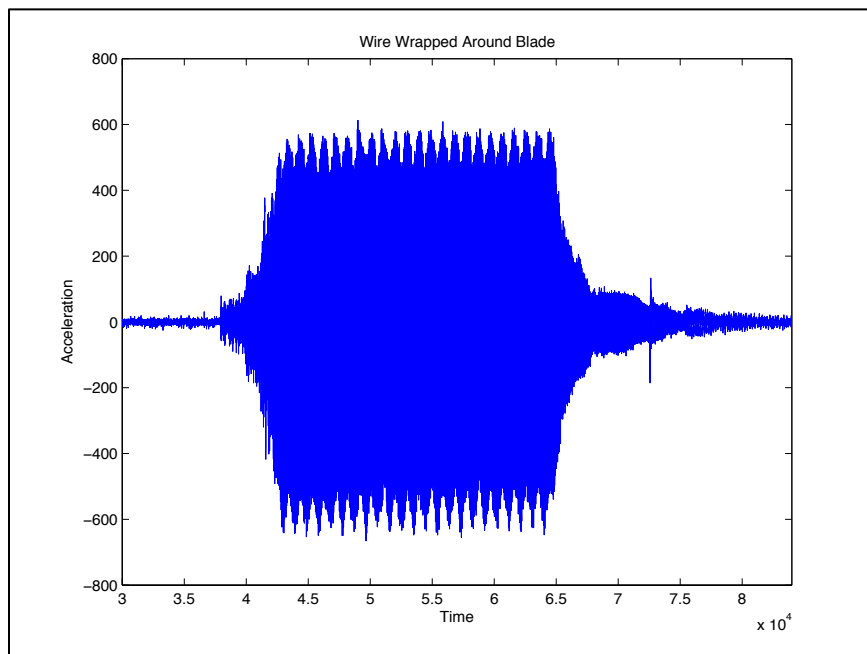


Figure 44: Wire Wrapped Around Fan Blade in Lab (Appendix 9.2.4).

To determine the specific signature or unique characteristic of particular vibration sources, a numerically comparative solution was needed. VAMPIRE proposed that

the difference in vibration sources could be seen in the spin-down of the motor. To test this theory, the spectrum of vibration frequencies was analyzed from both tests during the motor spin-down. The most common format of a spectrogram is a graph with two geometric dimensions: the horizontal axis represents time, the vertical axis is frequency; a third dimension indicating the amplitude of a particular frequency at a particular time is represented by the intensity or color of each point in the image. In this case, a 2-D graph was created with the change in color representing the intensity of vibration at each point.

In MATLAB, the spectrogram function returns the short-time Fourier transform of the input signal and a matrix P containing the power spectral density (PSD) of each segment. For each real segment, P contains the one-sided modified periodogram estimate of the PSD of each segment. The elements of the PSD matrix P are given by $P(i, j) = k|S(i, j)|^2$ where k is a real-valued scalar defined as

$$k = \frac{2}{F_s \sum_{n=1}^L |\omega(n)|^2} \quad (1)$$

where $w(n)$ denotes the window function (Hamming by default) and F_s is the sampling frequency. At zero and the Nyquist frequencies, the factor of 2 in the numerator is replaced by 1.

Figure 45 depicts the entire spectrogram for the two tests run in the lab in the Z direction during the motor spin-down. Each direction, X, Y, and Z, were analyzed, but the Z direction showed the greatest difference in vibration between the two tests. The graph on the left is the baseline test while the graph on the right shows wire wrapped around the fan. The darker colors (yellow, orange, and red) on the right demonstrate the increase in intensity on the fan due to the wire.

Of particular interest is the tail “whisker” at the bottom of the graphs beginning at the rotational frequency of the fan, 60 Hz. Figure 46 depict the spectrogram after running the data through a low pass filter to focusing on the tail wisp for a more detailed comparison for the Z-Axis. The Z-Axis depicts the radial axis with respect to the rotating shaft in this case and illustrates the worst case scenario, the one when the highest vibrations are experienced by the fan. Even in the worst case scenario, these spectrograms still do not categorize or diagnose the type of vibrations; another tool was needed.

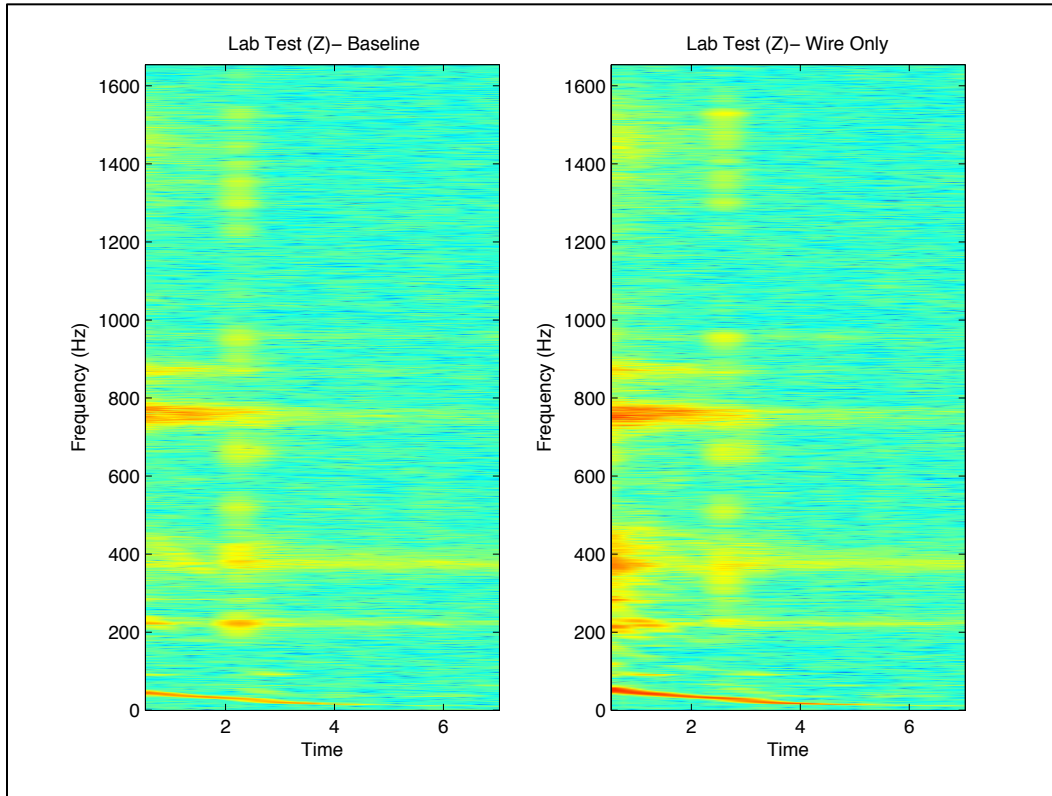


Figure 45: Lab Comparison Between a Baseline Run and a Wire Wrapped Around Rotor Blade on Z-Axis (Appendix 9.2.4).

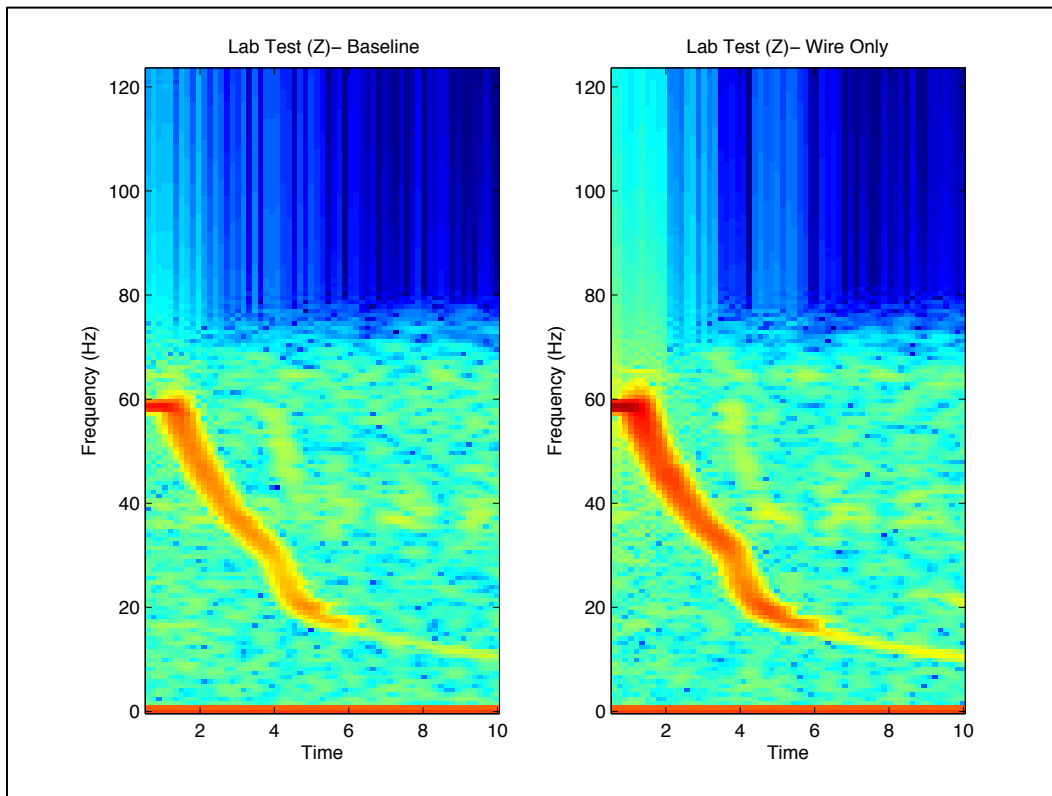


Figure 46: Lab Comparison of Imbalance on a Smaller Frequency Scale on Z-Axis (Appendix 9.2.4).

The MATLAB Whisker Diagnostic Tool was developed by Chris Schantz to analyze the spin-down of the motors. The program is capable of processing data from either a CAPTCHA device or Gulf Coast accelerometer with four columns of data (time, X, Y, and Z axis) or a series of data with two columns (X and Y axis). In addition to the accelerometer data as an initial input, the program requires the nominal rotations per minute (rpm) of the rotating machine and the sampling frequency of the data collection device. If known, the program will also accept the spin down friction parameters as inputs. The spin-down friction parameters govern the rotational energy loss of the motor or machine's shaft during spin down and therefore, can estimate the spin down behavior over time of the machine from the steady state shaft speed at the instant power is turned off. The power off time and initial shaft speed are visually selected by the user via graphical input overlaid on a vibration signal time frequency plot, like that shown in Figure 47. In most cases, the frequency content of the shaft rotation is dominant and near the expected nominal speed of the motor.

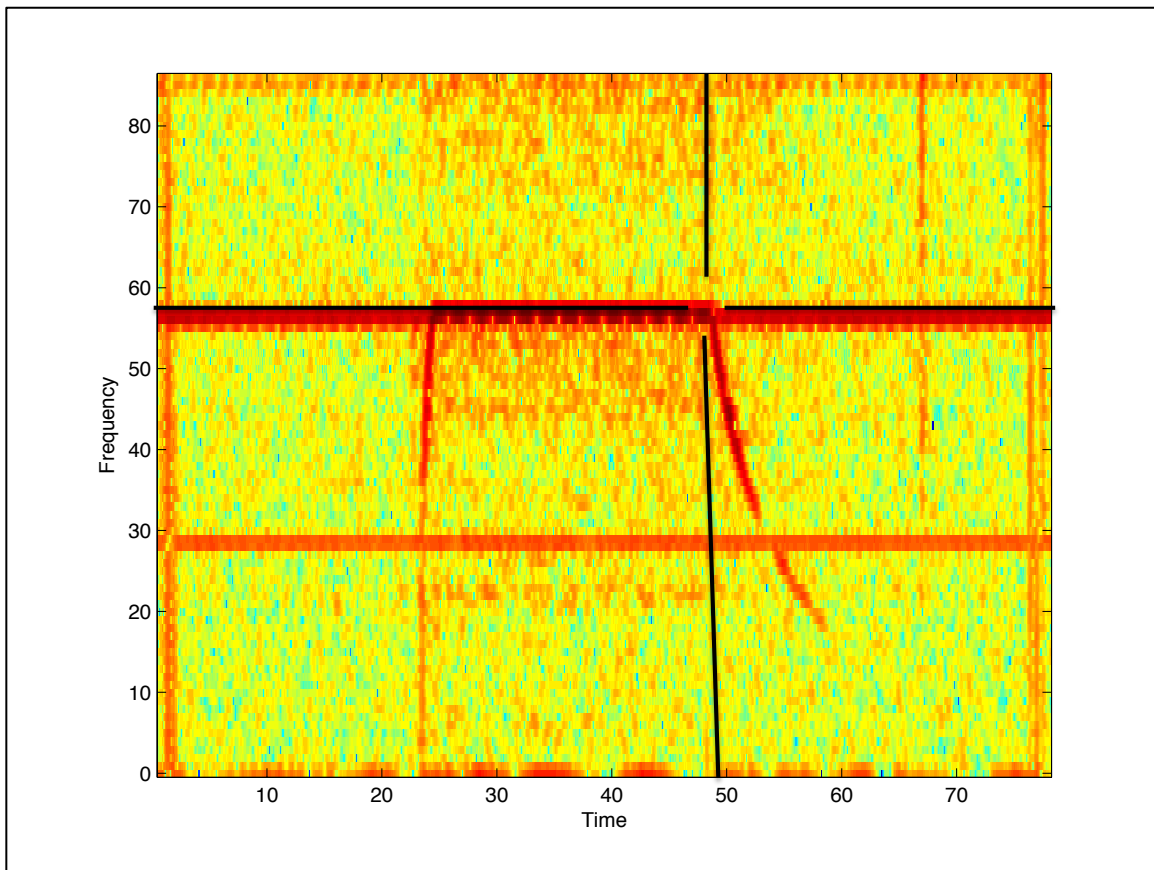


Figure 47: Operational Profile of Motor (Appendix 9.2.2).

If the friction parameters are not known, the function estimates the parameters via a non linear, least squares estimation utilizing a two parameter friction model with both linear and squared friction coefficients shown in Equation 2.

$$\frac{d \omega_r}{dt} = f_1 * \omega_r + f_2 * \omega_r^2$$

(2)

The user is asked to trace out the dominant spin down frequency content in the time frequency plot. The locations of this trace serve as inputs to the friction parameter fitting algorithm shown in Figure 48. Once the parameters are found, an overlaid spin-down curve is plotted on top of the time frequency plot to allow the user to check the accuracy of the spin down estimation. The solid black line in Figure 49 depicts the overlaid spin-down curve. Figure 49 also contains dashed “error bars” on either side of the solid black line estimating the extent of the extracted signal during the filtering step described in the paragraphs below. The friction parameters and user-selected time of power off are outputs of the function to allow for their values to be stored along with the vibration data and facilitate rapid automatic re-processing of the data in the future.

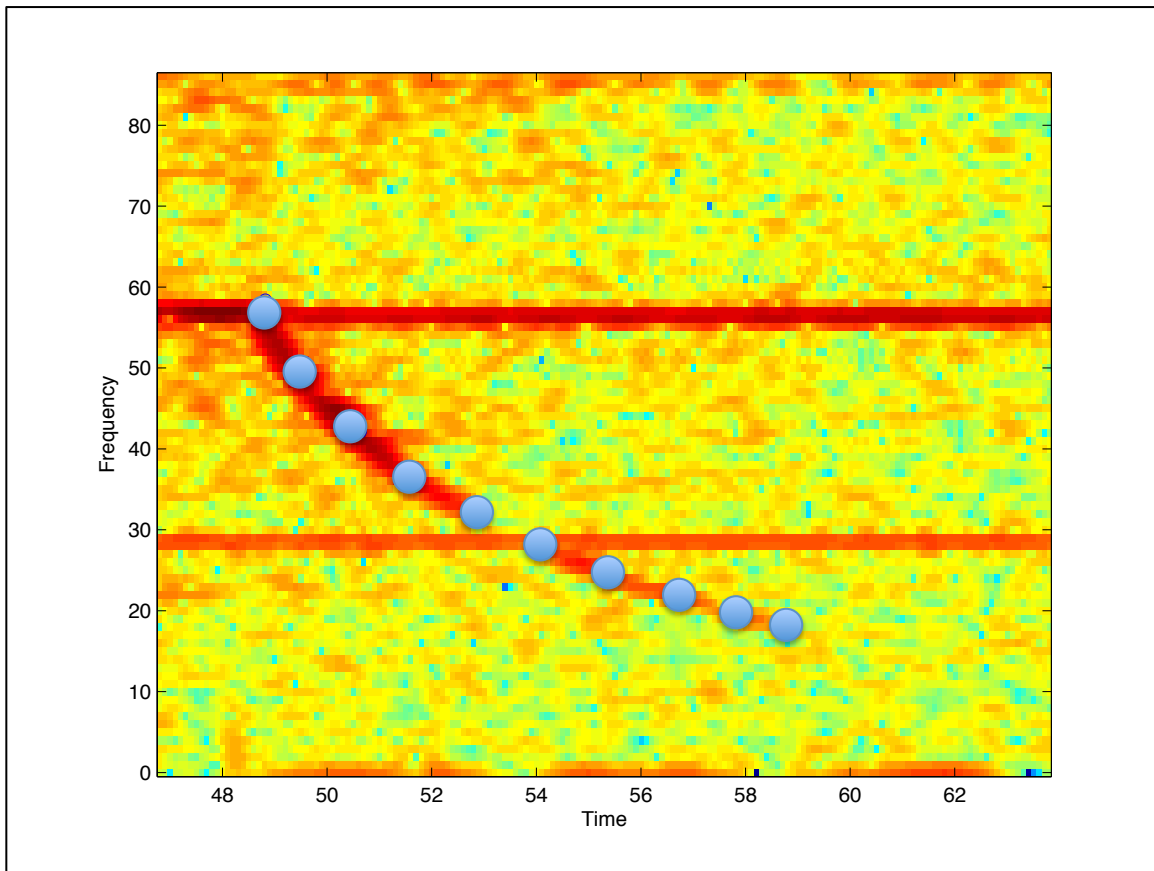


Figure 48: Selecting Points Along the Spin-down (Selection Made by Indication of Blue Dots) (Appendix 9.2.2).

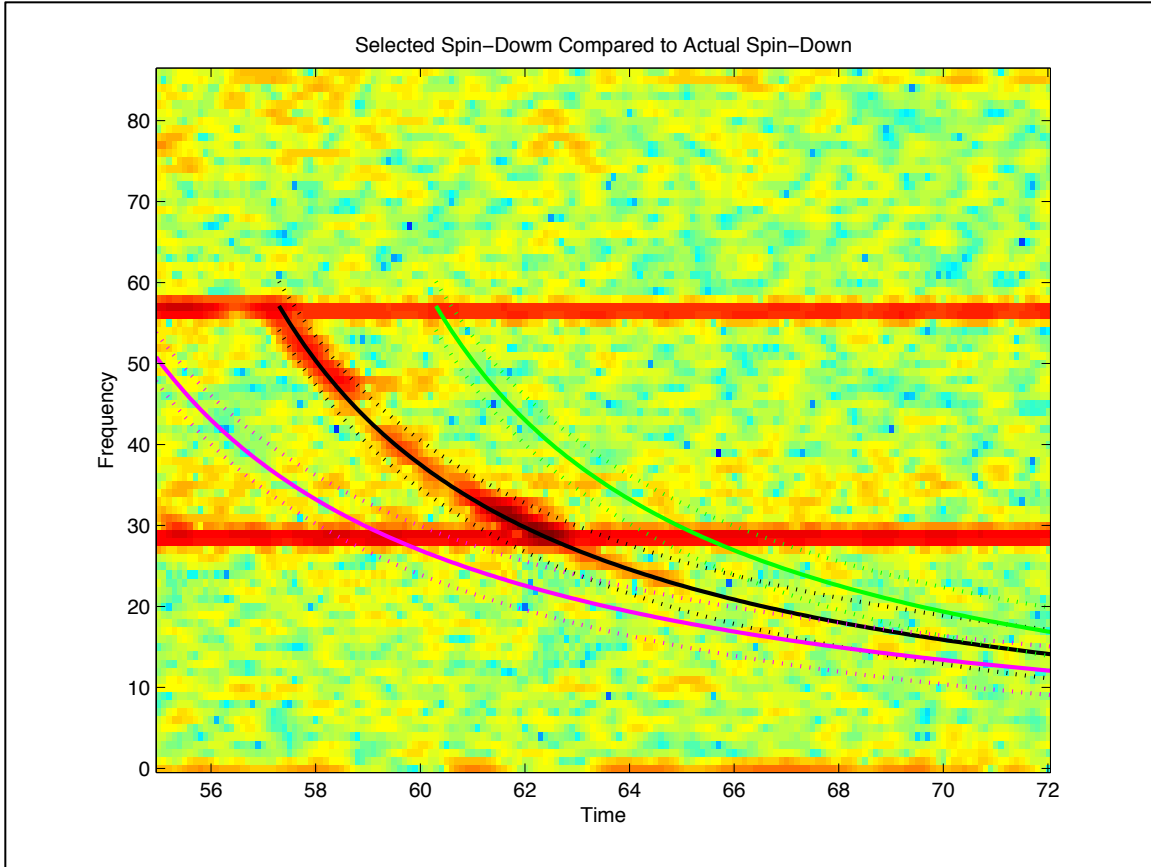


Figure 49: Whisker Tracing for Spin-down with Plus or Minus Three Times the Sampling Frequency (Appendix 9.2.2).

The program implements a time varying band pass filter to remove as much of the vibration signal content as possible not associated with the spin-down of the machine. The variable filtering is conducted by creating a complex mixing signal from the estimated spin-down shaft speed $\omega_r(t)$ via the following formula.

$$m(t) = e^{i \int_0^t \omega_r(\tau) d\tau} \quad (3)$$

The vibration signal, starting at the time power is turned off, is multiplied by the mixing signal to create a new complex signal where the vibration content near the instantaneous spin down frequency is near DC. This new signal is then low pass filtered with an FIR filter with cutoff at 3 Hz. Since the data is being block processed, phase neutral “forward backward” filtering is used. Care is taken to deal with filter transients by appending signal data of length equal to the size of the filter before and after the spin down signal region, and then removing these data points after filtering.

After filtering, the complex signal is then divided by the mixing signal to recover what is termed the whisker signal. This whisker signal is complex, which allows straightforward amplitude envelope extraction via the absolute value function.

Plots of example whisker amplitude envelopes versus spin-down shaft speeds are shown in Figure 50.

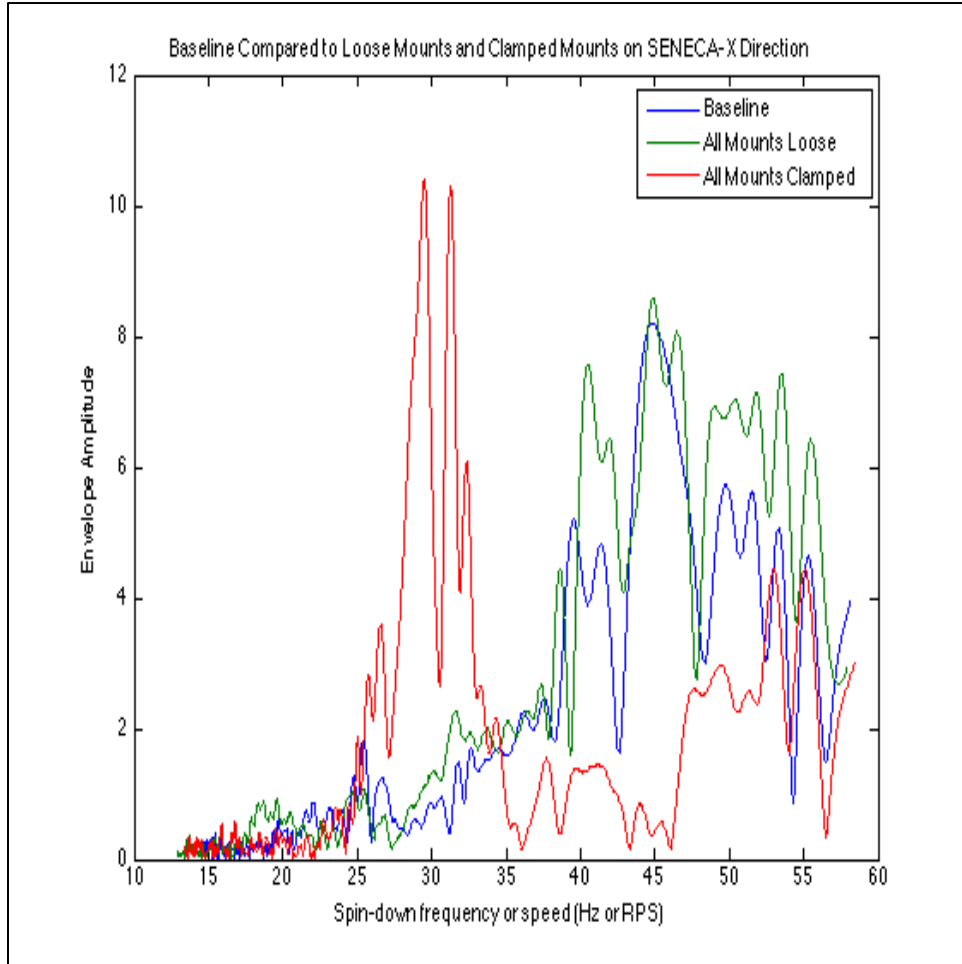


Figure 50: Fundamental Spin-down Diagnostic Graph Comparing a Baseline Run to Loose and Clamped Mount Scenarios (Appendix 9.2.2).

Pre and post whiskers are also extracted by offsetting the power off time to obtain an estimate of constant contaminating noise present in the environment from neighboring machines. If constant interfering vibration signal content is present in the data during the spin down vibration trace, the user can gain a measure of the extent of the signal contamination by examining these pre and post whiskers' amplitude envelopes. For example, in Figure 50 an external, interfering vibration can be seen on the clamped mounts scenario around 30 Hz. This spike can then be attributed to other equipment and disregarded during analysis.

4.0 Diagnostic Lab Tests

Prior to testing the CAPTCHAs on an actual ship, they were tested in the lab on two coast guard ventilation fans to determine if they could record vibration data and if the use of the MATLAB whiskers diagnostic tool could lead to the differentiation between types of vibrations- ie- imbalance and loose mounting. These tests were done in collaboration with Chris Schantz.

4.1 Rotor Imbalance

The most common type of vibration seen in machinery on USN and USCG ships is an imbalance. In order to simulate an imbalance in the lab, a wire was wrapped around one of the blades of the coast guard fan. The wire added weight to a single blade and created an imbalance as the fan turned.

Experimentally, the fan was first run without any alteration to get a baseline reading of the vibrations created by the operation of the fan. The CAPTCHA was placed on the side of the test fan as seen in Figure 51 using command strips as seen in Figure 52. The axis orientation for the CAPTCHA is seen in Figure 53.

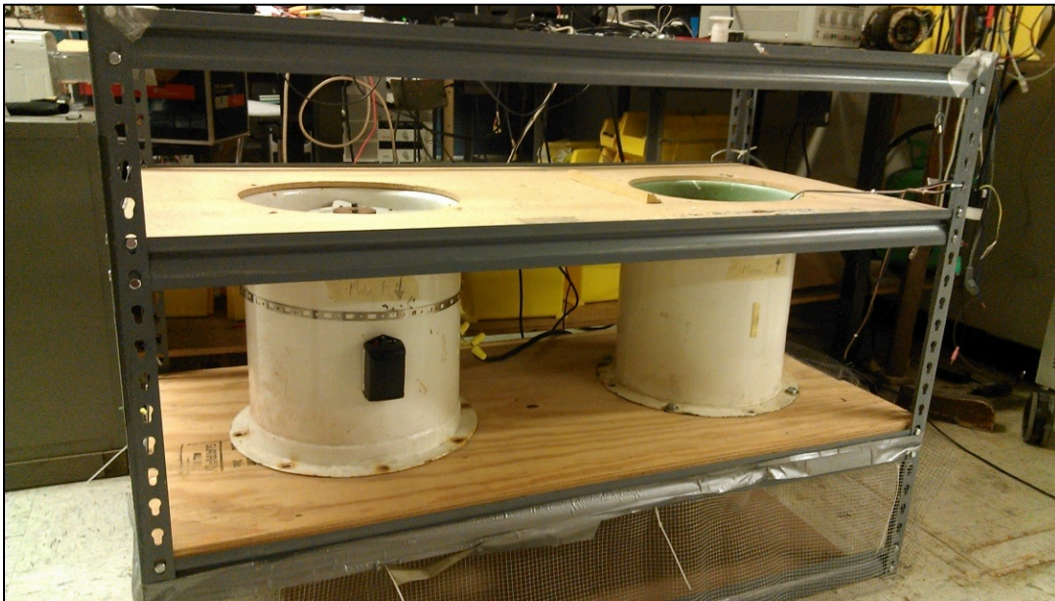


Figure 51: CAPTCHA Attached to Side of Fan with Command Strips.



Figure 52: CAPTCHA Attaches to Equipment Via Command Strips.

Lab Fan Side View

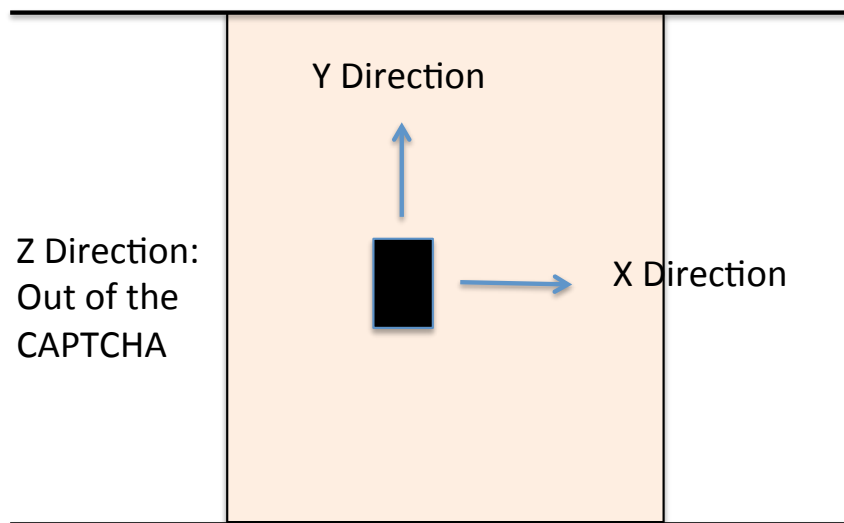


Figure 53: Axis Orientation on the CAPTCHA for the Lab Tests (Side View of Fan).

Once the baseline test was complete, a wire was wrapped around a single fan blade as seen in Figure 54 to incite an imbalance in the fan.

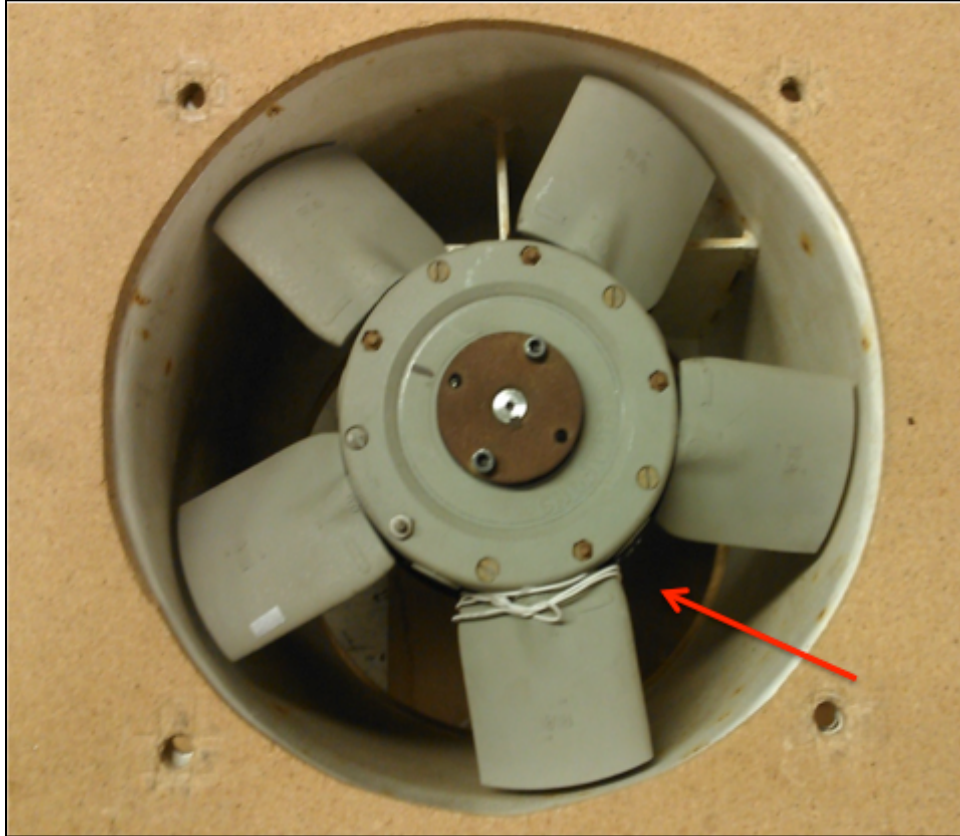


Figure 54: Wire Wrapped Around Single Fan Blade (See Red Arrow).

Data was then downloaded from the CAPTCHA and analyzed using the MATLAB whisker diagnostic tool as seen in Figure 55. Depicting the spin-down in the X-direction of the lab fan, these results reinforce the original concepts proposed in the VAMPIRE paper showing that an imbalance is excited throughout the spin-down. The green line, the fan with the wire wrapped around the blade, maintains a higher vibration amplitude throughout each spin-down frequency.

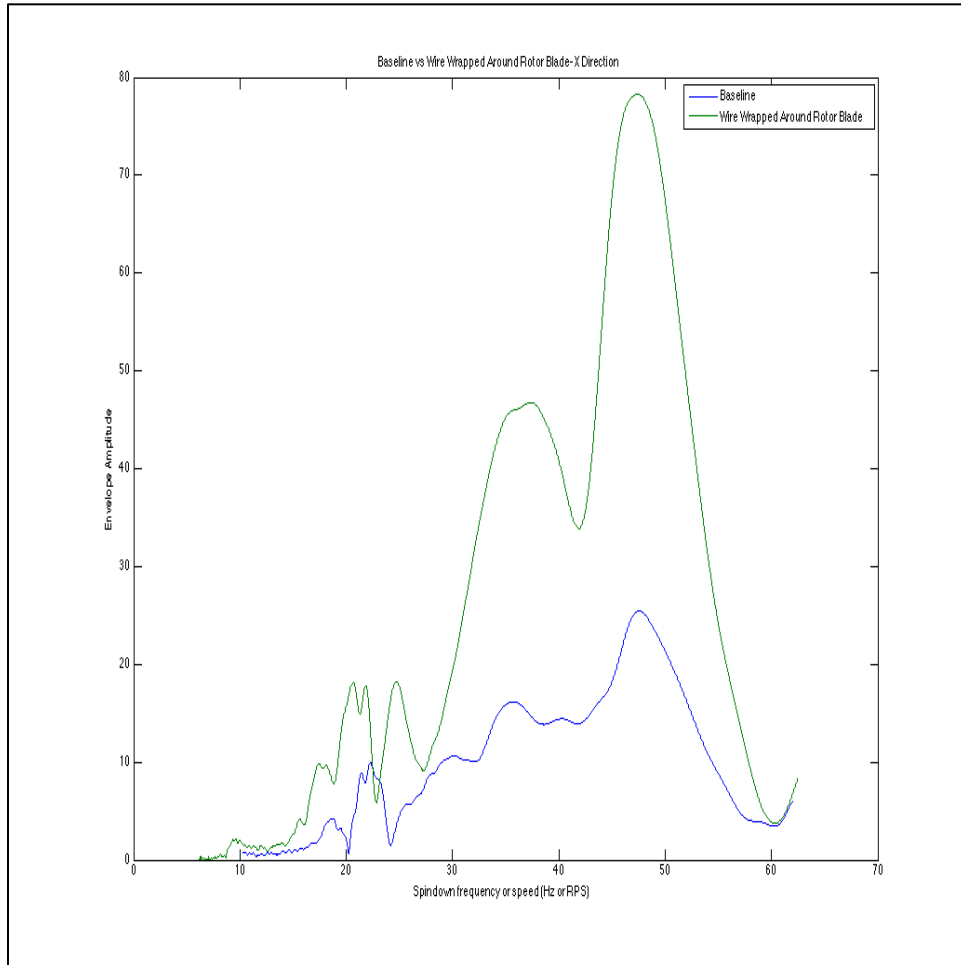


Figure 55: Baseline Run Compared to a Wire Wapped Around a Single Rotor Blade- 29 MARCH 2013 (Appendix 9.2.4).

4.2 Loose Mounts

The most common external source of vibration in machinery on USN and USCG ships is a loose mount. To simulate this in the lab, the coast guard fan used in the previous experiment was used again. This time, however, no wire was present to impede the blade. The mounting bolts seen in Figure 56 were removed one at a time to measure the increase in vibration. Four tests were run on these fans to induce a loose mount scenario on March 29, 2013 as outlined in Table 1. A second series of tests, Table 2, were also run on April 5, 2013 to determine if loosening the mounts could produce the same spin-down affects as the removed mounts and to simulate the exact tests used for the VAMPIRE paper.

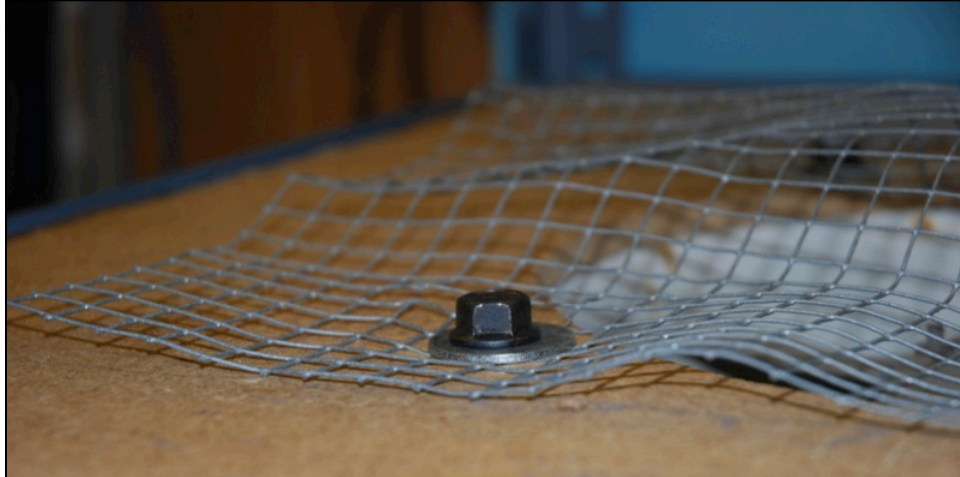


Figure 56: Corner Mounting Bolt on a Lab Test Fan.

Test #	Experimental Set-Up
1	Baseline- All Bolts Tightened
2	One Bolt Removed
3	Two Bolts Removed
4	All Bolts Removed

Table 1: Experiments Conducted on Lab Fan to Induce a Loose Mount Scenario-29 MARCH 2013.

Test #	Experimental Set-Up
1	Baseline Run on Motor 1, Motor 2 off
2	Baseline Run on Motor 2, Motor 1 off
3	All Four Bolts Loose on Motor 1, Motor 2 off
4	All Four Bolts Loose on Motor 1, Motor 1 off, Motor 2 on
5	All Four Bolts Removed on Motor 1, Motor 1 on, Motor 2 off
6	All Four Bolts Removed on Motor 1, Motor 1 off, Motor 2 on

Table 2: Second Set of Tests Run on Coast Guard Lab Fan- 5 APRIL 2013.

Figure 57 shows motor 1 with all four bolts removed, thereby creating the most extreme loose mount condition. As the lab fan is mounted to a steel frame only, the bolts completely removed allowed the fan the greatest opportunity to move while in operation.

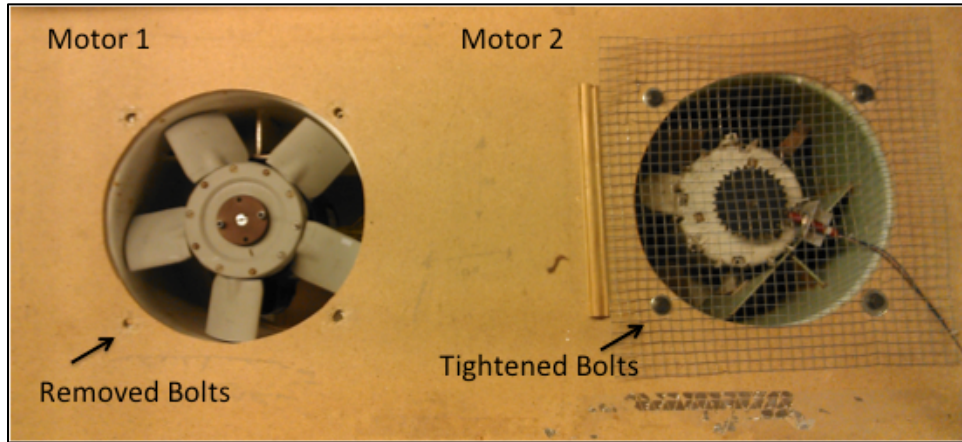


Figure 57: Lab Fans Configured with All Four Bolts Removed on Motor 1.

In an effort to find a signature distinct to a loose mount, the same analysis was conducted on the mounting tests as previously applied to the imbalanced fan. Initially, a time-series comparison was conducted to see if there was a basic, amplitude difference between fan acceleration during steady state. Figure 58 depicts the time-series comparison in the X-direction between the baseline run and all four mounts loosened, the worst-case scenario for loose mounts. As it is not abundantly clear that the amplitudes of vibrations are larger for the loose mounts, the Z-direction was also graphed to ensure ample distinction between the two cases in Figure 59.

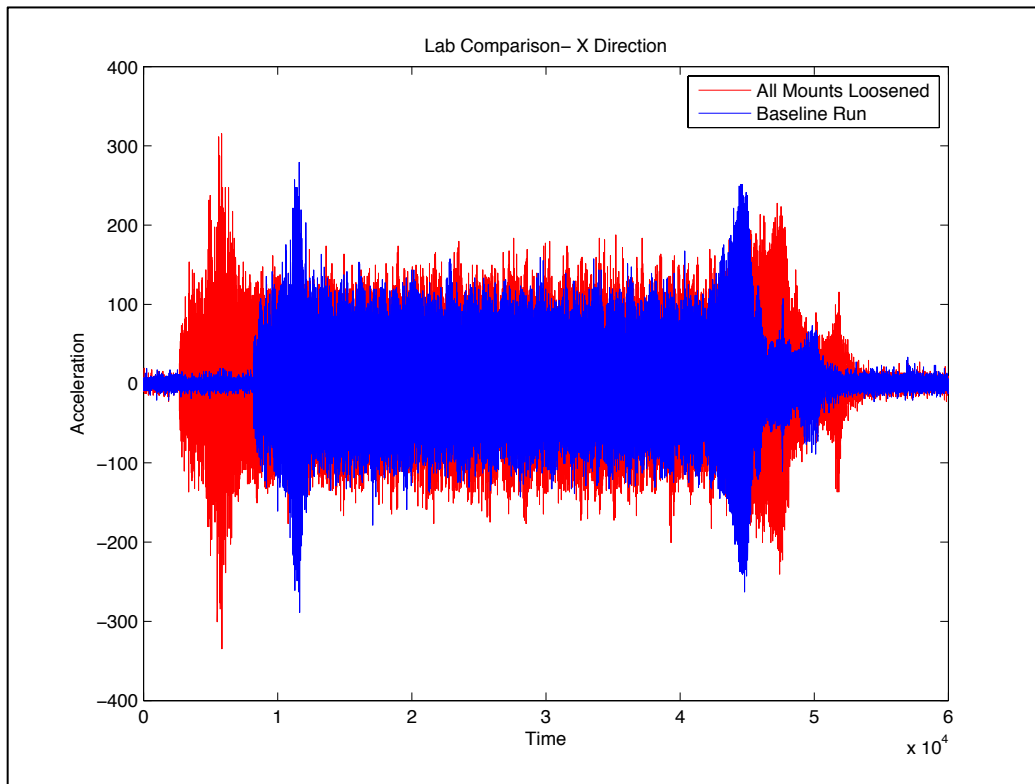


Figure 58: Time- Series Lab Comparison of Baseline Fan and Loose Mounting in X Direction (Appendix 9.2.4).

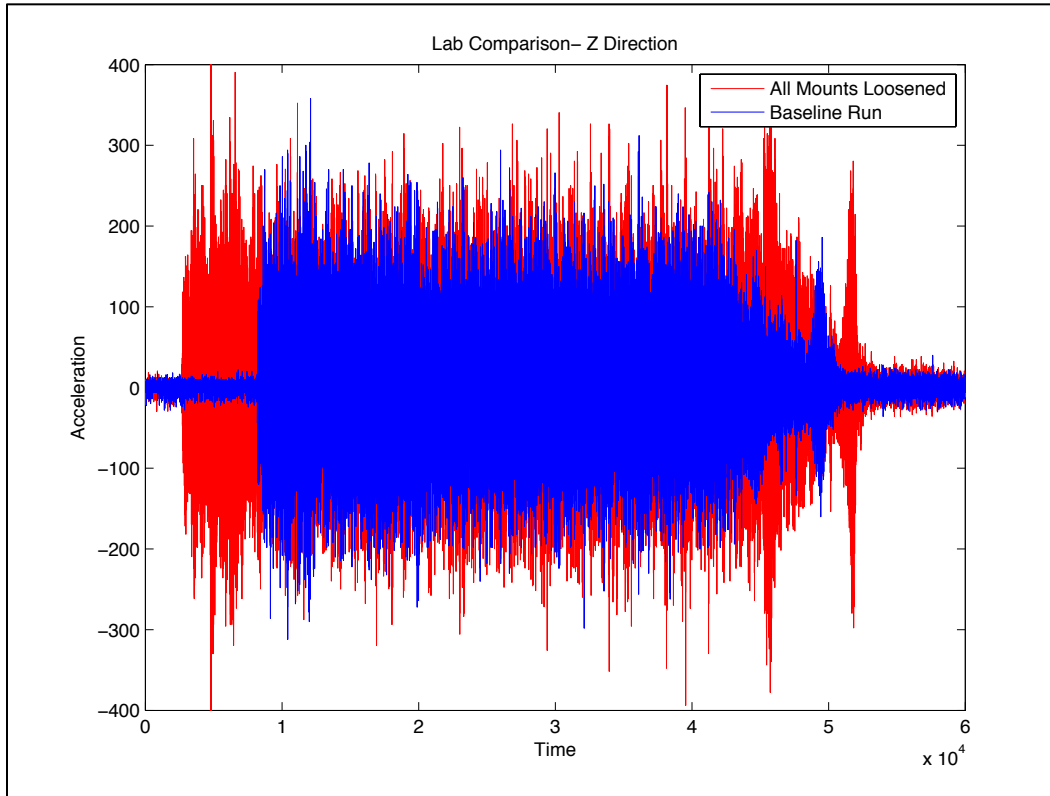


Figure 59: Time- Series Lab Comparison of Baseline Fan and Loose Mounting in Z Direction (Appendix 9.2.4).

Both of these graphs, once again, reinforce the VAMPIRE paper findings, which state that during steady state, the vibration amplitudes are higher for loose mounts (and imbalanced fans).

Once vibration differences were deemed discernable for the loose mounts, a spectrogram in the Z-direction was created for the spin-down of the baseline fan condition and the worst-case scenario of all four mounts loose as seen in Figure 60 and Figure 61. The CAPTCHA was oriented in the same direction as the wire imbalance test and thus, the Z direction demonstrated the most vibrations.

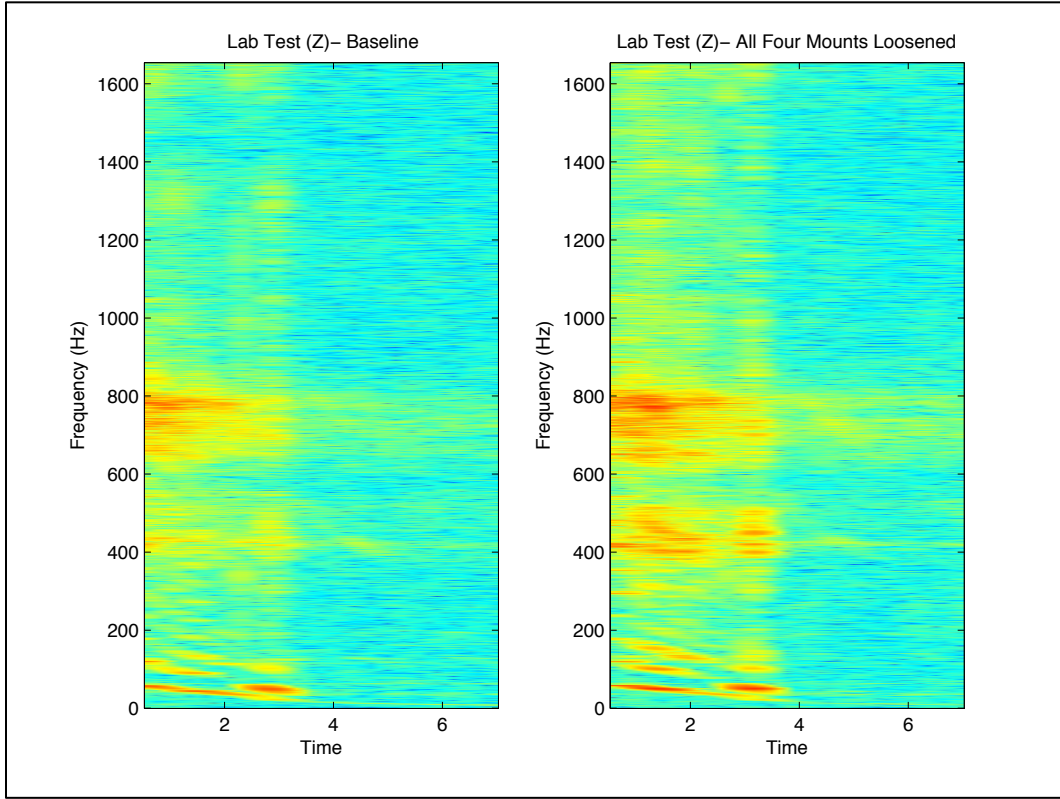


Figure 60: Lab Comparison Between Baseline Run and Four Loose Mounts (Appendix 9.2.4).

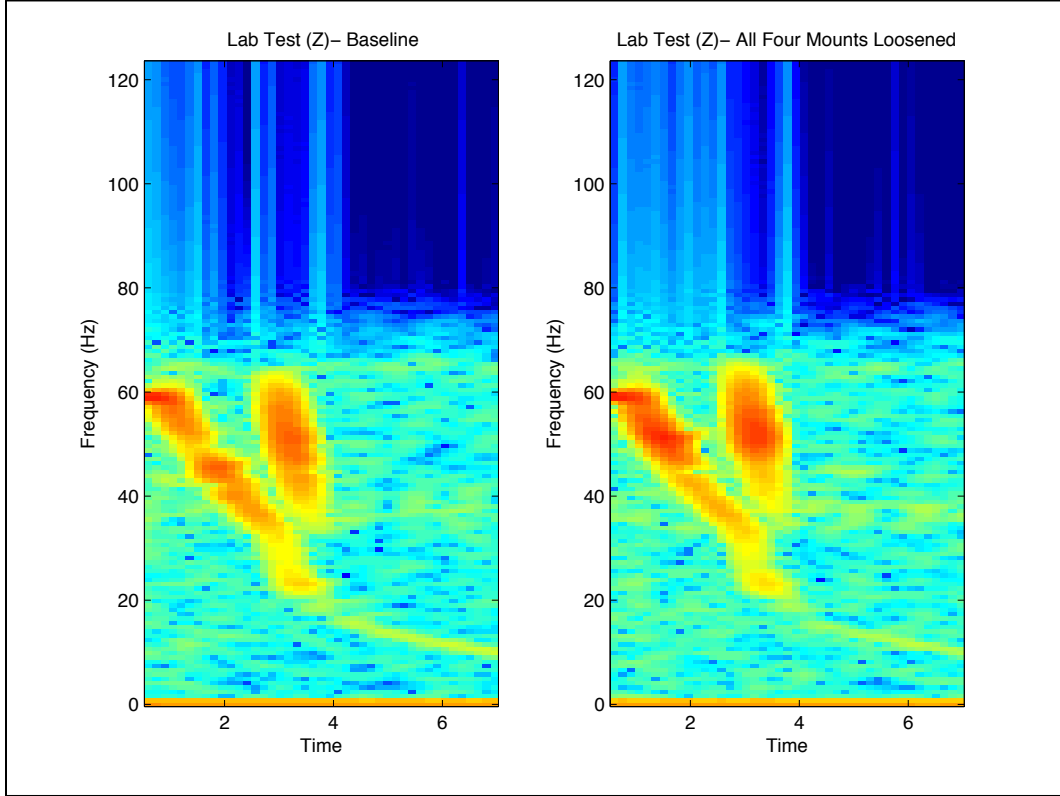


Figure 61: Lab Comparison Between Baseline Run and Four Loose Mounts Truncated by a Low Pass Filter (Appendix 9.2.4).

With these sets of data, the whisker diagnostic tool was implemented to produce a frequency spin-down graph in Figure 62. In this graph, several observations can be made. First, as expected, only loosening the mounts produces lower vibration amplitudes during spin-down than removing the mounts completely. Second, both the loose and removed mounts (green and red lines) are initially excited upon spin-down, but around roughly 30 Hz begin to blend back in with the baseline vibration signature (blue line). Finally, these findings corroborate the VAMPIRE paper’s findings, establishing that to distinguish between the two types of vibrations, loose mounts and an imbalance, one needs to look at the frequency spin-down of the equipment.

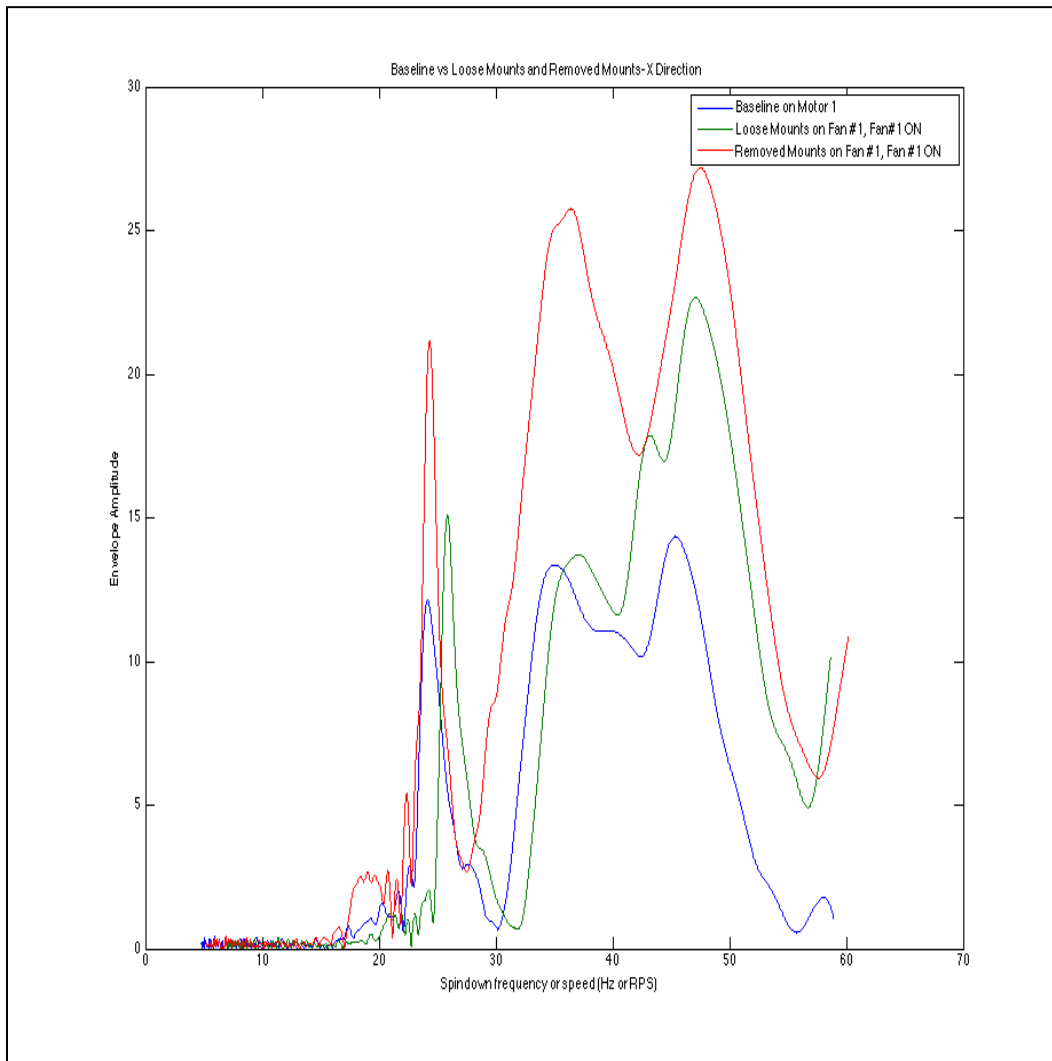


Figure 62: Lab Test Spin-down for Loose Mounts and Completely Removed Mounts- 5 APRIL 2013 (Appendix 9.2.4).

4.3 Comparison

In order to discretely compare the vibration sources, Figure 63 and Figure 64 shows the whisker diagnostic tool of both a loose mount scenario and an imbalanced fan scenario in the X-direction. Each test was run on two different motors so there are

two different baselines in these graphs. The effects of loose mounts can be seen on the left while the imbalanced fan can be seen on the right. The imbalanced fan is excited throughout the spin-down while the loosely mounted fan is more damped during spin-down. The spike in the 30 Hz area in the loosely mounted fan spin-down is attributed to an external source of vibration in the lab; another motor in the lab was on while the tests were being conducted. These results strengthen the arguments made in the VAMPIRE paper and lead to the tests run on Naval and Coast Guard vessels for further substantiation.

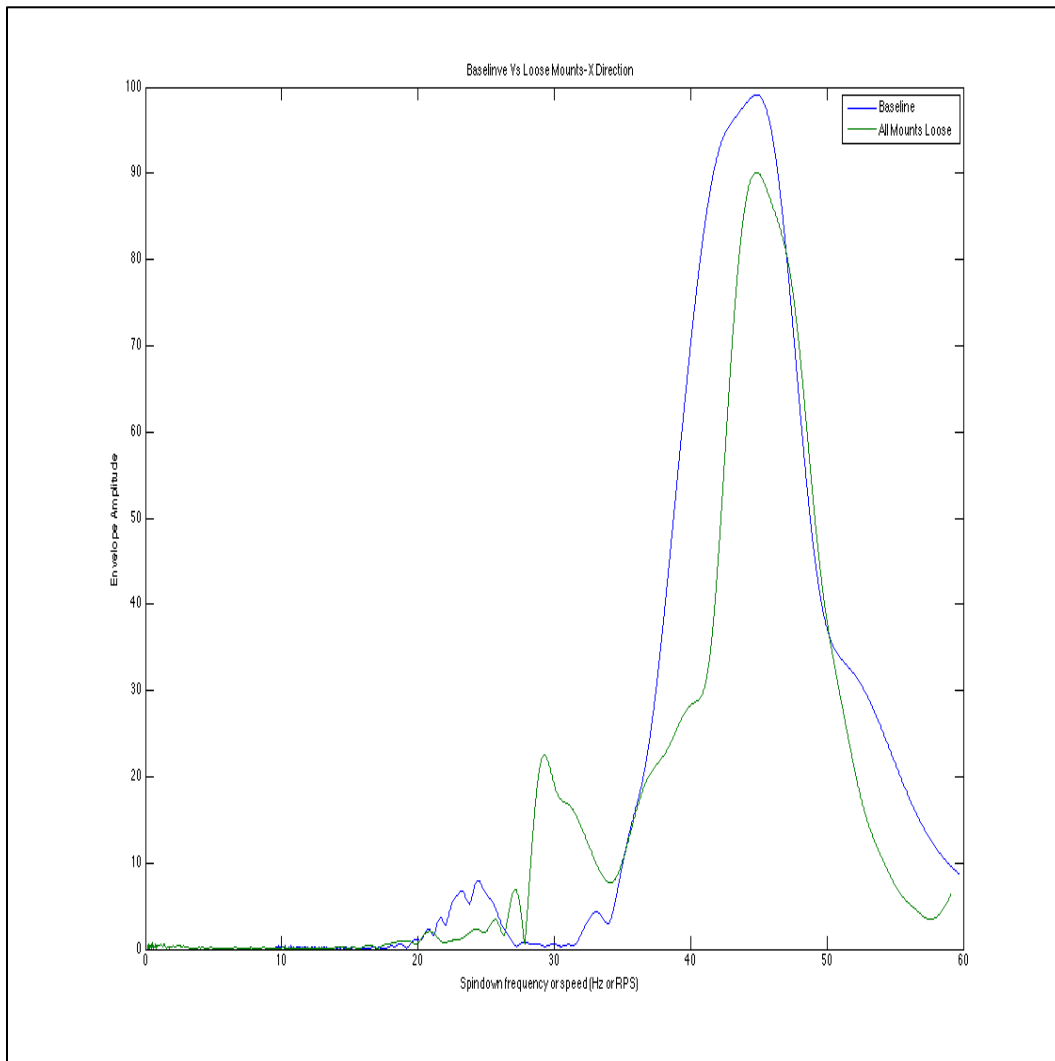


Figure 63: Baseline Comparison to Motor with Loose Mounts in the Lab- 29 MARCH 2013 (Appendix 9.2.4).

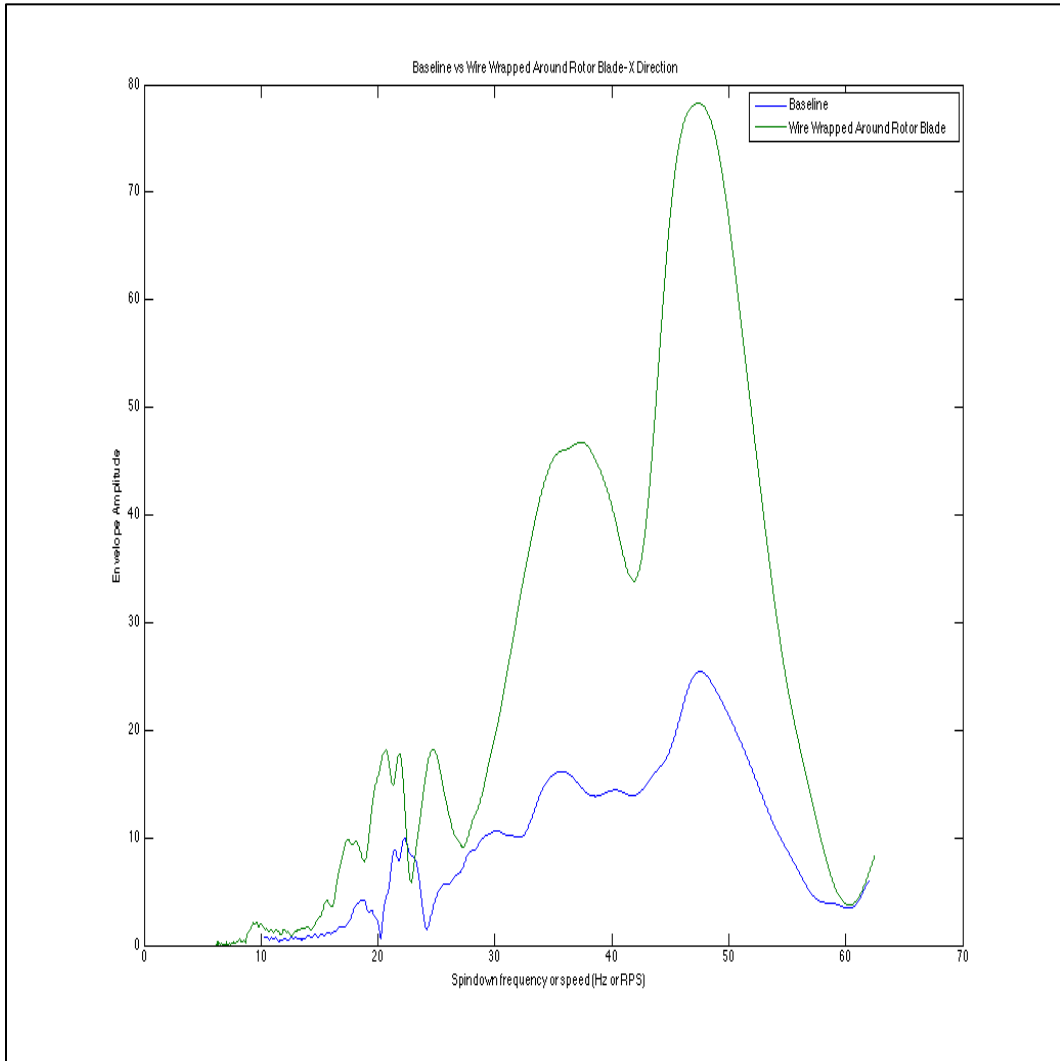


Figure 64: Baseline Comparisons to an Imbalanced Fan (right)-29 MARCH 2013 (Appendix 9.2.4).

5.0 Diagnostic Validation on a USCGC SENECA

In order to validate the lab diagnostic results and observations, representative tests conducted on commissioned vessels were required. With the permission and assistance of LT Jon Cox, the Engineering Officer aboard the USCGC SENECA, two sets of tests were run on a supply ventilation fan, inducing the same types of vibrations as in the lab tests. The first set of tests, Table 3, were run on March 20, 2013 and the second set of tests, Table 4, were run on March 29, 2013. These tests include imbalancing the fan and loosening the mounts to simulate the lab tests. These tests were conducted with the assistance of Chris Schantz, John Donnal, and Bart Sievenpiper.

Test #	Experimental Set-Up
1	Baseline Run
2	All Four Mounts Clamped With Wood
3	Left Side (x2) Mounts Clamped With Wood
4	Forward (x2) Mounts Clamped With Wood
5	Back Corner (x1) Mount Clamped With Wood
6	Wire Wrapped Around Rotor Blades, No Clamping
7	Wire Wrapped Around Blade, All Four Mounts Clamped
8	Wire Wrapped Around Blade, 2 Mounts Clamped
9	Wire Wrapped Around Blade, 1 Mount Clamped

Table 3: Tests Run on the USCGC SENECA on March 20, 2013.

Test #	Experimental Set-Up
1	Baseline Run
2	One Mount Loose
3	Two Opposite Mounts Loose
4	All Four Mounts Loose
5	All Four Mounts Loose Plus Two Mounts Clamped
6	Baseline Recalibration
7	All Mounts Tight, All Mounts Clamped

Table 4: Tests Run on the USCGC SENECA on March 29, 2013.

The CAPTCHA axis orientation for each set of tests can be seen in Figure 65 and Figure 66. For each test, a CAPTCHA was placed on the terminal box, the location of the envisioned VAMPIRE accelerometer, the side structure, and the base of the fan to pick up any structural resonance.

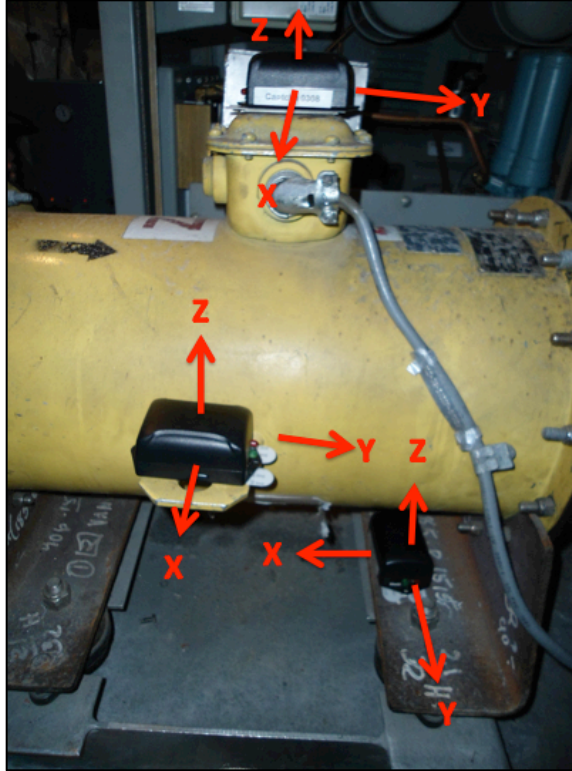


Figure 65: Axis Orientation for the CAPTCHAs During March 20, 2013 Tests.

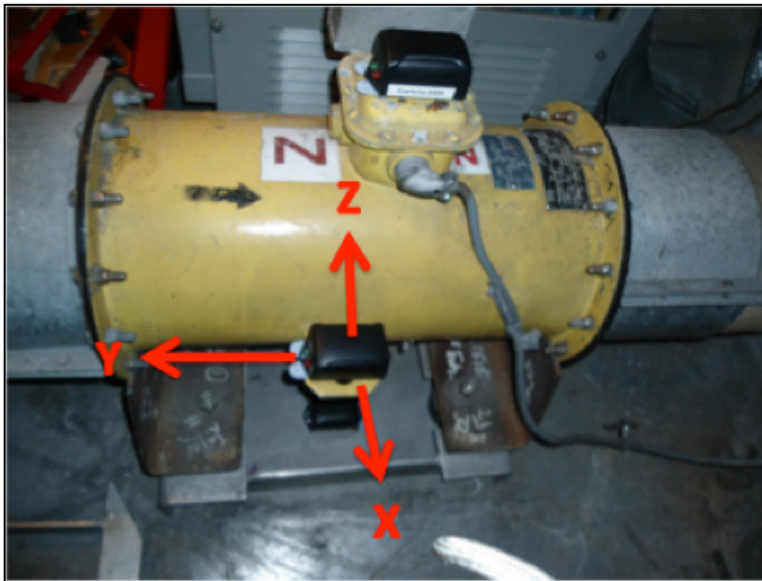


Figure 66: Axis Orientation for CAPTCHAs During March 29, 2013 Tests.

5.1 Rotor Imbalance

The first source of vibration induced on the ventilation fan was a rotor imbalance. A copper wire was attached to one of the fan blades via an opening in the fan as seen in Figure 67. The wire was taped down to the blade using electrical tape so as not to fly off and break or injure the fan.

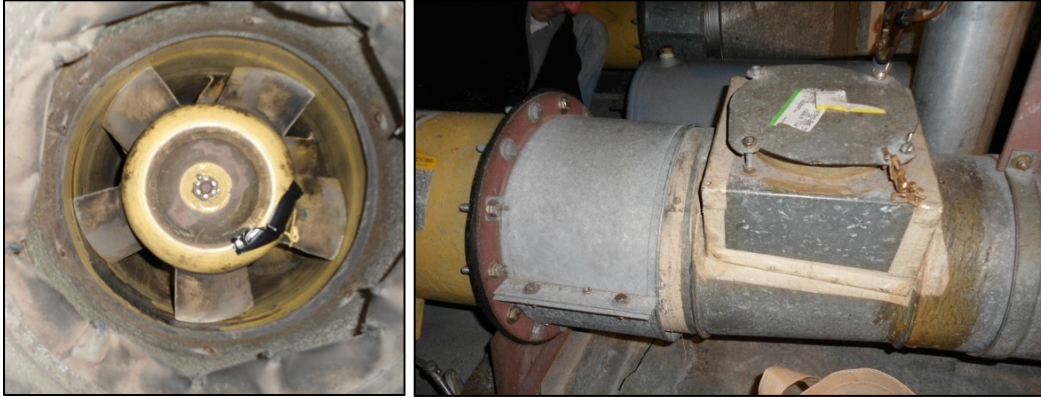


Figure 67: Imbalance Induced on SENECA Fan via Wire Wrapped on Rotor Blade (left) Through Fan Access (right).

After the tests listed earlier were run, the data was analyzed using the whisker diagnostic tool to compare to the lab data. Again, the imbalanced fan was excited throughout the entire spin-down as seen in Figure 68, which reinforced the VAMPIRE proposals.

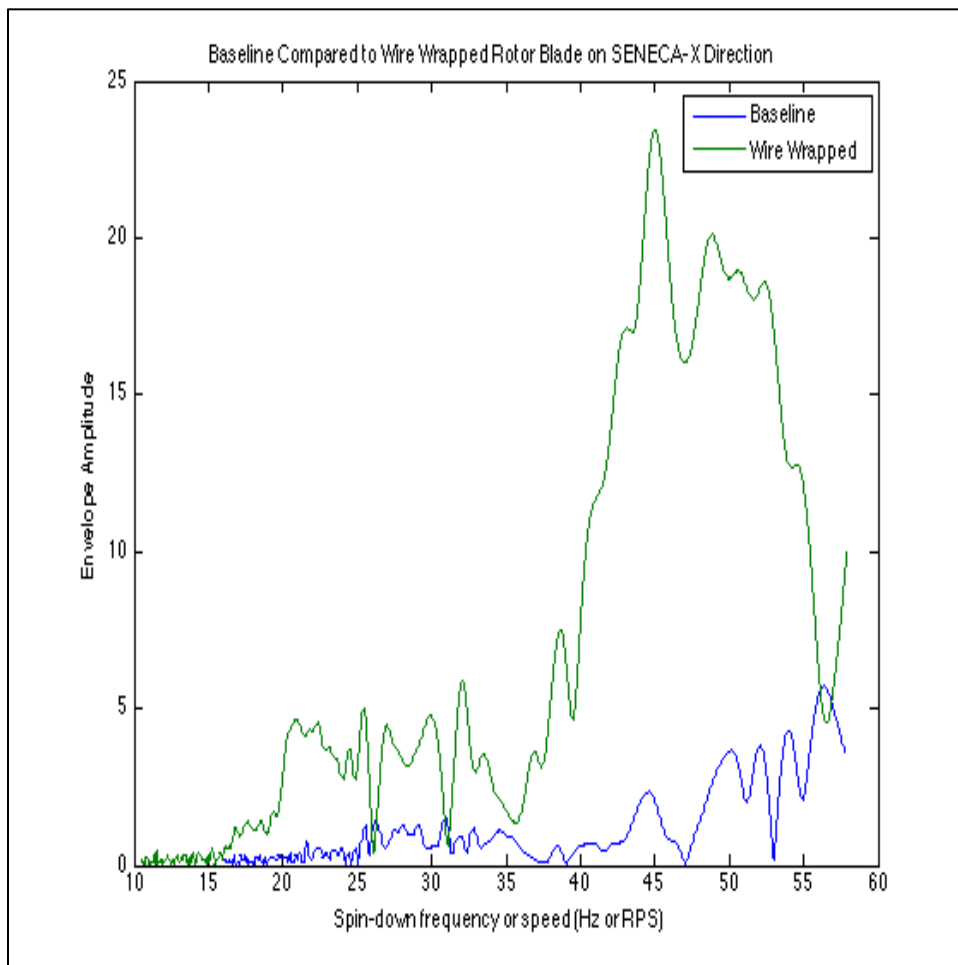


Figure 68: Baseline Run vs Wire Wrapped Around Rotor Blade on USCGC SENECA (Appendix 9.2.5).

5.2 Loose Mounts

In order to model a loose mounting condition on the SENECA fan, the mounting screw was loosened as depicted by the yellow arrow in Figure 69. A side view of the mounts can be seen in Figure 70.



Figure 69: Vibration Mounts for Ventilation Fan on SENECA.



Figure 70: Side View of Vibration Mounts on SENECA.

In addition to loosening the mounts, the mounts were additionally clamped to observe the difference in the two conditions. Each of the four mounts were clamped to induce damping conditions with C-clamps and wooden blocks as seen in Figure 71 and Figure 72.



Figure 71: SENECA Mounts Clamped.



Figure 72: Clamped Mounts on SENECA Fans with C-Clamps and Wooden Blocks.

Several tests were run with the fans in this condition and then the data was analyzed using the whisker diagnostic tool. The results for these tests are seen in Figure 73 and Figure 74. Figure 73 depicts the SENECA ventilation fan baseline signature as compared to the sequential loosening of the vibration mounts. Overall, the fan signatures in each condition follow closely with the baseline signature. There

is some excitation initially as the fan begins to spin-down; however, in the lower frequencies, the loosened mounts taper off.

Figure 74 depicts the baseline run as compared to the fan when the mounts are clamped and loosened. As seen, the vibration signature of the fan with the mounts loosened is very similar to the baseline signature of the fan. There is some excitation at the beginning of the spin-down, but almost nothing in the lower frequencies. Initially, it was expected to have seen more excitation at the beginning of the spin-down than what was actually seen. However, this could be due to the style of vibration mounts and the style of the fan. In this particular scenario, the fan changed very little with the loosening of the mounts due to the stiffness of the mounts. This particular type of vibration mount maintained stiffness throughout the test. Even with only a slight increase in vibration at the beginning of the spin-down, these results corroborate the findings in the lab and VAMPIRE paper.

The clamped mounts, though, did have an effect on the signature of the vibrations. As expected, clamping the mounts dampened the acceleration of the mounts. To note, the spike around 30 Hz in the clamped mount signature is due to a compressor in the space turning on during the run.

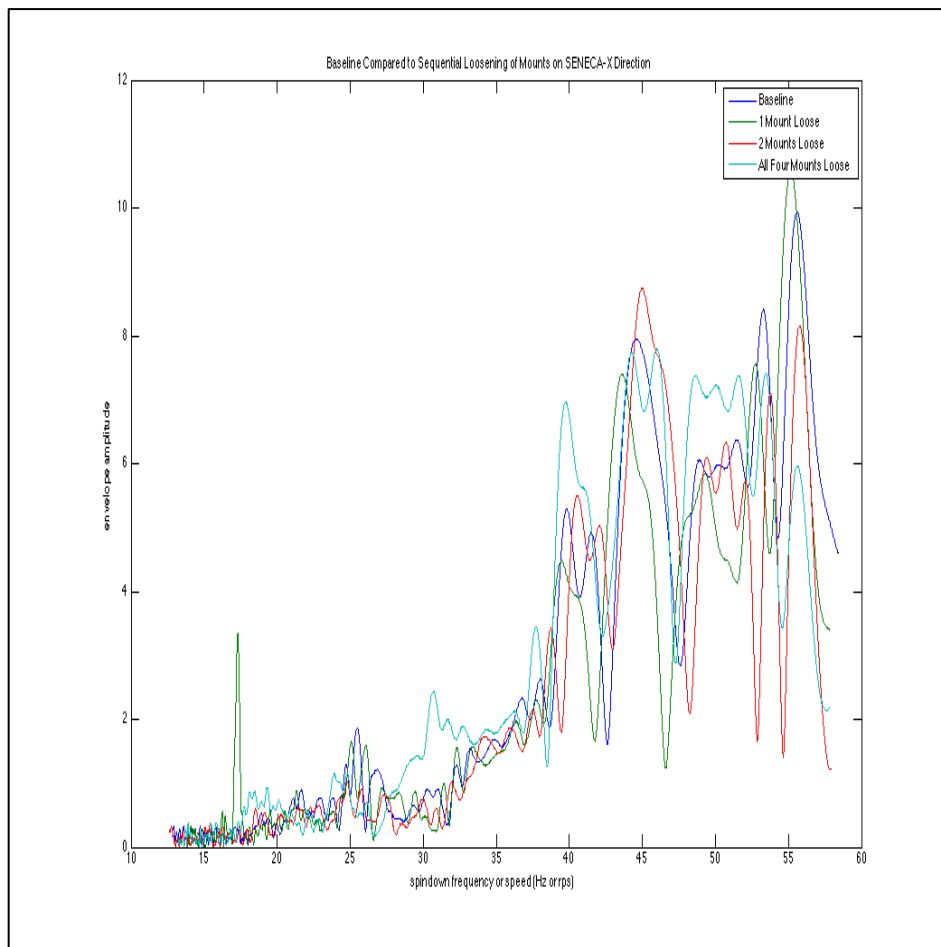


Figure 73: Fundamental Spin-down of SENECA Fan Baseline vs Sequential Loosening of the Mounts (Appendix 9.2.5).

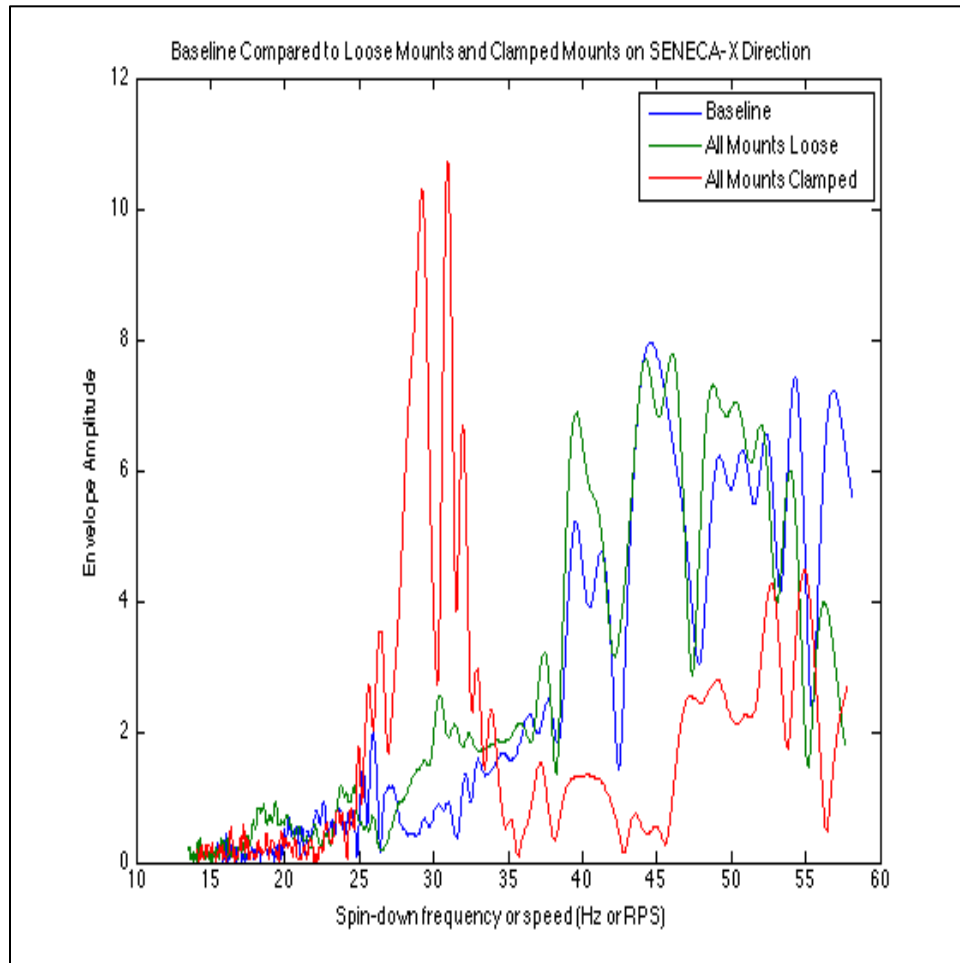


Figure 74: Fundamental Spin-down of SENECA Fan Baseline vs Loose Mounts and Clamped Mounts (Appendix 9.2.5).

5.3 Comparison

On a real-time platform, some of the results from testing are not as clear-cut as they are in the lab; however, they do agree with the initial VAMPIRE findings. As seen in Figure 75, the imbalanced fan produces a vibration signature much higher than the baseline throughout the motor spin-down while the loose mounts is only slightly excited at the beginning of the spin-down. In this particular situation, the loose mount signature is very similar to the baseline run. This could be due to the stiffness of the mounts, the light weight of the fan, the inport condition of the ship, or even the other equipment in the space forcing air through the fan even after shut-off.

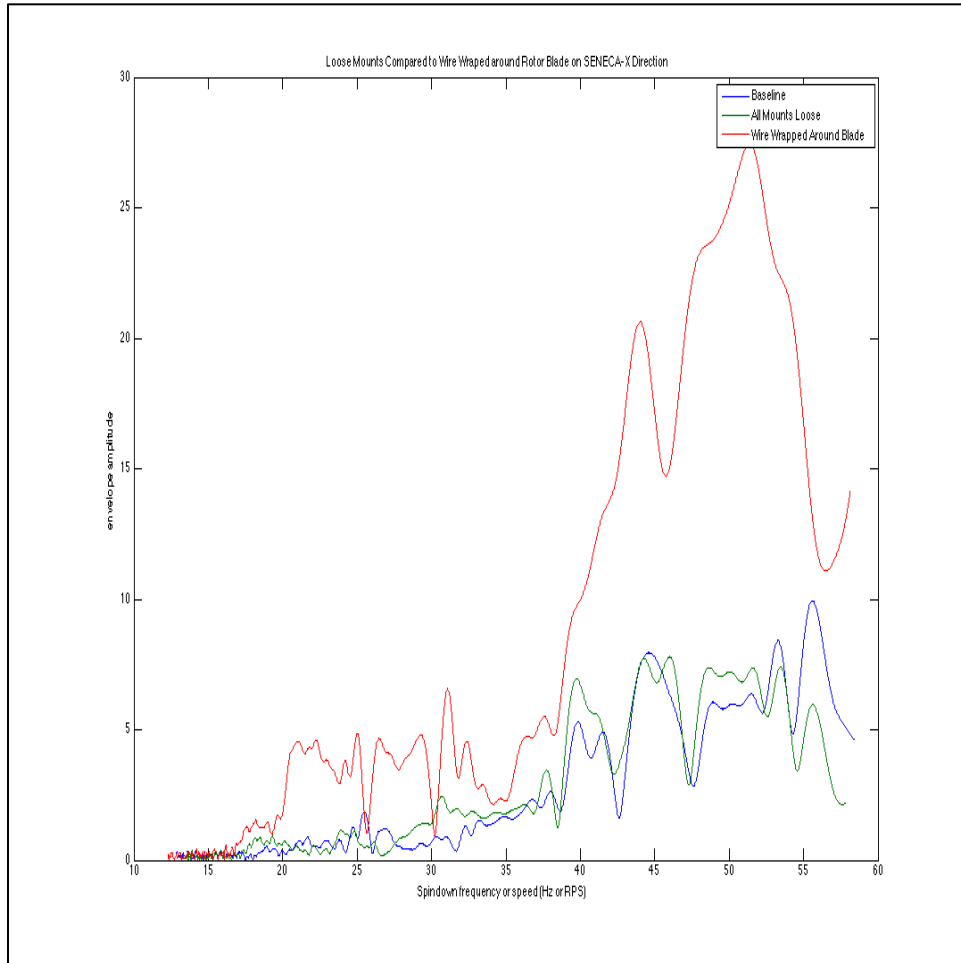


Figure 75: Fundamental Spin-down of SENECA Fan Baseline vs Loose Mounts and Wire Wrapped Rotor Blade.

However, the similarity in the baseline run and the loose mount scenario could lead to an interesting observation. Figure 77 adds the clamped mount vibration signature to the scenarios seen in Figure 75. Seeing that the loose mount signature and the baseline signature are similar, the baseline run is removed from the analysis and Figure 77 only includes the wire wrapped blade, the clamped mounts, and the loose mounts. From these signatures, it could be observed that if there is no baseline data available from an unfamiliar, fleet-based piece of equipment, the loose mount signature could provide a baseline comparison for higher or lower vibrations.

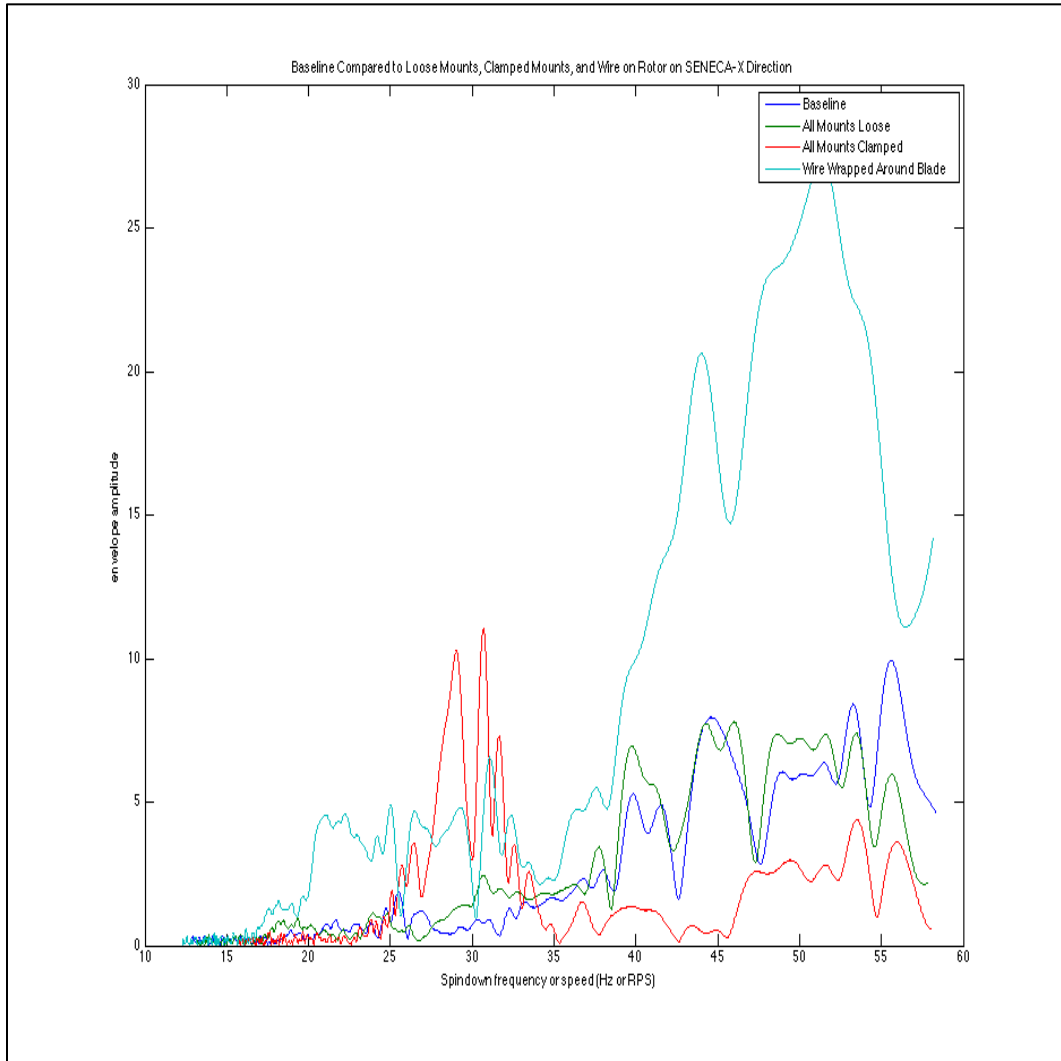


Figure 76: Fundamental Spin-down of SENECA Fan- Baseline vs Various Vibration Sources (Appendix 9.2.5).

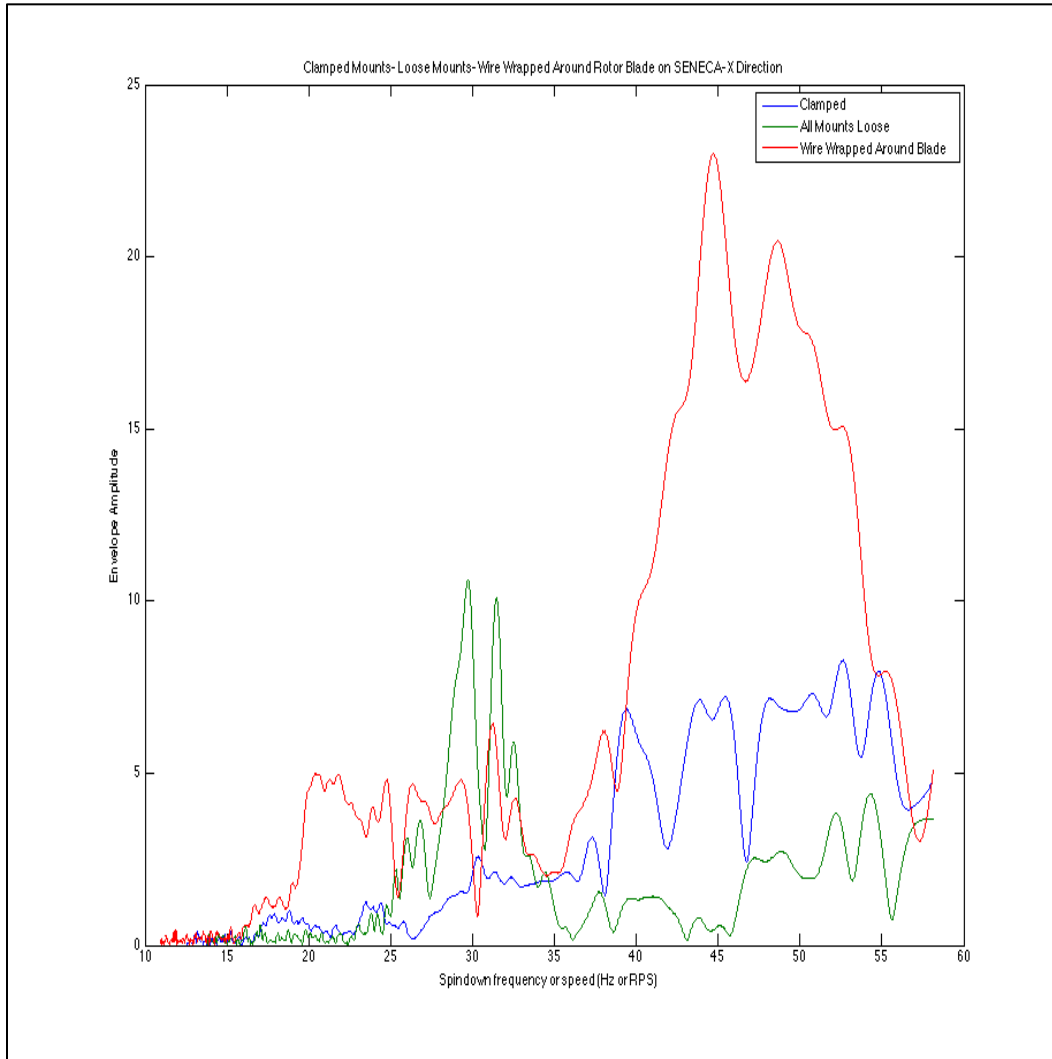


Figure 77: Fundamental Spin-down of SENECA Fan- Clamped and Loose Mounts vs Wire Wrapped Around Rotor Blade (Appendix 9.2.5).

6.0 USN and USCG Fleet Vibration Testing

Once the diagnostic testing in the lab was corroborated on the USCGC SENECA, a commissioned Coast Guard vessel operating out of the Boston Harbor, data was sampled onboard other USN and USCG vessels to observe shipboard vibrations in an attempt to determine the sources of any perceived high vibrations.

6.1 WMSL 750- USCGC BERTHOLF & WMSL 752- USCGC STRATTON

Two USCG vessels analyzed were the USCGC BERTHOLF and USCGC STRATTON as mentioned in Section 2.3.2.1. These two ships have similar hulls are of the same class, ideal for equipment comparison. For each ship, a series of data was collected as outlined in Table 5 and Table 6. This data was collected with the assistance of Bart Sievenpiper.

Test #	Equipment	Experimental Set-Up
1	Helo Hangar Fan (1-14-2)	Initially Off, Start in Slow, Stop, Start in Fast, Stop
2	FWD Supply Venilation Fan (1-42-4)	Both Running, Stop, Bottom Fan on, Stop, Top Fan on, Stop, Both On
3	FWD Supply Venilation Fan (1-42-2)	
4	Chill Water Pump #1	A. 1&3 on, 2 off. B. 2 & 3 off, 1 on. C. 1 & 2on, 3 off. D. 1 & 3 off, 2 on. E. 1 on, 2 & 3 off.
5	Chill Water Pump #2	
6	Chill Water Pump #3	
7	Fire Pump #1	Initially Off, then on, then off.

Table 5: Data Collected From the USCGC BERTHOLF on January 8, 2013.

Test #	Equipment	Experimental Set-Up
1	Helo Hangar Fan (1-14-2)	Initially Off, Start in Slow, Stop, Start in Fast, Stop
2	FWD Supply Venilation Fan (1-42-4)	Both Running, Stop, Bottom Fan on, Stop, Top Fan on, Stop, Both On
3	FWD Supply Venilation Fan (1-42-2)	
4	Chill Water Pump #1	A. 2 on, 1 & 3 off. B. 1 & 2 on, 3 off. C. 1 on, 2 & 3 off. D. 1 & 3 on, 2 off. E. 1 & 2 off, 3 on. F. 1 off, 2 & 3 on. G. 1 & 3 off, 2 on.
5	Chill Water Pump #2	
6	Chill Water Pump #3	
7	Fire Pump #1	Initially Off, then on, then off.
8	Sea Water Cooling Pump #2	Initially Off, then on, then off.
9	Sea Water Cooling Pump #3	Initially Off, then on, then off.

Table 6: Data Collected From the USCGC STRATTON on January 9, 2013.

While on board these ships, the BERTHOLF's crew reported that the forward ventilation fan was exceedingly loud and seemed to be experiencing high vibrations. No diagnostic tests had been run on the fan prior to the CAPTCHA testing and the port engineer was notified about the fan at the same time the team was on board. The BERTHOLF's fans, seen in Figure 78 and Figure 79, were then compared to the STRATTON's ventilation fans as seen in Figure 80 and Figure 81. Data was captured and then analyzed utilizing the whisker diagnostic tool to determine what type of vibrations are causing the BERTHOLF's fan to shake.

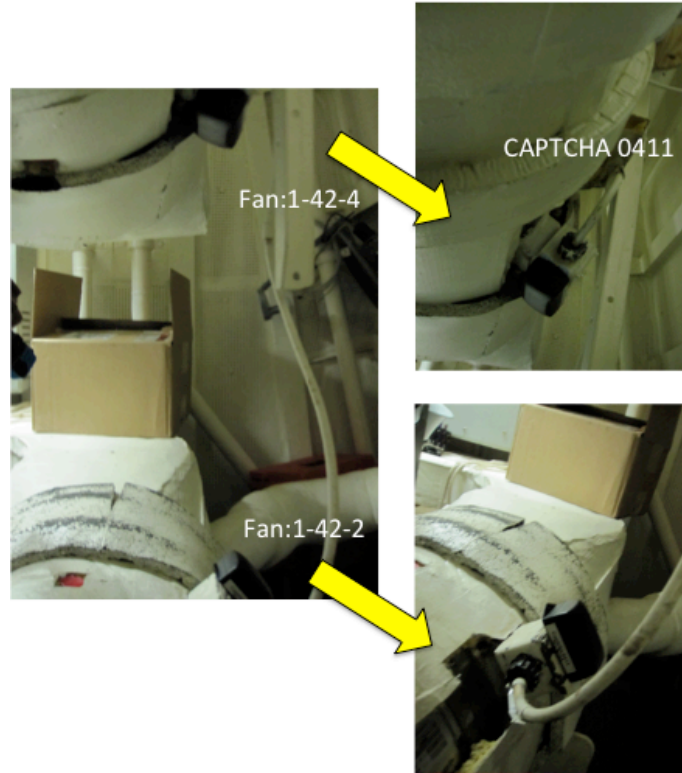


Figure 78: USCGC BERTHOLF Forward Ventilation Fans.

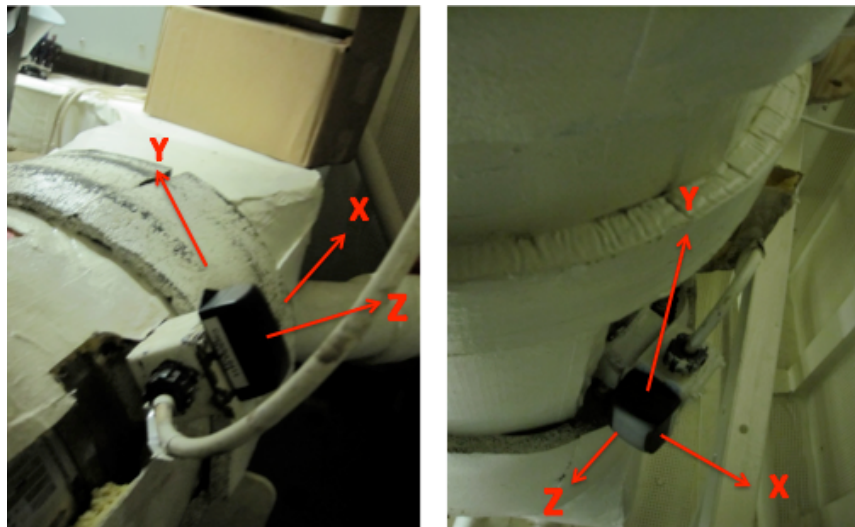


Figure 79: CAPTCHA Axis Orientation on BERTHOLF Ventilation Fans. Bottom Fan (left), Top Fan (right).

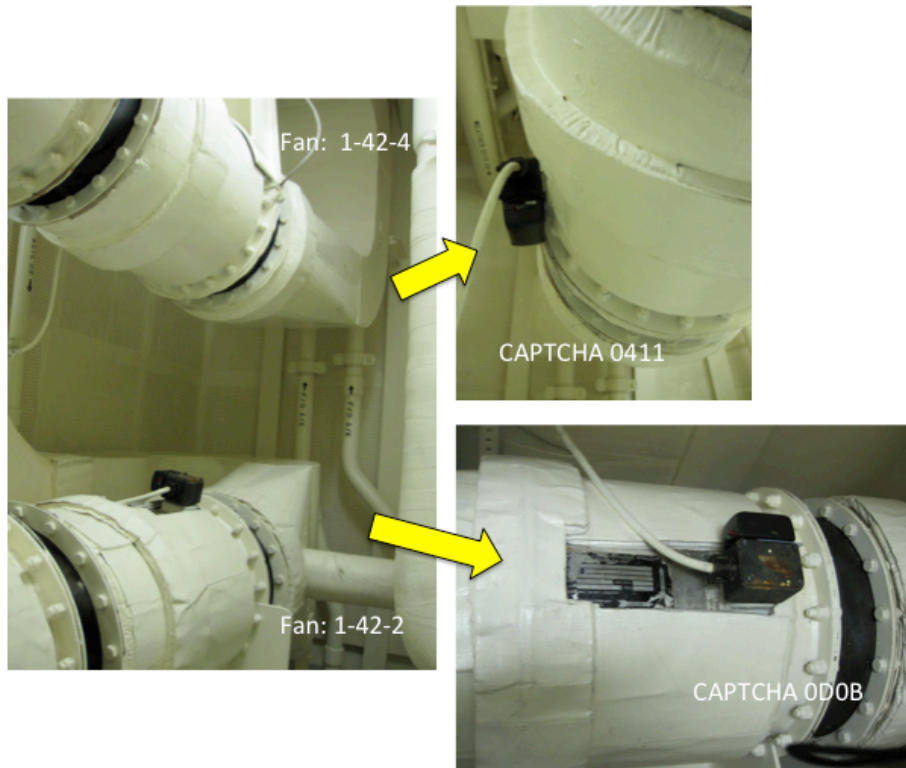


Figure 80: USCGC STRATTON Ventilation Fans.

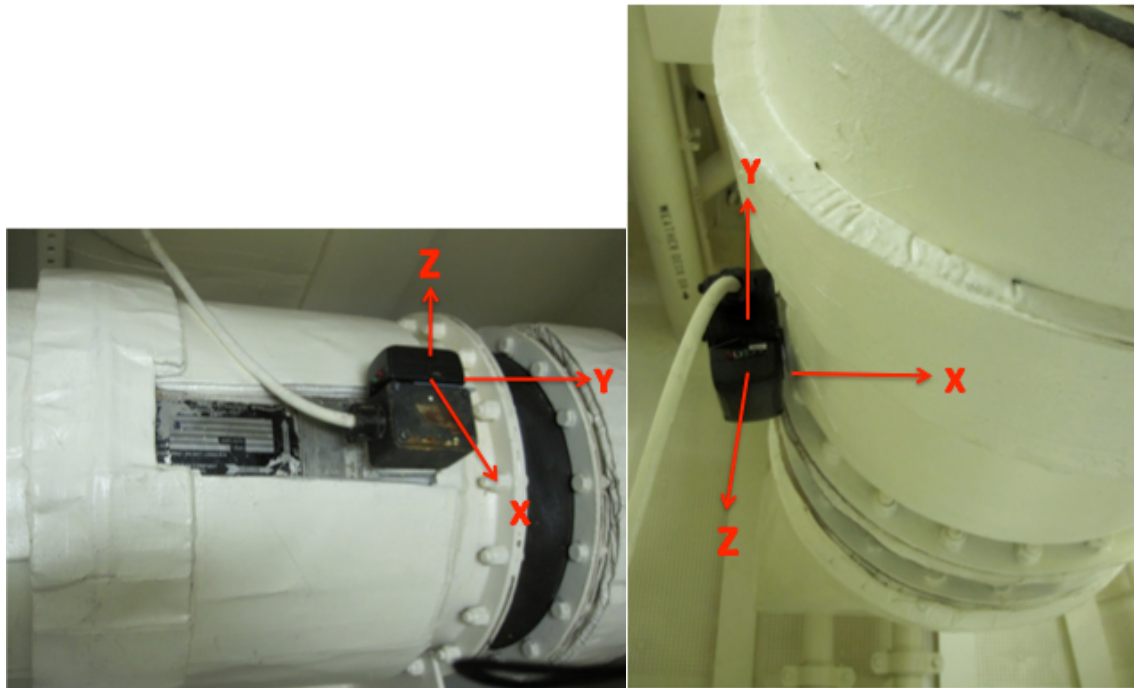


Figure 81: USCGC STRATTON Ventilation Fan CAPTCHA Orientation. Bottom Fan (left), Top Fan (right).

Implementing the whisker diagnostic tool, both the top set of ventilation fans and the bottom set of ventilation fans were compared between the two ships. Figure 82 depicts the two top ventilation fans on the BERTHOLF and the STRATTON. Both ships' crews believe these fans to be normal and non-vibration inducing. The

fundamental spin-down analysis agrees with this statement as both fans have a similar spin-down signature. The slightly higher accelerations on the BERTHOLF fan could be due to age and condition of the fan. The BERTHOLF fan is two years older than the STRATTON fan, which could equate to two more years of salt and debris build-up in the fan.

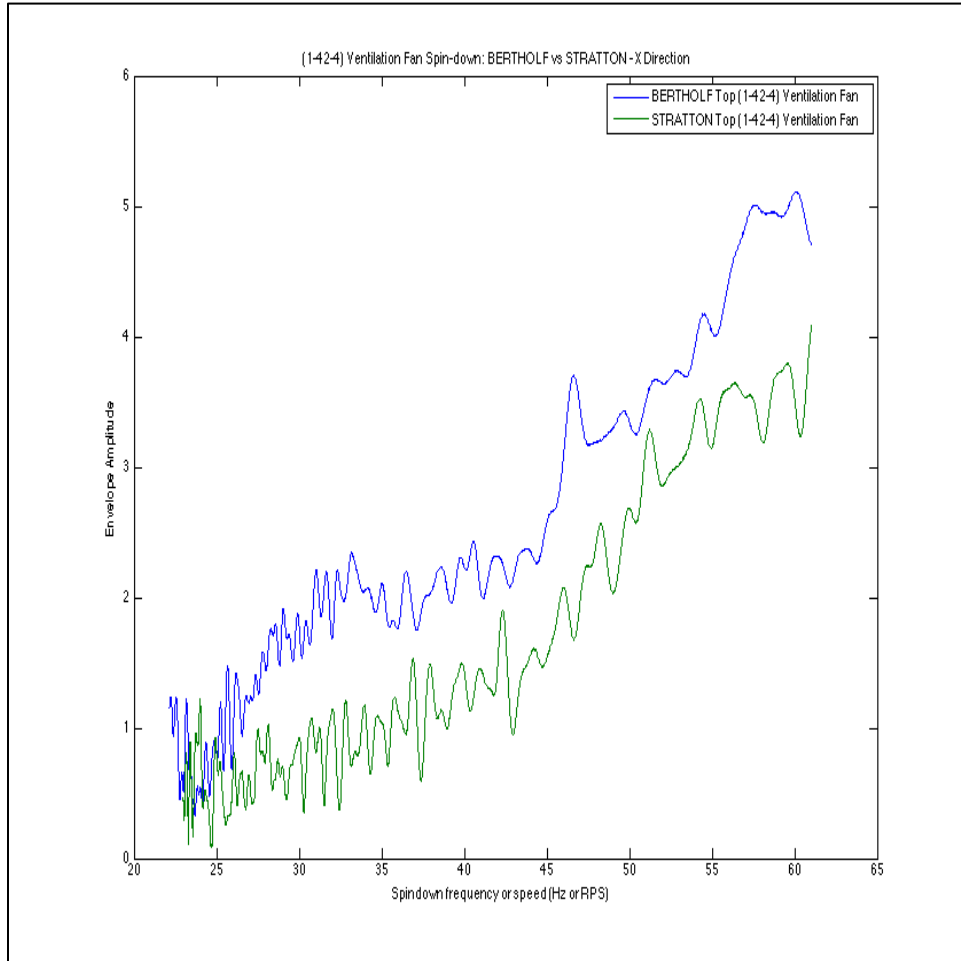


Figure 82: Top Ventilation Fans Compared on the Two National Security Cutters (Appendix 9.2.6).

However, Figure 83 presents the comparison between the BERTHOLF's bottom ventilation fan and the STRATTON's bottom ventilation fan from the same space on both ships. It is clear to see that the BERTHOLF's ventilation fan has higher vibrations than the STRATTON's in this fundamental spin-down depiction. Not only are the vibrations higher, but they are higher throughout the entire spin-down. Based upon earlier testings in the lab and on the USCGC SENECA, these vibrations could be due to salt build-up in the fan causing an imbalance internally. Although this induction can only be verified via the workshop when the fan is offloaded and taken apart, this type of data and observation epitomizes the VAMPIRE proceedings.

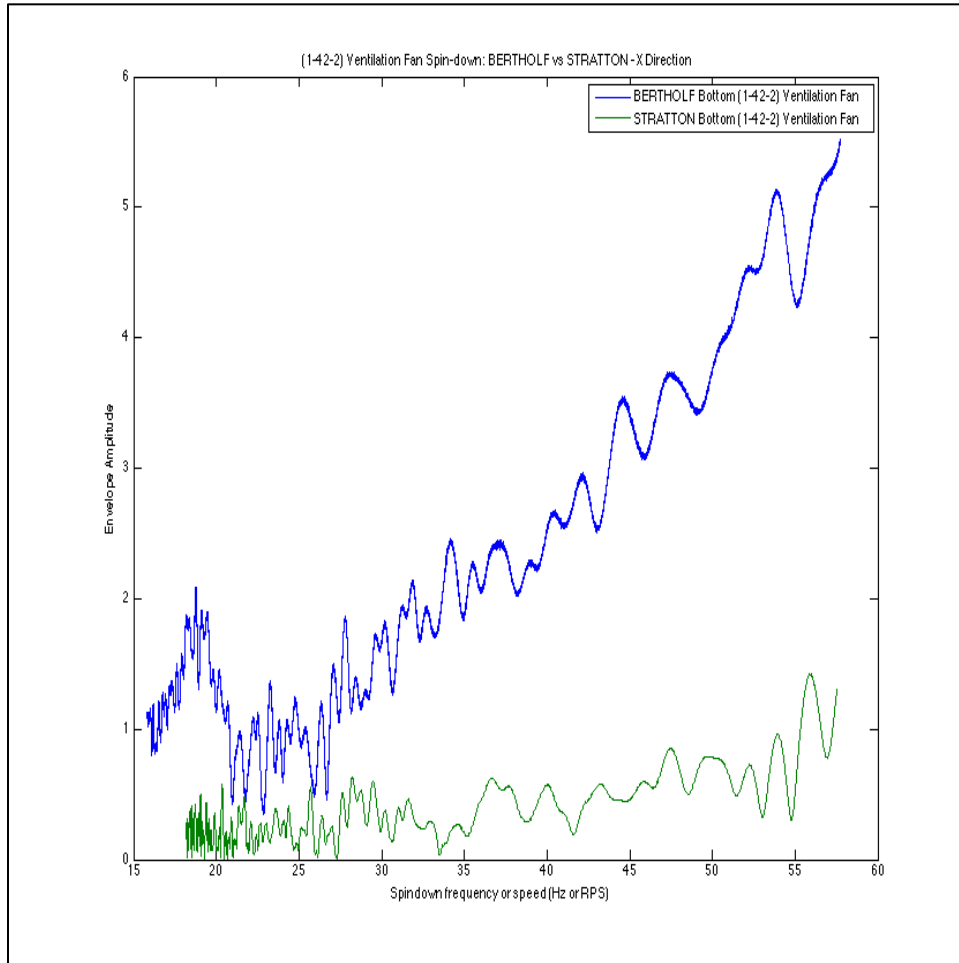


Figure 83: Bottom Ventilation Fans Compared on the Two National Security Cutters (Appendix 9.2.6).

Taking the observation one step further, Figure 84 shows all four fans during spin-down. The BERTHOLF bottom fan (green line) can be audibly distinguished from the top fan in the ventilation space; however, according to the spin-down signature, the top fan's spin-down signature is just below the bottom fan's. As such, higher vibrations due to an imbalance could be being experienced on the top fan as well, just not audibly yet. After this study, it is recommended that the top fan as well as the bottom fan be maintenance and rotor blades cleared of any foreign object debris (FOD) that could cause vibrations.

Although the STRATTON is a newer ship and neither fan has the crew concerned about high vibrations, it could be predicted from these results that the top ventilation fan on the STRATTON will exhibit characteristics of high vibrations first. With a spin-down signature nearing the BERTHOLF's fans, the top ventilation fan on the STRATTON should be checked for obstruction within the fan which could result in an imbalanced fan.

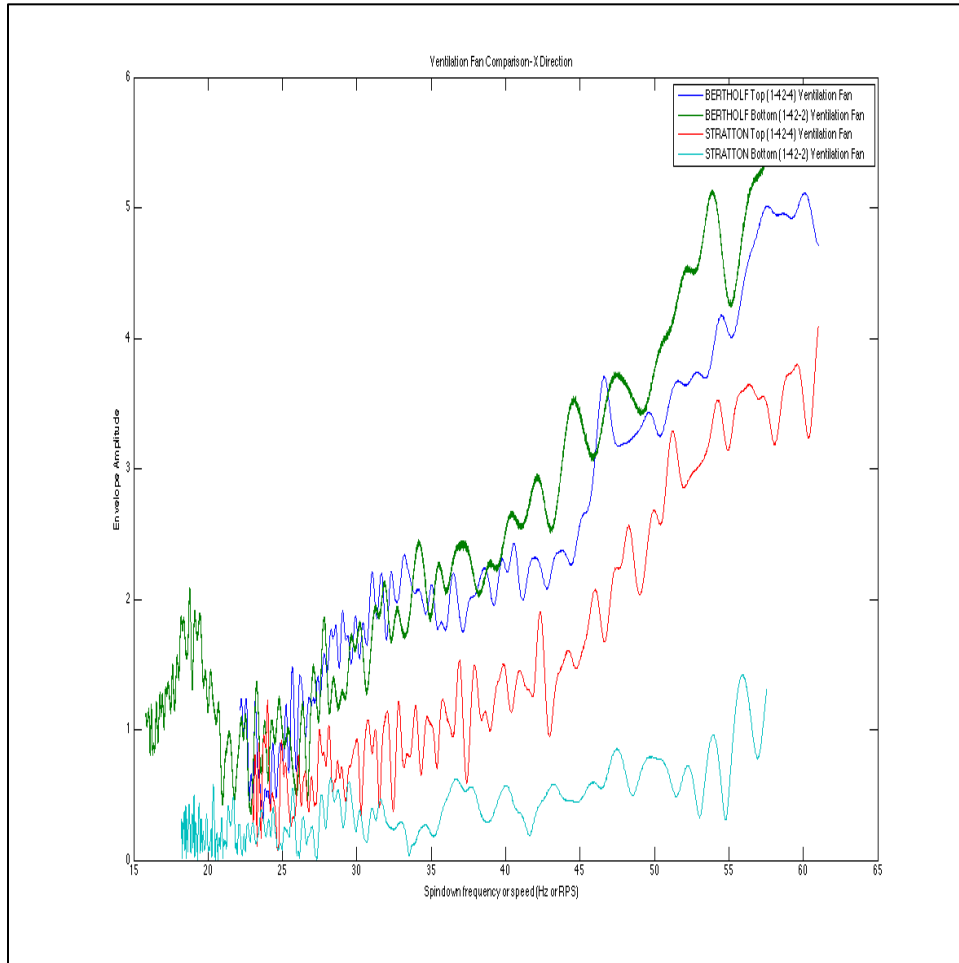


Figure 84: All Four Ventilation Fans Compared for Vibrations During Spin-down (Appendix 9.2.6).

6.2 USS MICHAEL MURPHY (DDG 112)

Three USN ships were visited and data collected from including the USS INDEPENDENCE (LCS 2), the USS SAN DIEGO (LPD 22), and the USS MICHAEL MURPHY (DDG 112). The newest of the ARLEIGH BURKE Class Destroyers, the data collected from the USS MICHAEL MURPHY was the most useful and provided for a legitimate equipment comparative analysis.

An accelerometer was placed on each of the six fire pumps on the DDG 112 to collect and analyze vibration data. However, only three fire pump signatures were recorded using the higher quality, lab designed CAPTCHAs, while the other three were monitored using the COTS accelerometers. Due to the low fidelity and lower sampling rate, the COTS accelerometers were not reliable and unable to discern the spin-down signature of the fire pumps. The COTS accelerometers were able to provide time-series data, but not data compatible with the whisker diagnostic tool. Table 7 outlines the fire pumps and CAPTCHAs used to gather vibration data from on the USS MICHAEL MURPHY. Figure 85, Figure 86, and Figure 87 depict the CAPTCHAs' axis orientation on each of the three fire pumps on DDG 112.

Fire Pump #	CAPTCHA #
2	0308
3	0DOB
5	0411

Table 7: Fire Pumps Tested on USS MICHAEL MURPHY.

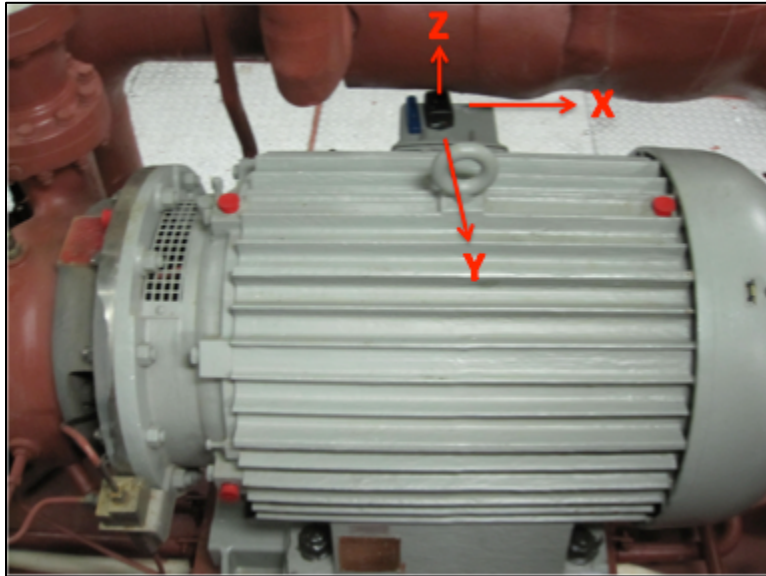


Figure 85: Fire Pump #2 on the MICHAEL MURPHY.

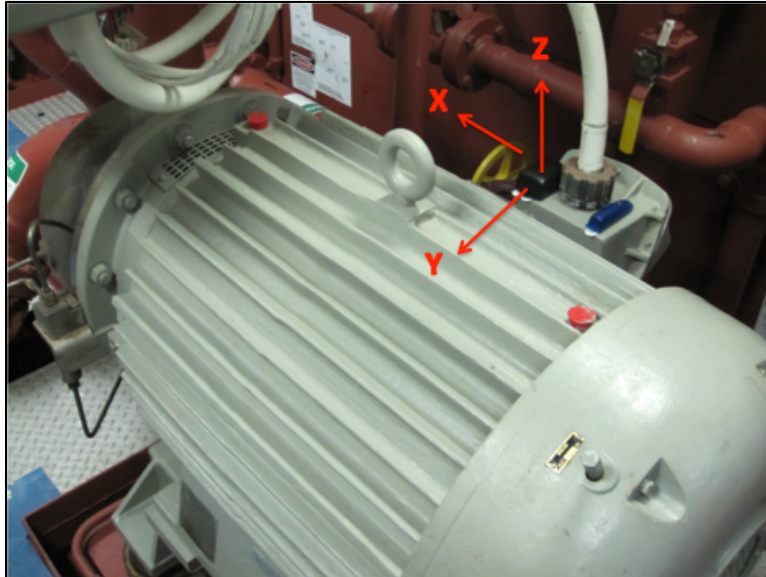


Figure 86: Fire Pump #3 on the MICHAEL MURPHY.

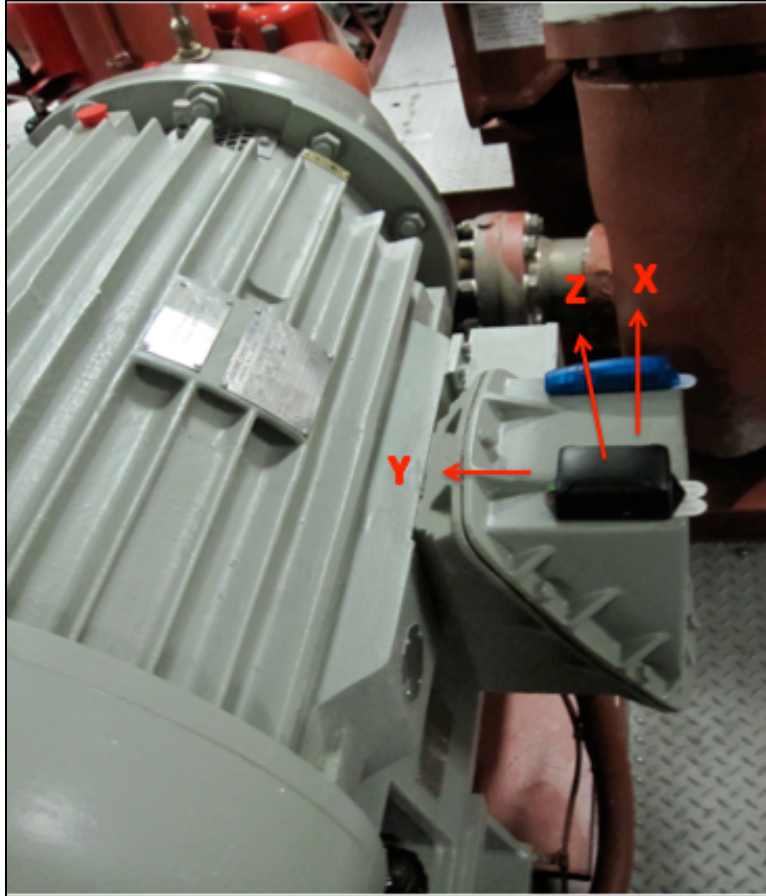


Figure 87: Fire Pump #5 on MICHAEL MURPHY (Z Direction up, out of the CAPTCHA; X Direction perpendicular to Y Direction).

Figure 88 depicts the data collected on each fire pump on the MICHAEL MURPHY after being analyzed with the whisker diagnostic tool. None of these fire pumps were reported by the crew to have known problems or being currently experiencing high vibrations. Looking at this graph, it could be assumed that the spike at 40 Hz seen in the spin-down on fire pump #2 and the spike at 20 Hz in fire pump #5 could be attributed to other equipment in those engineering spaces.

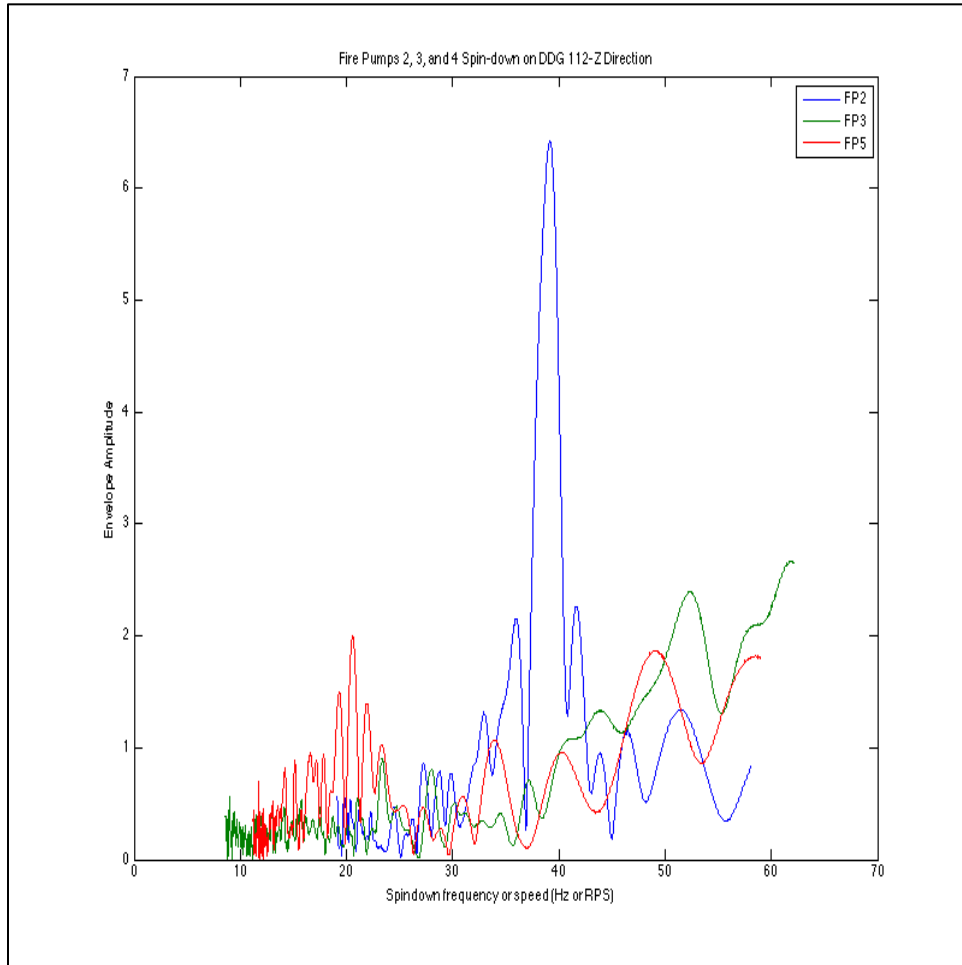


Figure 88: Comparison of the Three Fire Pumps on DDG 112 (Appendix 9.2.7).

Disregarding those interferences, these spin-downs are all very similar and hard to discern the magnitude of vibrations based upon this data only. What actually equates to a high vibration numerically? If there is no baseline data to compare these data points to, a standard could be used to determine if a vibration a machine emits is “high”. If MIL-STD 167-1 as discussed in Section 1.1.5 is used, none of the fire pumps on DDG 112 have high vibrations in steady state and are well under the 107 VdB threshold as seen in Figure 89.

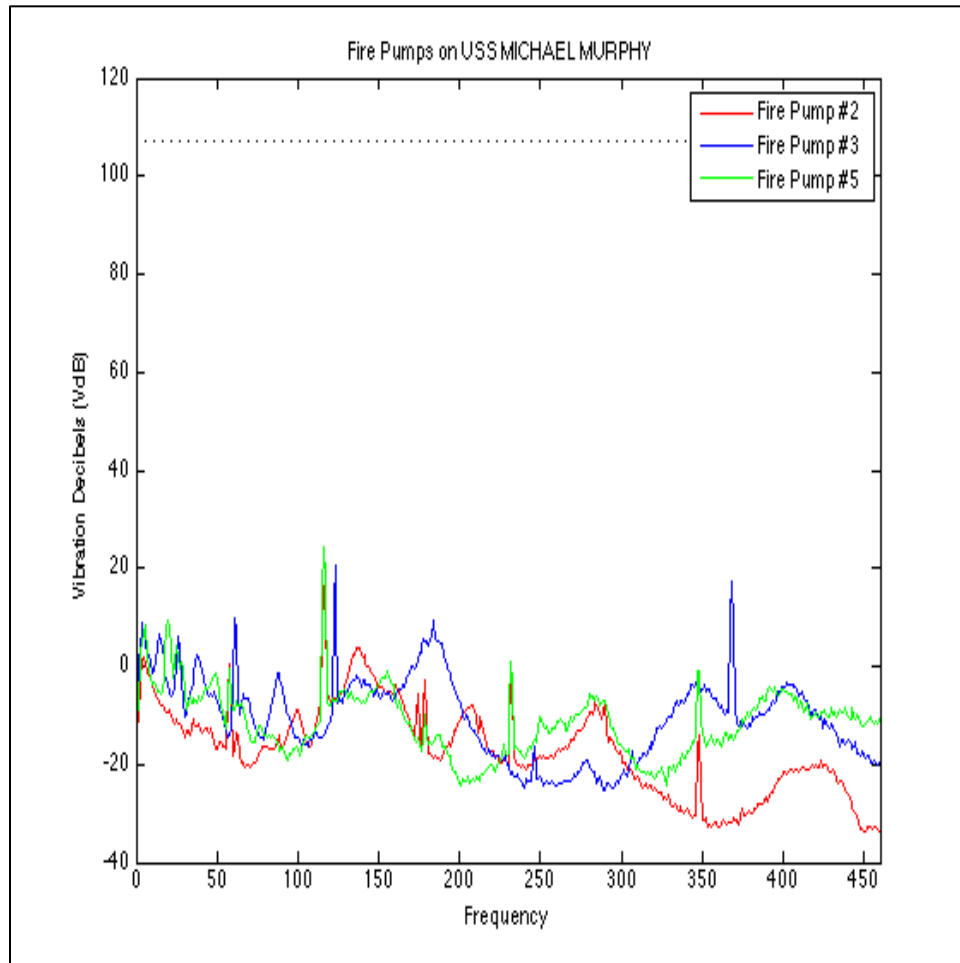


Figure 89: Fire Pumps on DDG 112 Compared to MIL-STD 167-1 (Appendix 9.2.7).

6.3 USS INDEPENDENCE (LCS 2)

Although the data from the LCS 2 did not clearly show the spin-downs of the fire pumps on board and therefore unable to be analyzed in the whisker diagnostic tool, the CAPTCHAs were still able to collect data on two of the fire pumps and verify high vibrations. Fire Pumps #3 was reported by the crew to have high vibrations and was tagged out for normal use due to these high vibrations. Figure 90 and Figure 91 depict the axis orientation for the CAPTCHAs on the two fire pumps.

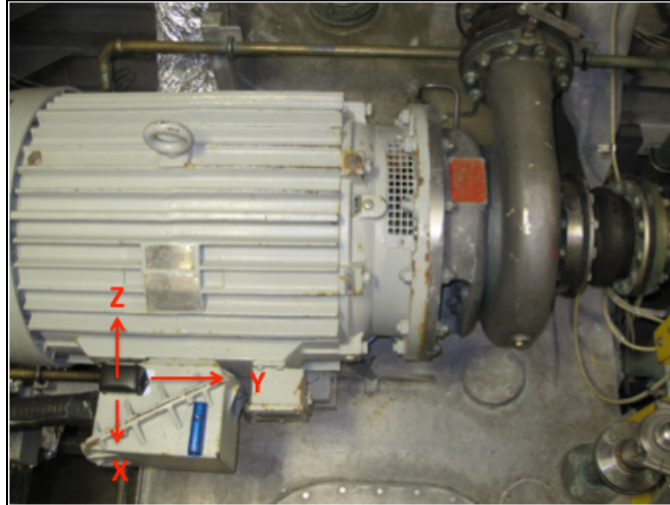


Figure 90: Axis Orientation on LCS 2's Fire Pump #1.

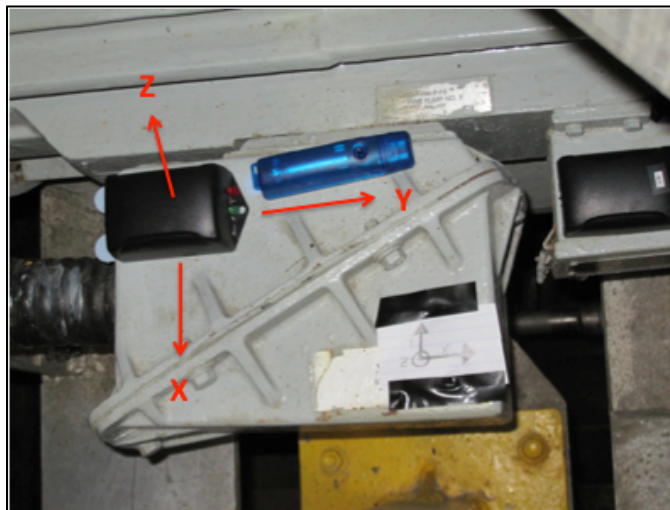


Figure 91: Axis Orientation on LCS 2's Fire Pump #3.

Since the whisker diagnostic tool was not an option with this set of data, the data collected from these two fire pumps was analyzed using a power spectral density function and plotted on a logarithmic scale. Figure 92 compares the vibration amplitude across the frequency spectrum for fire pumps #1 and #3. As it can be clearly seen, the vibration amplitudes for fire pump #3, the green line, are much higher than the vibration amplitudes for fire pump #1 therefore reinforcing the findings of the ship's crew.

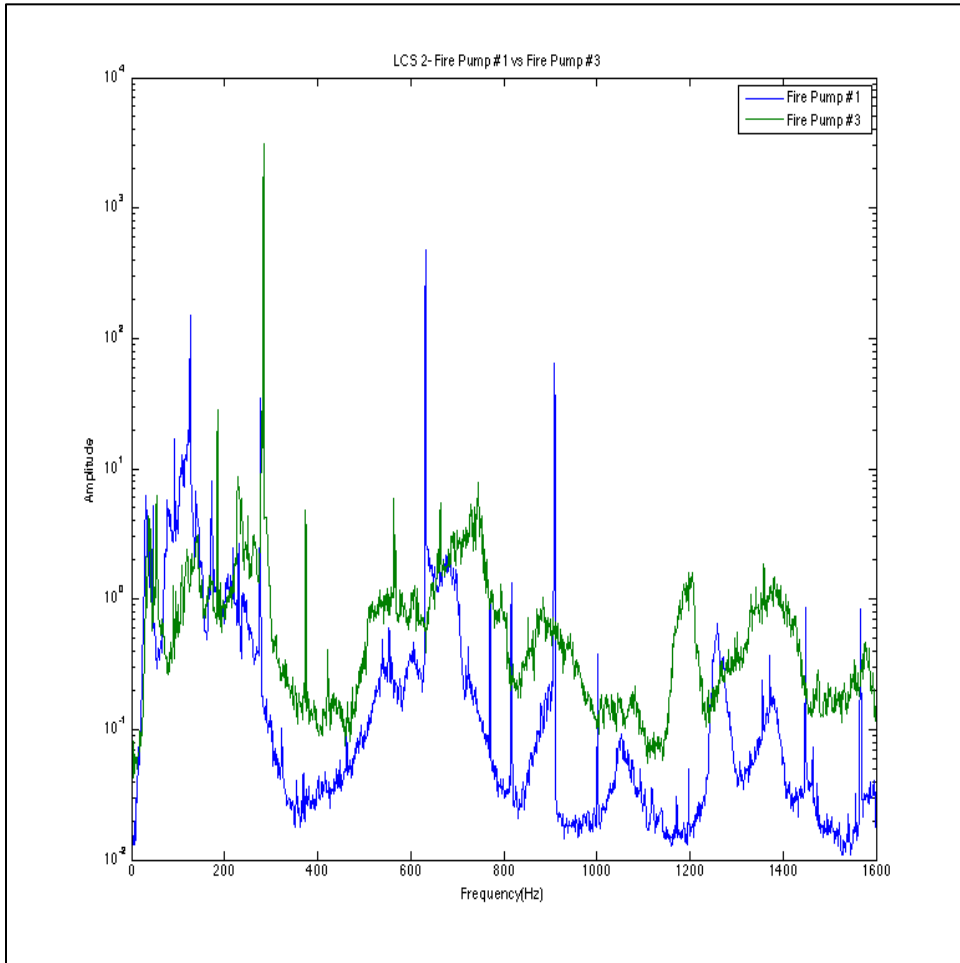


Figure 92: Power Spectral Density for Fire Pumps #1 and #3 on LCS 2 (Appendix 9.2.8).

7.0 Future Work

Currently, the VAMPIRE project is still a work in progress and there is still work to be completed in order for it to be a successful tool for the USN and USCG fleet. Additionally, there are outside parameters and standards that need to be agreed upon to create baseline vibration readings for each piece of equipment.

7.1 Continued Diagnostic Testing on Equipment

Currently, diagnostic testing was only completed on lab-based equipment and a single ventilation fan on the USCGC SENECA. These data points are valuable and allow for baseline observations to be made; however, conducting more diagnostic testing on several different types of equipment would make the analysis more robust. The testing on the SENECA could be a baseline for experiments conducted on other ships and other equipment to include fans, fire pumps, seawater pumps, chill water pumps, or any other rotating piece of equipment. Table 8 details a generic testing plan for future diagnostic testing. One of the most important lessons learned during this experiment was to have a solid experiment plan prior to testing. Before testing on the SENECA, pictures of the fan were obtained for planning purposes along with mount sizing and structure support size. Additionally, establishing a baseline vibration signature prior to and after testing allows for a stronger comparison study.

Test Outline	Explanation
Baseline Run	Run Equipment Prior to any Testing/Alteration
Imbalance	Imbalance the motor- ex- wrap a wire around a blade or add extra weight to one side
Baseline Re-run	Remove/Un-do any alterations to equipment. To monitor any change in the equipment
Mount Alteration	Induce external source of vibration- ex- Loosen or Clamp the Mounts.
Baseline Final Run	Run equipment again after placing equipment in original condition again.

Table 8: Generic Outline of Future Diagnostic Testing.

7.2 Diagnostic Signatures of Vibrations

The two most common sources of high vibrations are imbalances and loose mounts; however, there are other types of vibrations as seen in Figure 7 that are experienced throughout the USN and USCG fleets. Misalignments, bent shafts, broken gears, and bad bearings are other common problems experienced in USN and USCG motors. When installed on ships, the goal of VAMPIRE is to be able to present the operator with as much detailed information as possible in regards to the high vibrations of

equipment and how to fix it as quickly as possible. In order to have a realistic, well-rounded vibration measuring and diagnostic device, other types of vibrations should be analyzed and included in the vibration detection software.

7.3 Vibration Standards

The most common assumption with any vibration monitoring technique is the assumption that once a machine is placed into service and a baseline vibration signature is obtained, subsequent change in the material condition of the machinery will be reflected by a change in its vibration signature. Conversely, if there is no change in the vibration signature, then there has been no change in the material condition of the machine [2].

In order to create a software program internal to VAMPIRE that detects high vibrations, there is a need for baseline data on all of the USN and USCG equipment intended for installation of these accelerometers. A “high” vibration is defined as just that: a vibration that is higher than the original design was intended to vibrate. Having a baseline

7.4 Future Platform Tests

In addition to continued diagnostic tests, more platform tests need to be conducted to increase the fidelity of the data pool and test the hardware and software capabilities of the CAPTCHAs.

Like on the National Security Cutters, sets of ships of the same hull need to be examined for vibrations and comparative analysis. The National Security Cutters proved to have fruitful results, comparing one ship to another with the same type of equipment in the same spaces with the same ship layout. Running the same tests in parallel provides a consistent test subject with the most controllable test parameters.

USN ships recommended as test platforms include the DDG 51 ARLEIGH BURKE Class destroyers of the same flight, the CG 47 TICONDEROGA Class cruisers, and possibly the FFG 7 OLIVER HAZARD PERRY Class frigates. At least two of these ships can be found inport at any Naval Base at a given time, allowing for ease of access. Legacy ships, these vessels have been commissioned for several years and have already settled into operating routines- ie- no brand new equipment or testing equipment as seen on the LCS. Additionally, these three combatants were built with vibration mounts to reduce the noise emanating from the equipment and through the hull to the ocean. This means that data can be gathered on equipment and analyzed for mounting issues. USCG cutters recommended as test platforms include the Famous Class Cutters, Reliance Class Cutters, or the National Security Cutters. Each of these three classes are robust enough to provide sets of test models to collect data from and can be found on both coasts.

Furthermore, increasing the test locations would also be beneficial to the data collection process. About fifty percent of the data collected thus far from the USN and USCG ships have been taken while the ships were inport at discrete times. While

inport, ships turn off major propulsion and generation equipment and run only the necessary pumps and auxiliary equipment needed to keep the ship minimally operating. These conditions do not simulate the actual operating modes of the ship and thus the equipment. Vibrations may be increased or excited when the ship is full operational mode. As such, the ships should be tested inport, but also underway.

In addition to collecting more detailed discrete diagnostic testing on ships, it would be beneficial to collect diagnostic data over a given period of time. What changes are seen in an imbalanced fan over time? Can a bent shaft signature resemble a misalignment over time?

In an ideal situation, two similar ships would be able to take the CAPTCHAs underway for a patrol or deployment to monitor equipment degradation over time. In this way, the VAMPIRE development and analysis team could see the effects of equipment at sea and inport, compare different loading conditions, notice transients on the equipment, and have hulls to compare.

7.5 Steady State Analysis

Currently, the VAMPIRE project focuses on the spin-down of the motor to diagnose vibrations as seen in the whisker diagnostic tool. However, as seen in the LPD data and the LCS data, not all motors produce a discernable spin-down. The spin-down could show up very faint in the spectrum analysis or alias frequencies could interfere with the primary spin-down frequency.

The steady state time-series of a piece of equipment allows for quick comparison between a baseline motor and the affected or tested motor as seen in Figure 93. One can clearly see that during steady state, the top ventilation fan on the USCGC BETHOLF has lower vibration amplitudes than the bottom ventilation fan located in the same space. In the future, the steady state may also provide clues to the type of vibration. More analysis would be needed to delve into the data provided in a steady state signature of a particular motor.

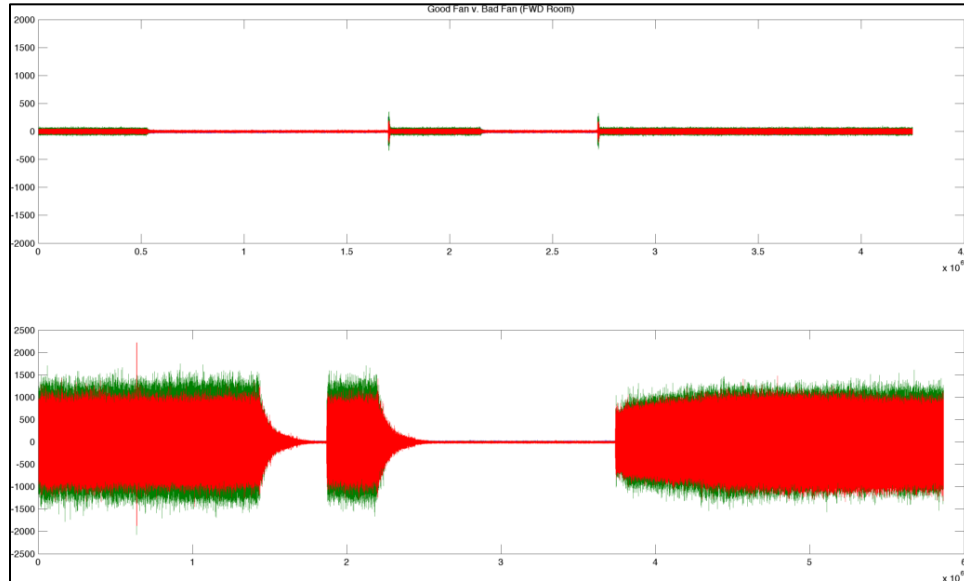


Figure 93: Steady State Comparison Between Two BERTHOLF Ventilation Fans. Good Fan (top) vs Bad Fan (bottom) (Appendix 9.2.6).

7.5 Hardware & Software Capabilities

Although this thesis deals mainly with the data processing and analysis portion of the VAMPIRE project, there are still some hardware and software strides that need to be made in order to be fully implemented in USN and USCG ships. The current CAPTCHAs are lithium battery-powered and are affixed to the equipment via command strips. For long term use, the LEES team is still working on the wireless and self-power harvesting capability. This will allow the accelerometers to be permanently installed inside the terminal box without the need for power replacement (ie-batteries) or cumbersome, expensive wiring.

Although not part of the initial VAMPIRE proposal, the information from the accelerometers could supplement the current ICAS system USN ships use today. If the software from the VAMPIRE accelerometers were compatible with the ICAS software, the accelerometers would not only provide immediate feedback to the crew for repair and parts replacement, but could also provide valuable data for distance support and maintenance facilities.

8.0 Conclusions and Recommendations

The VAMPIRE monitoring system clearly has the potential to simplify shipboard monitoring and maintenance. This potential is strengthened by the concept that the CAPTCHAs, tested in the current state, can record and, utilizing the whisker diagnostic tool, make observations about the source of vibrations for various rotating equipment. These early success stories support continued research on USN and USCG ships for detailed diagnostic and data analysis in an effort to enhance CBM, safeguard the maintenance budget, and assist in maintaining the high OPTEMPO of these two fleets.

Although the CAPTCHAs have been used to monitor vibrations in the lab and various commissioned USN and USCG ships, the next step in research is to conduct controlled testing on several sets of similar-hulled ships over long periods of time to collect and analysis equipment operations over time. Ongoing efforts should be aimed at increasing robustness of the data and designing a tool to examine the steady state of the equipment when a spin-down is inadequate.

9.0 Appendices

9.1 Background of Vibration Mounts

Vibration Mounts:

A rotating eccentric mass will generate a centrifugal force on its center pivot at a frequency of 1 times the turning speed. The direction of this force is radially outward, and its magnitude is calculated by the following formula:

$$F = I_m r \omega^2$$

where F is the imbalance force, I_m is equal to the mass, r is its distance from the pivot, and ω is the angular frequency, equal to 2π the frequency in Hz. If the structure holding the bearings in such a system is infinitely rigid as seen in Figure 94 and Figure 95, the center of rotation is constrained from moving and the centripetal force resulting from the imbalance can be found from the above equation.



Figure 94: Rigidly Mounted Rotating System (Ex. Fan).

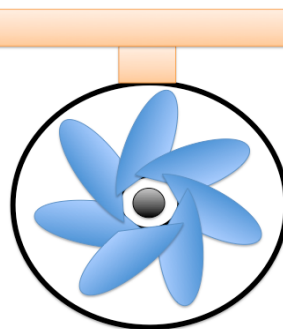


Figure 95: Cut Away of the Fan Rigidly Mounted Fan.

However, when the bearings are not rigidly constrained as seen in Figure 96, the shaft centerline is not constrained and the rotor will rotate around its center of gravity. The 1 x RPM force on the bearings will be very small. The double amplitude of vibration of the bearings will be equal to twice the distance between the center of gravity and the centerline of the rotor. Additionally, the bearing vibration is constant regardless of the rotor speed, provided the speed is higher than the natural frequency of the spring-rotor system.



Figure 96: Spring Mounted Rotating System (Ex. Vibration Mounted Fan).

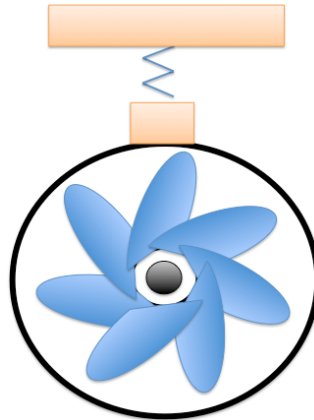


Figure 97: Cut Away of the Spring Mounted Fan.

At speeds below the natural frequency, the system is said to be “spring-controlled” and the centripetal force formula holds. Speeds above the natural frequency are in the “mass-controlled” region where the amplitude is constant and the bearing forces are not so easily predictable, be dependent on the equivalent mass of the bearing and springs [17].

9.2 Data Summary

The following sections summarize the equipment sampled, the type of device used to measure the vibrations, and the location of the data. The following is a quick overview of the data in the Appendix:

9.2.1- Table of Experimental Information including ship visited, accelerometer used, equipment tested, background information on the equipment, focus of the test, fidelity of the data, and data location.

9.2.2- MATLAB code, 'spindown_fitter.m', of the Whisker Diagnostic Tool developed by Chris Schantz. Code needed to process the motor spin-down.

9.2.3- MATLAB code, 'VAMPIRELabData.m' developed using the data collected from the LEES Coast Guard fan during the initial VAMPIRE experiments implementing the Whisker Diagnostic Tool. The data file, 'JohnLabData.mat', is made up of a two-columned vector, one the X-axis and the other the Y-axis. The data was recorded with LabJack and sampled at 8000 Hz.

9.2.4- MATLAB code, 'WhiskersLab.m', developed using the data collected from the LEES Coast Guard fan experiments that incite an imbalance in the motor and a loose mounting condition. This code takes this data and implements the Whisker Diagnostic Tool. The first set of data, 'Labtests.mat', is made up of two files. LABTEST 1 is made up of the baseline run (window: 3×10^5 : 4.1×10^5) and LABTEST 2 is made up of the wire rapped around the rotor blade run. The second set of data, 'LabTest2.mat' is made up of four variables. LAB1MTLOOSE represents the test conducted with one mount loose on the fan. LAB2MTLOOSE represents the test conducted with two mounts loose. LABALLLOOSE represents all the mounts on the fan loosened. Finally, LABBASELINE is the baseline run conducted before the mounts were loosened. All of these files are four column vectors equal to [Time X-Axis Y-Axis Z-Axis] in respect to the CAPTCHA orientation.

9.2.5- MATLAB code, 'Whiskers.m', developed using the data collected from the USCGC SENECA visits. This code imports data from three CAPTCHAs, 'CAPTCHA0308.mat' (Terminal box), 'CAPTCHA0411.mat' (Base of the fan), and 'CAPTCHA0D0B.mat' (Side structure) placed on the forward ventilation fan on the 20MAR2013 visit. During this visit, a wire was wrapped around a rotor blade and the base mounts were clamped. The code also incorporates data, 'SENECA29MARVISIT.mat', from the second visit to the SENECA on 29MAR2013 collected from the same ventilation fan. This set of data contains three sets of data collected from CAPTCHAs placed on the terminal box, base of the fan, and side structure of the fan.

9.2.6- MATLAB code, 'WhiskersNSCFans.m', developed using the data collected from USCGC BERTHOLF and USCGC STRATTON visits. This code imports data, 'NSCWhiskers.mat', from the tests conducted on ventilations fans on both NSCs. 'BottomFanBERT' and 'TopFanBERT' are two variables made up four column

vectors [time x-axis y-axis z-axis]. The same is the case for the 'BottomFanSTRATTON' and 'TopFanSTRATTON' variables.

9.2.7 MATLAB code, 'WhiskersDDG.m', developed using the data collected from USS MICHAEL MURPHY visit. This code calls upon data, 'DDGdata.mat', which is the transient data for Fire Pumps 2, 3, and 5. These were the only fire pump sets of data collected on the MURPHY with CAPTCHAs. The data consists of three four columned variables for 'FP1' as Fire Pump #1, 'FP2' as Fire Pump #2, and 'FP5' as Fire Pump #5.

9.2.8 MATLAB code, 'LCSVibes.m', developed using the data collected from USS INDEPENDENCE visit. This code graphs the two fire pumps monitored during the ship visit in a logarithmic scale to access the high vibes. The LCS data was unable to be seen clearly enough to use the whisker diagnostic tool.

9.2.1 Experimental Summary

The following table outlines the work completed over the past year and the location of the data. Dr. Steve Leeb has an electronic copy of all files. Additionally, the files are stored on Bucket. Each data file is a single .mat file made up of four columns of data set up as [Time X-Axis Y-Axis Z-Axis] with respect to the accelerometers orientation. The LabJack, recording the original VAMPIRE data, is the only exception with single files of two columns [X-Axis Y-Axis]. The data is sorted by equipment and accelerometer used during the test (ex. CAPTCHA 0411 or GCDC 2060) as denoted in the table.

The Labjack was set to read its bipolar -5 to 5 volt range (actually 5.07 to -5.18 volts) with 12 bit accuracy, but it streams 16 bit numbers for the data file. The ADXL has a 0 to 5 volt analog output corresponding to a range of plus or minus 1.7g nominally (0.68 g per volt). In order to convert the data to g's, first convert the data to voltage, then voltage to gravities:

$$Volts = \frac{Bits * 10.25}{65536} \tag{4}$$

Then, multiply by 0.68 g/volt to get units of gravities.

$$G = \frac{Bits * 10.25}{65536} * 0.68 \tag{5}$$

The value of 0 gravities is 2.5 volts, so this can be used to remove the mean of the measurement.

The accelerometer in the CAPTCHA provides digital values where the least significant bit corresponds to 0.0039 g. So the conversion formula is:

$$G = Bits * 0.0039$$

(6)

The sensitivity range of the device is configurable, with its maximum range of plus minus 16g, but all settings maintain the 0.0039 scale factor. The CAPTCHA was set to full range plus or minus 16g for all tests. As before, determining the mean 0g value is a matter of calibration and usually not required for vibration monitoring purposes.

The Gulf Coast accelerometers provides digital values where the least significant bit corresponds to 0.000977 g. So the conversion formula is:

$$G = Bits * 0.000977$$

The sensitivity range of the device is plus or minus 16g, but all settings maintain the 0.000977 scale factor. The Gulf Coast was set to full range plus minus 16g for all tests. As before determining the mean 0g value is a matter of calibration and usually not required for vibration monitoring purposes.

VAMPIRE Data Directory

Ship Name	Equipment	Accel. Location	Accelerometer #	Sampling Frequency	File Name	Variable Name	Testing/Other Info
VAMPIRE	Coast Guard Fan	Side of Fan	LabJack reading analog ADXL 203	8000 Hz	m1_baseline.mat	X,Y	Baseline on Motor 1, Motor 2 off
			LabJack reading analog ADXL 204		m1_baseline_m2_on.mat	X,Y	Motor 1 on, Motor 2 on
			LabJack reading analog ADXL 205		m1_loose.mat	X,Y	Motor 1 on, loose mount
			LabJack reading analog ADXL 206		m1_screw.mat	X,Y	Motor 1 on, screw imbalance
			LabJack reading analog ADXL 207		m1_screw_m2_on.mat	X,Y	Motor 1 on, Motor 2 on, screw imbalance
			LabJack reading analog ADXL 208		m1_screwnut.mat	X,Y	Motor 1 on, screw and nut imbalance
			LabJack reading analog ADXL 209		m1_screwnut_m2_on.mat	X,Y	Motor 1 on, Motor 2 on, screw and nut imbalance

Lab Data Directory

Ship Name	Equipment	Accel. Location	Accelerometer #	Sampling Frequency	File Name	Variable Name	Testing/Other Info
Lab	Coast Guard Fans	Side of Fan	CAPTCHA	3200 Hz	LABTEST1.mat (3*10^5:4.1*10^5)	Time, X, Y, Z	Baseline
					LABT2.mat	Time, X, Y, Z	Wire Wrapped Around Rotor Blade
					LABT3.mat	Time, X, Y, Z	One Mount Loose
					LABT4.mat	Time, X, Y, Z	Two Mounts Loose
					LABT5.mat	Time, X, Y, Z	All Four Mounts Loose
					LABT6.mat	Time, X, Y, Z	Baseline

SENECA Data Directory

Ship Name	Equipment	Accel. Location	Accelerometer #	Sampling Frequency	File Name	Variable Name	Testing/Other Info
SENECA	Fwd Ventilation Fan	Deck	CAPTCHA 0DOB	3200 Hz	DECK1.mat	Time, X, Y, Z	Baseline
					DECK2.mat	Time, X, Y, Z	One Loose Mount
					DECK3.mat	Time, X, Y, Z	Two Loose Mounts
					DECK4.mat	Time, X, Y, Z	All Four Loose Mounts
					DECK5.mat	Time, X, Y, Z	Four Loose Mounts, 2 Clamped
					DECK6.mat	Time, X, Y, Z	Baseline
					DECK7.mat	Time, X, Y, Z	All Four Mounts Clamped
	Fwd Ventilation Fan	Side Structure	CAPTCHA 0411	3200 Hz	SS1.mat	Time, X, Y, Z	Baseline
					SS2.mat	Time, X, Y, Z	One Loose Mount
					SS3.mat	Time, X, Y, Z	Two Loose Mounts
					SS4.mat	Time, X, Y, Z	All Four Loose Mounts
SS5.mat					Time, X, Y, Z	Four Loose Mounts, 2 Clamped	
SS6.mat					Time, X, Y, Z	Baseline	
SS7.mat					Time, X, Y, Z	All Four Mounts Clamped	
Fwd Ventilation Fan	Terminal Box	CAPTCHA 0308	3200 Hz	TB1.mat	Time, X, Y, Z	Baseline	
				TB2.mat	Time, X, Y, Z	One Loose Mount	
				TB3.mat	Time, X, Y, Z	Two Loose Mounts	
				TB4.mat	Time, X, Y, Z	All Four Loose Mounts	
				TB5.mat	Time, X, Y, Z	Four Loose Mounts, 2 Clamped	
				TB6.mat	Time, X, Y, Z	Baseline	
				TB7.mat	Time, X, Y, Z	All Four Mounts Clamped	
Fwd Ventilation Fan	Terminal Box	CAPTCHA 0308	3200 Hz	TERMBOX1	Time, X, Y, Z	Baseline	
				TERMBOX2	Time, X, Y, Z	All Four Mounts Clamped with Wood	
				TERMBOX3	Time, X, Y, Z	Left side only clamped	
				TERMBOX4	Time, X, Y, Z	Forward two mounts clamped.	
				TERMBOX5	Time, X, Y, Z	Back Corner Only Clamped	
				TERMBOX6	Time, X, Y, Z	One Side Clamped with metal	
				TERMBOX7	Time, X, Y, Z	Wire Around Rotor Blade	
				TERMBOX8	Time, X, Y, Z	Wire Wrapped on blade, all four mounts clamped	
				TERMBOX9	Time, X, Y, Z	Wire Wrapped on blade, forward two mounts clamped	
				TERMBOX10	Time, X, Y, Z	Wire Wrapped on blade, one mounted clamped	
				TERMBOX11	Time, X, Y, Z	Wire Wrapped on blade, one mout clamped with wood	
Fwd Ventilation Fan	Base	CAPTCHA 0411	3200 Hz	BASE1	Time, X, Y, Z	Baseline	
				BASE2	Time, X, Y, Z	All Four Mounts Clamped with Wood	
				BASE3	Time, X, Y, Z	Left side only clamped	
				BASE4	Time, X, Y, Z	Forward two mounts clamped.	
				BASE5	Time, X, Y, Z	Back Corner Only Clamped	
				BASE6	Time, X, Y, Z	One Side Clamped with metal	
				BASE7	Time, X, Y, Z	Wire Around Rotor Blade	
				BASE8	Time, X, Y, Z	Wire Wrapped on blade, all four mounts clamped	
				BASE9	Time, X, Y, Z	Wire Wrapped on blade, forward two mounts clamped	
				BASE10	Time, X, Y, Z	Wire Wrapped on blade, one mounted clamped	
				BASE11	Time, X, Y, Z	Wire Wrapped on blade, one mout clamped with wood	
Fwd Ventilation Fan	Side Structure	CAPTCHA 0DOB	3200 Hz	STRUCTURE1	Time, X, Y, Z	Baseline	
				STRUCTURE2	Time, X, Y, Z	All Four Mounts Clamped with Wood	
				STRUCTURE3	Time, X, Y, Z	Left side only clamped	
				STRUCTURE4	Time, X, Y, Z	Forward two mounts clamped.	
				STRUCTURE5	Time, X, Y, Z	Back Corner Only Clamped	
				STRUCTURE6	Time, X, Y, Z	One Side Clamped with metal	
				STRUCTURE7	Time, X, Y, Z	Wire Around Rotor Blade	
				STRUCTURE8	Time, X, Y, Z	Wire Wrapped on blade, all four mounts clamped	
				STRUCTURE9	Time, X, Y, Z	Wire Wrapped on blade, forward two mounts clamped	
				STRUCTURE10	Time, X, Y, Z	Wire Wrapped on blade, one mounted clamped	
				STRUCTURE11	Time, X, Y, Z	Wire Wrapped on blade, one mout clamped with wood	

SENECA (Continued)

Ship Name	Equipment	Accel. Location	Accelerometer #	Sampling Frequency	File Name	Variable Name	Testing/Other Info
SENECA	Aft Armory Fan	Terminal Box	CAPTCHA 0308	3200 Hz	ATERM1	Time, X, Y, Z	Baseline
					ATERM2	Time, X, Y, Z	Mount Clamped
					ATERM3	Time, X, Y, Z	Start at Slow speed, nothing clamped
					ATERM4	Time, X, Y, Z	High speed, nothing clamped
					ATERM5	Time, X, Y, Z	Mount clamped with metal
	Aft Armory Fan	Terminal Box	CAPTCHA 0308	3200 Hz	ABASE1	Time, X, Y, Z	Baseline
					ABASE2	Time, X, Y, Z	Mount Clamped
					ABASE3	Time, X, Y, Z	Start at Slow speed, nothing clamped
					ABASE4	Time, X, Y, Z	High speed, nothing clamped
					ABASE5	Time, X, Y, Z	Mount clamped with metal

BERTHOLF Data Directory

Ship Name	Equipment	Accel. Location	Accelerometer #	Sampling Frequency	File Name	Variable Name	Testing/Other Info
BERTHOLF	Helo Hangar Fan (1-14-2)	Terminal Box	CAPTCHA 0900	3200 Hz	HHBERT.mat	Time, X,Y,Z	
	FWD Supply Ventilation Fan (1-42-4)	Terminal Box	CAPTCHA 0D0B	3200 Hz	FWDTOPBERT.mat	Time, X,Y,Z	
	FWD Supply Ventilation Fan (1-42-2)	Terminal Box	CAPTCHA 0411	3200 Hz	FWDBOTTOMBERT.mat	Time, X,Y,Z	
	Chill Water Pump #1	Terminal Box	CAPTCHA 0308	3200 Hz	CW1BERT.mat	Time, X,Y,Z	
	Chill Water Pump #2	Terminal Box	CAPTCHA 0D0B	3200 Hz	CW2BERT.mat	Time, X,Y,Z	
	Chill Water Pump #3	Terminal Box	CAPTCHA 0411	3200 Hz	CW3BERT.mat	Time, X,Y,Z	
	Fire Pump #1	Terminal Box	CAPTCHA 0411	3200 Hz	FP1BERT.mat	Time, X,Y,Z	

STRATTON Data Directory

Ship Name	Equipment	Accel. Location	Accelerometer #	Sampling Frequency	File Name	Variable Name	Testing/Other Info
STRATTON	Helo Hangar Fan (1-14-2)	Terminal Box	CAPTCHA 0411	3200 Hz	HHSTRAT.mat	Time, X,Y,Z	
	FWD Supply Ventilation Fan (1-42-4)	Terminal Box	CAPTCHA 0D0B	3200 Hz	FWDTOPSTRAT.mat	Time, X,Y,Z	
	FWD Supply Ventilation Fan (1-42-2)	Terminal Box	CAPTCHA 0411	3200 Hz	FWDBOTTOMSTRAT.mat	Time, X,Y,Z	
	Chill Water Pump #1	Terminal Box	CAPTCHA 0411	3200 Hz	CW1STRAT.mat	Time, X,Y,Z	
	Chill Water Pump #2	Terminal Box	CAPTCHA 0D0B	3200 Hz	CW2STRAT.mat	Time, X,Y,Z	
	Chill Water Pump #3	Terminal Box	CAPTCHA 0308	3200 Hz	CW3STRAT.mat	Time, X,Y,Z	
	Fire Pump #1	Terminal Box	CAPTCHA 0D0B	3200 Hz	FP1TERMSTRAT.mat	Time, X,Y,Z	
	Fire Pump #1	Structure	CAPTCHA 0308	3200 Hz	FP1STRUCSTRAT.mat	Time, X,Y,Z	
	Fire Pump #1	Piping	CAPTCHA 0411	3200 Hz	FP1PIPESTRAT.mat	Time, X,Y,Z	
	Fire Pump #1	Terminal Box	CAPTCHA 0D0B	3200 Hz	FP1TERMSTRATB.mat	Time, X,Y,Z	
	Sea Water Cooling Pump #2	Terminal Box	CAPTCHA 0308	3200 Hz	ASWP2STRAT.mat	Time, X,Y,Z	
	Sea Water Cooling Pump #3	Terminal Box	CAPTCHA 0D0B	3200 Hz	ASWP3STRAT.mat	Time, X,Y,Z	

MICHAEL MURPHY Data Directory

Ship Name	Equipment	Accel. Location	Accelerometer #	Sampling Frequency	File Name	Variable Name	Testing/Other Info
DDG 112	Fire Pump #2	Terminal Box	CAPTCHA 0308	3200 Hz	FP2.mat	Time, Ax,Ay, Az	
	Fire Pump #3	Terminal Box	CAPTCHA 0D0B	3200 Hz	FP3.mat	Time, Ax,Ay, Az	
	Fire Pump #5	Terminal Box	CAPTCHA 0411	3200 Hz	FP5.mat	Time, Ax,Ay, Az	
	Fire Pump 1	Terminal Box	GCDC 2322	200 Hz	GC2322.mat	Time, Ax,Ay, Az	
	Fire Pump 1	Upper Foundation	GCDC 2054	200 Hz	GC2054.mat	Time, Ax,Ay, Az	
	Fire Pump 1	Lower Foundation	GCDC 2065	200 Hz	GC2065.mat	Time, Ax,Ay, Az	
	Fire Pump 2	Terminal Box	GCDC 2438	200 Hz	GC2438.mat	Time, Ax,Ay, Az	
	Fire Pump 3	Terminal Box	GCDC 2069	200 Hz	GC2069.mat	Time, Ax,Ay, Az	
	Fire Pump 4	Terminal Box	GCDC 2436	200 Hz	GC2436.mat	Time, Ax,Ay, Az	
	Fire Pump 5	Terminal Box	GCDC 2060	200 Hz	GC2060.mat	Time, Ax,Ay, Az	
	Fire Pump 5	Pump End	GCDC 2057	200 Hz	GC2057.mat	Time, Ax,Ay, Az	
	Fire Pump 6	Terminal Box	GCDC 2079	200 Hz	GC2079.mat	Time, Ax,Ay, Az	

INDEPENDENCE Data Directory

Ship Name	Equipment	Accel. Location	Accelerometer #	Sampling Frequency	File Name	Variable Name	Testing/Other Info
LCS 2	Fire Pump 1	Terminal Box	CAPTCHA 0805	3200 Hz		N/A	No data
	Fire Pump 1	Terminal Box	CAPTCHA 0411	3200 Hz	FP1_LCS.mat	Time, AX, AY, AZ	
	Fire Pump 1	Discharge	CAPTCHA 0E0C	3200 Hz		N/A	No data
	Fire Pump 1		GCDC 2079	200 Hz	GC2079LCS.mat	Time, AX,AY,AZ	Steady State only
	Fire Pump 2	Terminal Box	CAPTCHA 0D0B	3200 Hz	N/A		No data collected
	Fire Pump 2	Terminal Box	GCDC 2057	200 Hz	GC2057LCS.mat	Time, AX,AY,AZ	Garbage
	Fire Pump 3	Terminal Box	CAPTCHA 0900	3200 Hz	FP3_LCS.mat	Time, AX, AY, AZ	
	Fire Pump 3	Terminal Box	GCDC 2060	200 Hz	GC2060LCS.mat	Time, AX,AY,AZ	Steady State/Off
	HAVC	Terminal Box	GCDC 2065	200 Hz	GC2065LCS.mat	Time, AX,AY,AZ	Steady State only
	Sewage Vac Pump 1	Terminal Box	GCDC 2079_2	200 Hz	GC20792LCS.mat	Time, AX, AY, AZ	Transients
	Sewage Vac Pump 2	Terminal Box	GCDC 2054	200 Hz	GC2054LCS.mat	Time, AX, AY, AZ	Steady State only
	Lube Oil Pump 1	Terminal Box	CAPTCHA 0E0C_2	3200 Hz	N/A		No data
	Lube Oil 1	Terminal Box	CAPTCHA 0900_2	3200 Hz	N/A		No data
	Lube Oil 1	Terminal Box	CAPTCHA 0D0B_2	3200 Hz	N/A		No data
	Lube Oil Pump 2	Terminal Box	CAPTCHA 0411_2	3200 Hz	N/A		No data

SAN DIEGO Data Directory

Ship Name	Equipment	Accel. Location	Accelerometer #	Sampling Frequency	File Name	Variable Name	Testing/Other Info
SAN DIEGO	Fire Pump 1	Terminal Box	GCDC 2337	200 Hz	GC2337LPD.mat	Time, AX, AY, AZ	Turn-On/Steady State
	Fire Pump 1	Terminal Box	CAPTCHA 0308_2	3200 Hz	Fire Pump 1 CAPTCHA 0308_2.xls	Time, AX, AY, AZ	Steady State Only
	Fire Pump 1	Hull Plate	GCDC 2068	200 Hz	GC2068LPD.mat	Time, AX, AY, AZ	No Transients
	Fire Pump 1	Hull Plate	CAPTCHA 0900_2	3200 Hz	N/A		No good data
	Fire Pump 2	Terminal Box	GCDC 2331	200 Hz	GC2331LPD.mat	Time, AX, AY, AZ	Steady State Only
	Fire Pump 3	Terminal Box	GCDC 2065	200 Hz	GC2065LPD.mat	Time, AX, AY, AZ	Steady State Only
	Fire Pump 4	Terminal Box	GCDC 2079	200 Hz	GC2079LPD.mat	Time, AX, AY, AZ	Steady State Only
	Fire Pump 4	Mount	CAPTCHA 0411	3200 Hz	FP4 CAPTCHA0411.xls	Time, X, Y, Z	Possible Spin-Down (loud diessels)
	Fire Pump 5	Terminal Box	GCDC 2060	200 Hz	GC2060LPD.mat	Time, AX, AY, AZ	Steady State Only
	Main Sea Water Pump 1B	Terminal Box	CAPTCHAv2	3200 Hz	N/A		No good data
	Aux SW Pump 1	Terminal Box	CAPTCHA 020B	3200 Hz	N/A		No good data
	Aux SW Pump 1	Mount	CAPTCHA 0E0C	3200 Hz	N/A		No good data
	Fire Pump 6	Terminal Box	GCDC 2057	200 Hz	GC2057LPD.mat	Time, AX, AY, AZ	Spin-Down, Steady Sate
	Fire Pump 7	Terminal Box	GCDC 2069	200 Hz	GC2069LPD.mat	Time, AX, AY, AZ	Steady State Only
	Fire Pump 8	Terminal Box	GCDC 2436	200 Hz	GC2436LPD.mat	Time, AX, AY, AZ	Steady State Only
	Fire Pump 9	Terminal Box	GCDC2438	200 Hz	N/A		No good data
	Fire Pump 10	Terminal Box	GCDC 2054	200 Hz	GC2054LPD.mat	Time, AX, AY, AZ	Steady State Only
	Fire Pump 10	Terminal Box	CPATCHA 0900	3200 Hz	Fire Pump 10 CAPTCHA 0900.xls	Time, X, Y, Z	Turn-On/Steady State
	Fire Pump 10	Motor Frame	CAPTCHA 0308	3200 Hz	Fire Pump 10 Motor Frame.xls	Tmie, X,Y, A	Turn-On/Steady State

9.2.2 Whisker Diagnostic Tool

```
function [data_whisker pre_whisker post_whisker speed_freq
friction_params, motor_stop_time, motor_stop_ind] =
spindown_fitter(data, fs, nominal_rpm, friction_params)

whisker_length = 15; %in seconds

if size(data,2) == 4
    temp = mean(data(:,2:4),2);
    mask = isnan(temp);
    data(mask,:) = [];
    data(:,2) = data(:,2)-mean(data(:,2));
    data(:,3) = data(:,3)-mean(data(:,3));
    data(:,4) = data(:,4)-mean(data(:,4));
    X = data(:,2);
elseif size(data,2) == 1
    data(isnan(data)) = [];
    data = data - mean(data);
    X = data;
else
    error('data input vector wring size, needs to be a colomn vector
with 1 or 4 columns');
end
```

```

max_freq = round(nominal_rpm/60*1.5);

[S F T] = spectrogram(X,fs,round(0.9*fs),fs,fs);

[~, ind] = min(abs(F-max_freq));

imagesc(T,F(1:ind),log(abs(S(1:ind,:)))); axis xy; figure(gcf)
hold on;
disp('Please click turnoff time first, and then click whisker if
friction params not provided')
time = [];
speed = [];

[temp_time, temp_speed] = ginput(1);

hold off
close all

start_time = temp_time(1);

[~, start_ind] = min(abs(T-start_time));

spindown_span = max(start_ind-20, 1):start_ind+min(length(T)-
start_ind,round(whisker_length/mean(diff(T))));

imagesc(T(spindown_span),F(1:ind),log(abs(S(1:ind,spindown_span))));
axis xy; figure(gcf)
hold on;

[temp_time, temp_speed] = ginput(1);
start_time = temp_time(1);

[~, start_ind] = min(abs(T-start_time));

if nargin < 4 % friction params not provided

    while ~isempty(temp_time)
        time(end+1) = temp_time;
        speed(end+1) = temp_speed;
        plot(temp_time,temp_speed,'bo')
        [temp_time, temp_speed] = ginput(1);
    end

    time = time';
    speed = speed';

    time = time - time(1);

    params2 = lsqnonlin(@spindown_param2_model,[-0.01; -0.001]);
    a1 = params2(1);
    a2 = params2(2);

```

```

else
    speed = temp_speed;
    a1 = friction_params(1);
    a2 = friction_params(2);

end
friction_params(1) = a1;
friction_params(2) = a2;

spindown2 = @(t,x)a1.*x(1)+a2.*x(1).^2;

[tout, yout] = ode45(spindown2,T(start_ind):mean(diff(T)):T(end),
speed(1));

imagesc(T,F(1:ind),log(abs(S(1:ind,:)))); axis xy; figure(gcf)
hold on;
plot(tout, yout, '-k','LineWidth',2)
plot(tout, yout+3, ':k','LineWidth',2)
plot(tout, yout-3, ':k','LineWidth',2)

plot(tout-3, yout, '-m','LineWidth',2)
plot(tout-3, yout+3, ':m','LineWidth',2)
plot(tout-3, yout-3, ':m','LineWidth',2)

plot(tout+3, yout, '-g','LineWidth',2)
plot(tout+3, yout+3, ':g','LineWidth',2)
plot(tout+3, yout-3, ':g','LineWidth',2)

hold off

temp = load('LP_whisker_filter_coeficients.mat');
Num = temp.Num;

L_coef = length(Num); % need to append this much extra data to account
for filter transients

data_start_ind = round(start_time*fs);

% for output
motor_stop_time = start_time;
motor_stop_ind = data_start_ind;

data_time = (0:length(data)-1)/fs;

remaining_index = length(data)-data_start_ind-1-L_coef;
% if remaining_index < ((whisker_length+3)*fs) % not enough data
remaining, will need to use what remains.

trail_time = min(floor(remaining_index/fs), whisker_length);

data_ind = (data_start_ind-
L_coef):round(data_start_ind+trail_time*fs+L_coef);

```

```

[tout, speed_freq] =
ode45(spindown2,data_time(data_start_ind):1/fs:data_time(round(data_start_ind+trail_time*fs)), speed(1));

tout = data_time(data_ind)';

speed_freq = [speed_freq(1)*ones(L_coef,1); speed_freq;
speed_freq(end)*ones(L_coef,1)];

% figure
% plot(tout,speed_freq)

mixing_signal = exp(1i*cumtrapz(tout,2*pi*speed_freq));

if size(data,2) == 4

    data_signals = data(data_ind,2:4);
    pre_signals = data(data_ind-round(3*fs),2:4);

    data_whisker = [whisker(data_signals(:,1), mixing_signal),
whisker(data_signals(:,2), mixing_signal), whisker(data_signals(:,3),
mixing_signal)];
    pre_whisker = [whisker(pre_signals(:,1), mixing_signal),
whisker(pre_signals(:,2), mixing_signal), whisker(pre_signals(:,3),
mixing_signal)];

    if data_ind(end)+round(3*fs) > length(data)
        post_whisker = [];
    else
        post_signals = data(data_ind+round(3*fs),2:4);

        post_whisker = [whisker(post_signals(:,1), mixing_signal),
whisker(post_signals(:,2), mixing_signal), whisker(post_signals(:,3),
mixing_signal)];
    end
else

    data_signals = data(data_ind);
    pre_signals = data(data_ind-round(3*fs));

    data_whisker = [whisker(data_signals(:,1), mixing_signal)];
    pre_whisker = [whisker(pre_signals(:,1), mixing_signal)];

    if data_ind(end)+round(3*fs) > length(data)
        post_whisker = [];
    else

        post_signals = data(data_ind+round(3*fs));
        post_whisker = [whisker(post_signals(:,1), mixing_signal)];
    end
end

```



```

end

speed_freq = speed_freq(length(Num)+1:end-length(Num));

% figure
% plot(tout,real(mixing_signal));

% figure
% plot(tout,real(data_signal.*mixing_signal));

function W = whisker(signal, mixer)
    temp = signal.*mixer;
    tempF = filtfilt(Num,1,temp);
    tempW = tempF./mixer;
    W = tempW(length(Num)+1:end-length(Num));
end

function F = spindown_param2_model(params)
    a1 = params(1);
    a2 = params(2);
    spindown2 = @(t,x)a1.*x(1)+a2.*x(1).^2;
    [tout, yout] = ode45(spindown2,time, speed(1));
    F = speed-yout;
end

end

```

9.2.3 VAMPIRE MATLAB Code

```

clear
clc
close all

%% Lab Experiments that were run for the VAMPIRE Paper
load('JohnLabData.mat')

% m1_baseline
% m1_baseline_m2_on
% m1_loose
% m1_screw
% m1_screw_m2_on
% m1_screwnut
% m1_screwnut_m2_on

% m1_baseline= m1_baseline(4.75*10^5:5.6*10^5,:);
% % m1_baseline_m2_on= m1_baseline_m2_on(1.045*10^6:
1.15*10^6,:); % Motor 1 Spin-down
% m1_baseline_m2_on= m1_baseline_m2_on(4.5*10^5:
5.6*10^5,:); % Motor 2 Spin-down
% m1_loose= m1_loose(9.45*10^5:10.4*10^5,:);
% m1_screw= m1_screw(9.3*10^5:10.4*10^5,:);
% % m1_screw_m2_on= m1_screw_m2_on(4.5*10^5:5.4*10^6,:); % Motor 1
Spin-down (middle)
% m1_screw_m2_on= m1_screw_m2_on(1.05*10^6:1.15*10^6,:); % Motor 2

```

```

Spin-down (end)
% m1_screwnut=m1_screwnut(4.5*10^5:5.5*10^5,:);
% m1_screwnut_m2_on= m1_screwnut_m2_on(4.425*10^5: 5.6*10^5,:); %
Only have Motor 2 spin-down
%

fs= 8000;
nom_rpm= 3450;

% friction = friction = [-0.0202,   -0.0030]; % just a quick fit to TB1.
%M1= motor 1, M2= motor 2

% Baseline on M1
[data_w1, pre_w1, post_w1, ff1, friction1, stop_time1, stop_index1] =
spindown_fitter(m1_baseline(:,1), fs, nom_rpm);
% the outputs are form the pre (magenta), post (green), and "data"
(black)
% whiskers.

% Baseline spin-down for M2 when M1 is on
[data_w2, pre_w2, post_w2, ff2, friction2, stop_time2, stop_index2] =
spindown_fitter(m1_baseline_m2_on(:,1), fs, nom_rpm);

% M1 with Loose Bolts
[data_w3, pre_w3, post_w3, ff3, friction3, stop_time3, stop_index3] =
spindown_fitter(m1_loose(:,1), fs, nom_rpm);

%Screw Imbalance on M1
[data_w4, pre_w4, post_w4, ff4, friction4, stop_time4, stop_index4] =
spindown_fitter(m1_screw(:,1), fs, nom_rpm);

% Screw Imbalance: spin-down for M2 when M1 is on
[data_w5, pre_w5, post_w5, ff5, friction5, stop_time5, stop_index5] =
spindown_fitter(m1_screw_m2_on(:,1), fs, nom_rpm);

% Screw AND Nut Imbalance on M1
[data_w6, pre_w6, post_w6, ff6, friction6, stop_time6, stop_index6] =
spindown_fitter(m1_screwnut(:,1), fs, nom_rpm);

% Screw AND Nut Imbalance on Motor 1: spin-down for M2 when M1 is on
[data_w7, pre_w7, post_w7, ff7, friction7, stop_time7, stop_index7] =
spindown_fitter(m1_screwnut_m2_on(:,1), fs, nom_rpm);

% basic plot: does X,Y,Z
% If you only want one of those guys, then data_W is :, 1= x, :,2= Y, :,
3=
% Z
%% Baseline compared on Motor 1 when Motor is off and on

figure (2)
plot(ff1,abs(data_w1(:,1)), ff2,abs(data_w2(:,1)))
title('Baseline Lab Comparison with M2 OFF/ON- X Direction')
legend('M1 Baseline- M2 Off ', 'M2 Baseline- M1 On');
ylabel('Envelope Amplitude');
xlabel('Spindown frequency or speed (Hz or RPS)');

```

```

figure (3)
plot(ff1,abs(data_w1(:,2)), ff2,abs(data_w2(:,2)))
title('Baseline Lab Comparison with M2 OFF/ON- Y Direction')
legend('M1 Baseline- M2 Off ', 'M2 Baseline- M1 On');
ylabel('Envelope Amplitude');
xlabel('Spindown frequency or speed (Hz or RPS)');

figure (4)
plot(ff1,abs(data_w1(:,3)), ff2,abs(data_w2(:,3)))
title('Baseline Lab Comparison with M2 OFF/ON- Z Direction')
legend('M1 Baseline- M2 Off ', 'M2 Baseline- M1 On');
ylabel('Envelope Amplitude');
xlabel('Spindown frequency or speed (Hz or RPS)');

% Baseline compared to Loose Mount

figure (5)
plot(ff1,abs(data_w1(:,1)), ff3,abs(data_w3(:,1)))
title('Baseline vs Loose Mounts- X Direction')
legend('Baseline M1 (M2 OFF)', 'Loose Mounts');
ylabel('Envelope Amplitude');
xlabel('Spindown frequency or speed (Hz or RPS)');

figure (6)
plot(ff1,abs(data_w1(:,2)), ff3,abs(data_w3(:,2)))
title('Baseline vs Loose Mounts- Y Direction')
legend('Baseline M1 (M2 OFF)', 'Loose Mounts');
ylabel('Envelope Amplitude');
xlabel('Spindown frequency or speed (Hz or RPS)');

figure (7)
plot(ff1,abs(data_w1(:,3)), ff3,abs(data_w3(:,3)))
title('Baseline vs Loose Mounts- Z Direction')
legend('Baseline M1 (M2 OFF)', 'Loose Mounts');
ylabel('Envelope Amplitude');
xlabel('Spindown frequency or speed (Hz or RPS)');

% Baseline compared to Screw Imbalance

figure (8)
plot(ff1,abs(data_w1(:,1)), ff4,abs(data_w4(:,1)))
title('Baseline vs Screw Imbalance on M1 (M2 OFF)- X Direction')
legend('Baseline on Motor 1', 'Screw Imbalance on Motor 1');
ylabel('Envelope Amplitude');
xlabel('Spindown frequency or speed (Hz or RPS)');

figure (9)
plot(ff1,abs(data_w1(:,2)), ff4,abs(data_w4(:,2)))
title('Baseline vs Screw Imbalance on M1 (M2 OFF)- Y Direction')
legend('Baseline on Motor 1', 'Screw Imbalance on Motor 1');
ylabel('Envelope Amplitude');
xlabel('Spindown frequency or speed (Hz or RPS)');

figure (10)
plot(ff1,abs(data_w1(:,3)), ff4,abs(data_w4(:,3)))

```

```

title('Baseline vs Screw Imbalance on M1 (M2 OFF)- Z Direction')
legend('Baseline on Motor 1', 'Screw Imbalance on Motor 1');
ylabel('Envelope Amplitude');
xlabel('Spindown frequency or speed (Hz or RPS)');

% Baseline compared to Screw and Nut Imbalances

figure (11)
plot(ff1,abs(data_w1(:,1)), ff4,abs(data_w4(:,1)),
ff6,abs(data_w6(:,1)))
title('Baseline vs Screw Imbalance on M1(M1 ON/M2 OFF) - X Direction')
legend('Baseline on Motor 1', 'Screw Imbalance on Motor 1', 'Screw and
Nut Imbalance on Motor 1');
ylabel('Envelope Amplitude');
xlabel('Spindown frequency or speed (Hz or RPS)');

figure (12)
plot(ff1,abs(data_w1(:,2)), ff4,abs(data_w4(:,2)),
ff6,abs(data_w6(:,2)))
title('Baseline vs Screw Imbalance on M1(M1 ON/M2 OFF) - Y Direction')
legend('Baseline on Motor 1', 'Screw Imbalance on Motor 1', 'Screw and
Nut Imbalance on Motor 1');
ylabel('Envelope Amplitude');
xlabel('Spindown frequency or speed (Hz or RPS)');

figure (13)
plot(ff1,abs(data_w1(:,3)), ff4,abs(data_w4(:,3)),
ff6,abs(data_w6(:,3)))
title('Baseline vs Screw Imbalance on M1(M1 ON/M2 OFF) - Z Direction')
legend('Baseline on Motor 1', 'Screw Imbalance on Motor 1', 'Screw and
Nut Imbalance on Motor 1');
ylabel('Envelope Amplitude');
xlabel('Spindown frequency or speed (Hz or RPS)');

% Baseline compared to Loose and both imbalances

figure (14)
plot(ff1,abs(data_w1(:,1)), ff3,abs(data_w3(:,1)),
ff4,abs(data_w4(:,1)), ff6,abs(data_w6(:,1)))
title('Baseline vs Loose Mounts, Screw Imbalance and Screw and Nut
Imbalance- X Direction')
legend('Baseline on Motor 1', 'Loose Mounts', 'Screw Imbalance on Motor
1', 'Screw and Nut Imbalance on Motor 1');
ylabel('Envelope Amplitude');
xlabel('Spindown frequency or speed (Hz or RPS)');

figure (15)
plot(ff1,abs(data_w1(:,2)), ff3,abs(data_w3(:,2)),
ff4,abs(data_w4(:,2)), ff6,abs(data_w6(:,2)))
title('Baseline vs Loose Mounts, Screw Imbalance and Screw and Nut
Imbalance- Y Direction')
legend('Baseline on Motor 1', 'Loose Mounts', 'Screw Imbalance on Motor
1', 'Screw and Nut Imbalance on Motor 1');
ylabel('Envelope Amplitude');
xlabel('Spindown frequency or speed (Hz or RPS)');

figure (16)

```

```

plot(ff1,abs(data_w1(:,3)), ff3,abs(data_w3(:,3)),
ff4,abs(data_w4(:,3)), ff6,abs(data_w6(:,3)))
title('Baseline vs Loose Mounts, Screw Imbalance and Screw and Nut
Imbalance (M1 ON/M2 OFF)- Z Direction')
legend('Baseline on Motor 1', 'Loose Mounts', 'Screw Imbalance on Motor
1', 'Screw and Nut Imbalance on Motor 1');
ylabel('Envelope Amplitude');
xlabel('Spindown frequency or speed (Hz or RPS)');

```

```

%Effects on Motor 2

```

```

figure (17)
plot(ff2,abs(data_w2(:,1)), ff5,abs(data_w5(:,1)),
ff7,abs(data_w7(:,1)))
title('Baseline on M2 vs Spin-down of M2 during Screw Imbalance and
Screw+Nut Imbalance- X Direction')
legend('Baseline on Motor 2', 'Screw Imbalance on Motor 2', 'Screw and
Nut Imbalance on Motor 2');
ylabel('Envelope Amplitude');
xlabel('Spindown frequency or speed (Hz or RPS)');

```

```

figure (18)
plot(ff2,abs(data_w2(:,2)), ff5,abs(data_w5(:,2)),
ff7,abs(data_w7(:,2)))
title('Baseline on M2 vs Spin-down of M2 during Screw Imbalance and
Screw+Nut Imbalance- Y Direction')
legend('Baseline on Motor 2', 'Screw Imbalance on Motor 2', 'Screw and
Nut Imbalance on Motor 2');
ylabel('Envelope Amplitude');
xlabel('Spindown frequency or speed (Hz or RPS)');

```

```

figure (19)
plot(ff2,abs(data_w2(:,3)), ff5,abs(data_w5(:,3)),
ff7,abs(data_w7(:,3)))
title('Baseline on M2 vs Spin-down of M2 during Screw Imbalance and
Screw+Nut Imbalance- Z Direction')
legend('Baseline on Motor 2', 'Screw Imbalance on Motor 2', 'Screw and
Nut Imbalance on Motor 2');
ylabel('Envelope Amplitude');
xlabel('Spindown frequency or speed (Hz or RPS)');

```

```

%% Normalized Graphs
% "excitation normalized plot:
% Comparison Between Mounts

```

```

figure(20)
plot(ff1,abs(data_w1(:,1))./(ff1.^2), ff3,abs(data_w3(:,1))./(ff3.^2),
ff4,abs(data_w4(:,1))./(ff4.^2))
title('Baseline vs Loose Mounts and Screw Imbalance (Normalized
Spindown Whiskers)- X Direction');
legend('Baseline', 'All Mounts Loose', 'Screw Imbalance');
ylabel('Envelope Amplitude');
xlabel('Spindown frequency or speed (Hz or RPS)');

```

```

figure(21)
plot(ff1,abs(data_w1(:,2))./(ff1.^2), ff3,abs(data_w3(:,2))./(ff3.^2),
ff4,abs(data_w4(:,2))./(ff4.^2))

```

```

title('Baseline vs Loose Mounts and Screw Imbalance (Normalized
Spindown Whiskers)- X Direction');
legend('Baseline', 'All Mounts Loose', 'Screw Imbalance');
ylabel('Envelope Amplitude');
xlabel('Spindown frequency or speed (Hz or RPS)');

figure(22)
plot(ff1,abs(data_w1(:,3))./(ff1.^2), ff3,abs(data_w3(:,3))./(ff3.^2),
ff4,abs(data_w4(:,3))./(ff4.^2))
title('Baseline vs Loose Mounts and Screw Imbalance (Normalized
Spindown Whiskers)- X Direction');
legend('Baseline', 'All Mounts Loose', 'Screw Imbalance');
ylabel('Envelope Amplitude');
xlabel('Spindown frequency or speed (Hz or RPS)');

% Baseline vs all conditions

figure(23)
plot(ff1,abs(data_w1(:,1))./(ff1.^2), ff3,abs(data_w3(:,1))./(ff3.^2),
ff4,abs(data_w4(:,1))./(ff4.^2), ff6,abs(data_w6(:,1))./(ff6.^2))
title('Baseline vs Loose Mounts, Screw Imbalance, and Screw+Nut
Imbalance (Normalized Spindown Whiskers)- X Direction');
legend('Baseline', 'All Mounts Loose', 'Screw Imbalance', 'Screw and
Nut Imbalance');
ylabel('Envelope Amplitude');
xlabel('Spindown frequency or speed (Hz or RPS)');

figure(24)
plot(ff1,abs(data_w1(:,2))./(ff1.^2), ff3,abs(data_w3(:,2))./(ff3.^2),
ff4,abs(data_w4(:,2))./(ff4.^2), ff6,abs(data_w6(:,2))./(ff6.^2))
title('Baseline vs Loose Mounts, Screw Imbalance, and Screw+Nut
Imbalance (Normalized Spindown Whiskers)- Y Direction');
legend('Baseline', 'All Mounts Loose', 'Screw Imbalance', 'Screw and
Nut Imbalance');
ylabel('Envelope Amplitude');
xlabel('Spindown frequency or speed (Hz or RPS)');

figure(25)
plot(ff1,abs(data_w1(:,3))./(ff1.^2), ff3,abs(data_w3(:,3))./(ff3.^2),
ff4,abs(data_w4(:,3))./(ff4.^2), ff6,abs(data_w6(:,3))./(ff6.^2))
title('Baseline vs Loose Mounts, Screw Imbalance, and Screw+Nut
Imbalance (Normalized Spindown Whiskers)- Z Direction');
legend('Baseline', 'All Mounts Loose', 'Screw Imbalance', 'Screw and
Nut Imbalance');
ylabel('Envelope Amplitude');
xlabel('Spindown frequency or speed (Hz or RPS)');

% Baseline vs Conditions on Motor 2

figure(26)
plot(ff2,abs(data_w2(:,1))./(ff2.^2), ff5,abs(data_w5(:,1))./(ff5.^2),
ff7,abs(data_w7(:,1))./(ff7.^2))
title('Baseline on M2 vs Screw Imbalance on M2 and Screw+ Nut Imbalance
on M2 (Normalized Spindown Whiskers)- X Direction');
legend('Baseline for Motor 2', 'Screw Imbalance on Motor 2', 'Screw and
Nut Imbalance on Motor 2');
ylabel('Envelope Amplitude');

```

```

xlabel('Spindown frequency or speed (Hz or RPS)');

figure(27)
plot(ff2,abs(data_w2(:,2))./(ff2.^2), ff5,abs(data_w5(:,2))./(ff5.^2),
ff7,abs(data_w7(:,2))./(ff7.^2))
title('Baseline on M2 vs Screw Imbalance on M2 and Screw+ Nut Imbalance
on M2 (Normalized Spindown Whiskers)- Y Direction');
legend('Baseline for Motor 2', 'Screw Imbalance on Motor 2', 'Screw and
Nut Imbalance on Motor 2');
ylabel('Envelope Amplitude');
xlabel('Spindown frequency or speed (Hz or RPS)');

figure(28)
plot(ff2,abs(data_w2(:,3))./(ff2.^2), ff5,abs(data_w5(:,3))./(ff5.^2),
ff7,abs(data_w7(:,3))./(ff7.^2))
title('Baseline on M2 vs Screw Imbalance on M2 and Screw+ Nut Imbalance
on M2 (Normalized Spindown Whiskers)- Z Direction');
legend('Baseline for Motor 2', 'Screw Imbalance on Motor 2', 'Screw and
Nut Imbalance on Motor 2');
ylabel('Envelope Amplitude');
xlabel('Spindown frequency or speed (Hz or RPS)');

```

9.2.4 Lab MATLAB Code

```

clc
close all

%% Lab Runs- 29 MARCH 2013 and 5 APRIL 2013
load('Labtests.mat')
load('LabTest2.mat')

% Baseline= AX1(3.4*10^5:4.1*10^5)
% Two Wire Wraps= AX2

LT1= LABTEST1(3*10^5:4.1*10^5,:);

fs= 3200;
nom_rpm= 3450;

% friction = friction = [-0.0202, -0.0030]; % just a quick fit to TB1.
%
% Baseline in Lab- Before Loose Mounts
[data_w1, pre_w1, post_w1, ff1, friction1, stop_time1, stop_index1] =
spindown_fitter(LABBASLINE, fs, nom_rpm);
% the outputs are form the pre (magenta), post (green), and "data"
(black)
% whiskers.

% One Loose Mount
[data_w2, pre_w2, post_w2, ff2, friction2, stop_time2, stop_index2] =
spindown_fitter(LAB1MTLOOSE, fs, nom_rpm);

% Two Loose Mounts
[data_w3, pre_w3, post_w3, ff3, friction3, stop_time3, stop_index3] =
spindown_fitter(LAB2MTLOOSE, fs, nom_rpm);

% All Four Loose Mounts

```

```

[data_w4, pre_w4, post_w4, ff4, friction4, stop_time4, stop_index4] =
spindown_fitter(LABALLLOOSE, fs, nom_rpm);

% % Baseline Recalibration- Before Wire Test
[data_w6, pre_w6, post_w6, ff6, friction6, stop_time6, stop_index6] =
spindown_fitter(LT1, fs, nom_rpm);

% Wire Wrapped Around Fan
[data_w7, pre_w7, post_w7, ff7, friction7, stop_time7, stop_index7] =
spindown_fitter(LABTEST2, fs, nom_rpm);

% basic plot: does X,Y,Z
% If you only want one of those guys, then data_W is :, 1= x, :,2= Y, :,
3=
% Z

% Baseline compared to sequential Loosing of All Mounts
figure (2)
plot(ff1,abs(data_w1(:,1)), ff2,abs(data_w2(:,1)),
ff3,abs(data_w3(:,1)), ff4,abs(data_w4(:,1)))
title('Baseline vs Sequential Loosening of the Mounts- X Direction')
legend('Baseline', '1 Mount Loose', '2 Mounts Loose', 'All Four Mounts
Loose');
ylabel('Envelope Amplitude');
xlabel('Spindown frequency or speed (Hz or RPS)');

figure (3)
plot(ff1,abs(data_w1(:,2)), ff2,abs(data_w2(:,2)),
ff3,abs(data_w3(:,2)), ff4,abs(data_w4(:,2)))
title('Baseline vs Sequential Loosening of the Mounts- Y Direction')
legend('Baseline', '1 Mount Loose', '2 Mounts Loose', 'All Four Mounts
Loose');
ylabel('Envelope Amplitude');
xlabel('Spindown frequency or speed (Hz or RPS)');

figure (4)
plot(ff1,abs(data_w1(:,3)), ff2,abs(data_w2(:,3)),
ff3,abs(data_w3(:,3)), ff4,abs(data_w4(:,3)))
title('Baseline vs Sequential Loosening of the Mounts- Z Direction')
legend('Baseline', '1 Mount Loose', '2 Mounts Loose', 'All Four Mounts
Loose');
ylabel('Envelope Amplitude');
xlabel('Spindown frequency or speed (Hz or RPS)');

%Baseline- All Loose- Baseline- All Clamped
figure (5)
plot(ff1,abs(data_w1(:,1)),ff4,abs(data_w4(:,1)), ff6,abs(data_w6(:,1)),
ff7,abs(data_w7(:,1)))
title('Baseline vs Loose, Wire Wrapped Around a Rotor Blade- X
Direction')
legend('Baseline', 'All Loose', 'Baseline', 'Wire Wrapped Around Rotor
Blade');
ylabel('Envelope Amplitude');
xlabel('Spindown frequency or speed (Hz or RPS)');

figure (6)
plot(ff1,abs(data_w1(:,2)),ff4,abs(data_w4(:,2)), ff6,abs(data_w6(:,2)),

```



```

ff7,abs(data_w7(:,2)))
title('Baseline vs Loose, Wire Wrapped Around a Rotor Blade- Y
Direction')
legend('Baseline', 'All Loose', 'Baseline', 'Wire Wrapped Around Rotor
Blade');
ylabel('Envelope Amplitude');
xlabel('Spindown frequency or speed (Hz or RPS)');

figure (7)
plot(ff1,abs(data_w1(:,3)),ff4,abs(data_w4(:,3)), ff6,abs(data_w6(:,3)),
ff7,abs(data_w7(:,3)))
title('Baseline vs Loose, Wire Wrapped Around a Rotor Blade- Z
Direction')
legend('Baseline', 'All Loose', 'Baseline', 'Wire Wrapped Around Rotor
Blade');
ylabel('Envelope Amplitude');
xlabel('Spindown frequency or speed (Hz or RPS)');

%Baseline- Baseline
figure (8)
plot(ff1,abs(data_w1(:,1)), ff6,abs(data_w6(:,1)))
title('Baseline Comparison- X Direction')
legend('Baseline', 'Baseline Recalibration');
ylabel('Envelope Amplitude');
xlabel('Spindown frequency or speed (Hz or RPS)');

figure (9)
plot(ff1,abs(data_w1(:,2)), ff6,abs(data_w6(:,2)))
title('Baseline Comparison- Y Direction')
legend('Baseline', 'Baseline Recalibration');
ylabel('Envelope Amplitude');
xlabel('Spindown frequency or speed (Hz or RPS)');

figure (10)
plot(ff1,abs(data_w1(:,3)), ff6,abs(data_w6(:,3)))
title('Baseline Comparison- Z Direction')
legend('Baseline', 'Baseline Recalibration');
ylabel('Envelope Amplitude');
xlabel('Spindown frequency or speed (Hz or RPS)');

%Baseline- Loose Mouts
figure (11)
plot(ff1,abs(data_w1(:,1)), ff4,abs(data_w4(:,1)))
title('Baseline Vs Loose Mounts- X Direction')
legend('Baseline', 'All Mounts Loose');
ylabel('Envelope Amplitude');
xlabel('Spindown frequency or speed (Hz or RPS)');

figure (12)
plot(ff1,abs(data_w1(:,2)), ff4,abs(data_w4(:,2)))
title('Baseline Vs Loose Mounts- Y Direction')
legend('Baseline', 'All Mounts Loose');
ylabel('Envelope Amplitude');
xlabel('Spindown frequency or speed (Hz or RPS)');

figure (13)
plot(ff1,abs(data_w1(:,3)), ff4,abs(data_w4(:,3)))

```

```

title('Baseline Vs Loose Mounts- Z Direction')
legend('Baseline', 'All Mounts Loose');
ylabel('Envelope Amplitude');
xlabel('Spindown frequency or speed (Hz or RPS)');

% Baseline- Wire Wrapped
figure (14)
plot(ff6,abs(data_w6(:,1)), ff7,abs(data_w7(:,1)))
title('Baseline vs Wire Wrapped Around Rotor Blade- X Direction')
legend('Baseline', 'Wire Wrapped Around Rotor Blade');
ylabel('Envelope Amplitude');
xlabel('Spindown frequency or speed (Hz or RPS)');

figure (15)
plot(ff6,abs(data_w6(:,2)), ff7,abs(data_w7(:,2)))
title('Baseline vs Wire Wrapped Around Rotor Blade- Y Direction')
legend('Baseline', 'Wire Wrapped Around Rotor Blade');
ylabel('Envelope Amplitude');
xlabel('Spindown frequency or speed (Hz or RPS)');

figure (16)
plot(ff6,abs(data_w6(:,3)), ff7,abs(data_w7(:,3)))
title('Baseline vs Wire Wrapped Around Rotor Blade- Z Direction')
legend('Baseline', 'Wire Wrapped Around Rotor Blade');
ylabel('Envelope Amplitude');
xlabel('Spindown frequency or speed (Hz or RPS)');

% Baseline- Loose-Wire
figure (17)
plot(ff1,abs(data_w1(:,1)), ff4,abs(data_w4(:,1)),
ff7,abs(data_w7(:,1)))
title('Baseline vs Loose vs Wire Wrapped Around Rotor Blade- X
Direction')
legend('Baseline','Loose', 'Wire Wrapped Around Rotor Blade');
ylabel('Envelope Amplitude');
xlabel('Spindown frequency or speed (Hz or RPS)');

figure (18)
plot(ff1,abs(data_w1(:,2)), ff4,abs(data_w4(:,2)),
ff7,abs(data_w7(:,2)))
title('Baseline vs Loose vs Wire Wrapped Around Rotor Blade- Y
Direction')
legend('Baseline','Loose', 'Wire Wrapped Around Rotor Blade');
ylabel('Envelope Amplitude');
xlabel('Spindown frequency or speed (Hz or RPS)');

figure (19)
plot(ff1,abs(data_w1(:,3)), ff4,abs(data_w4(:,3)),
ff7,abs(data_w7(:,3)))
title('Baseline vs Loose vs Wire Wrapped Around Rotor Blade- Z
Direction')
legend('Baseline','Loose', 'Wire Wrapped Around Rotor Blade');
ylabel('Envelope Amplitude');
xlabel('Spindown frequency or speed (Hz or RPS)');

%% Normalized Graphs

```

```

% "excitation normalized plot:

% Sequential Mounts Loosening
figure(20)
plot(ff1,abs(data_w1(:,1))./(ff1.^2), ff2,abs(data_w2(:,1))./(ff2.^2),
ff3,abs(data_w3(:,1))./(ff3.^2), ff4,abs(data_w4(:,1))./(ff4.^2))
title('Baseline vs Sequential Loosening (Normalized Spindown Whiskers)-
X Direction');
legend('Baseline', '1 Mount Loose', '2 Mounts Loose', 'All Four Mounts
Loose');
ylabel('Envelope Amplitude');
xlabel('Spindown frequency or speed (Hz or RPS)');

figure(21)
plot(ff1,abs(data_w1(:,2))./(ff1.^2), ff2,abs(data_w2(:,2))./(ff2.^2),
ff3,abs(data_w3(:,2))./(ff3.^2), ff4,abs(data_w4(:,2))./(ff4.^2))
title('Baseline vs Sequential Loosening (Normalized Spindown Whiskers)-
Y Direction');
legend('Baseline', '1 Mount Loose', '2 Mounts Loose', 'All Four Mounts
Loose');
ylabel('Envelope Amplitude');
xlabel('Spindown frequency or speed (Hz or RPS)');

figure(22)
plot(ff1,abs(data_w1(:,3))./(ff1.^2), ff2,abs(data_w2(:,3))./(ff2.^2),
ff3,abs(data_w3(:,3))./(ff3.^2), ff4,abs(data_w4(:,3))./(ff4.^2))
title('Baseline vs Sequential Loosening (Normalized Spindown Whiskers)-
Z Direction');
legend('Baseline', '1 Mount Loose', '2 Mounts Loose', 'All Four Mounts
Loose');
ylabel('Envelope Amplitude');
xlabel('Spindown frequency or speed (Hz or RPS)');

% Baseline vs All Loose
figure(23)
plot(ff1,abs(data_w1(:,1))./(ff1.^2), ff4,abs(data_w4(:,1))./(ff4.^2))
title('Baseline vs All Loose (NormalizedSpindown Whiskers)- X
Direction');
legend('Baseline', 'All Four Mounts Loose');
ylabel('Envelope Amplitude');
xlabel('Spindown frequency or speed (Hz or RPS)');

figure(24)
plot(ff1,abs(data_w1(:,1))./(ff1.^2), ff4,abs(data_w4(:,1))./(ff4.^2))
title('Baseline vs All Loose (NormalizedSpindown Whiskers)- Y
Direction');
legend('Baseline', 'All Four Mounts Loose');
ylabel('Envelope Amplitude');
xlabel('Spindown frequency or speed (Hz or RPS)');

figure(25)
plot(ff1,abs(data_w1(:,1))./(ff1.^2), ff4,abs(data_w4(:,1))./(ff4.^2))
title('Baseline vs All Loose (NormalizedSpindown Whiskers)- Z
Direction');
legend('Baseline', 'All Four Mounts Loose');
ylabel('Envelope Amplitude');
xlabel('Spindown frequency or speed (Hz or RPS)');

```

```

% Baseline vs Wired
figure(26)
plot(ff6,abs(data_w6(:,1))./(ff6.^2), ff7,abs(data_w7(:,1))./(ff7.^2))
title('Baseline vs Wired(Normalized Spindown Whiskers)- X Direction');
legend('Baseline', 'Wire Wrapped Around Blade');
ylabel('Envelope Amplitude');
xlabel('Spindown frequency or speed (Hz or RPS)');

figure(27)
plot(ff6,abs(data_w6(:,2))./(ff6.^2), ff7,abs(data_w7(:,2))./(ff7.^2))
title('Baseline vs Wired(Normalized Spindown Whiskers)- Y Direction');
legend('Baseline', 'Wire Wrapped Around Blade');
ylabel('Envelope Amplitude');
xlabel('Spindown frequency or speed (Hz or RPS)');

figure(28)
plot(ff6,abs(data_w6(:,3))./(ff6.^2), ff7,abs(data_w7(:,3))./(ff7.^2))
title('Baseline vs Wired(Normalized Spindown Whiskers)- Z Direction');
legend('Baseline', 'Wire Wrapped Around Blade');
ylabel('Envelope Amplitude');
xlabel('Spindown frequency or speed (Hz or RPS)');

% Baseline vs Baseline
figure(29)
plot(ff1,abs(data_w1(:,1))./(ff1.^2),ff6,abs(data_w6(:,1))./(ff6.^2))
title('Baseline vs Baseline (Normalized Spindown Whiskers)- X
Direction');
legend('Baseline- Before Loose MTS', 'Baseline-Before Wired');
ylabel('Envelope amplitude');
xlabel('Spindown frequency or speed (Hz or RPS)');

figure(30)
plot(ff1,abs(data_w1(:,2))./(ff1.^2),ff6,abs(data_w6(:,2))./(ff6.^2))
title('Baseline vs Baseline (Normalized Spindown Whiskers)- Y
Direction');
legend('Baseline- Before Loose MTS', 'Baseline-Before Wired');
ylabel('Envelope amplitude');
xlabel('Spindown frequency or speed (Hz or RPS)');

figure(31)
plot(ff1,abs(data_w1(:,3))./(ff1.^2),ff6,abs(data_w6(:,3))./(ff6.^2))
title('Baseline vs Baseline (Normalized Spindown Whiskers)- Z
Direction');
legend('Baseline- Before Loose MTS', 'Baseline-Before Wired');
ylabel('Envelope amplitude');
xlabel('Spindown frequency or speed (Hz or RPS)');

% Baseline vs Loose vs Wire Wrapped
figure(32)
plot(ff1,abs(data_w1(:,1))./(ff1.^2),
ff4,abs(data_w4(:,1))./(ff4.^2),ff6,abs(data_w6(:,1))./(ff6.^2),
ff7,abs(data_w7(:,1))./(ff7.^2))
title('Baseline vs Loose vs Wire Wrapped (NormalizedSpindown Whiskers)-
X Direction');
legend('Baseline', 'All Four Mounts Loose','Baseline', 'Wire Wrapped
Around Blade');

```

```

ylabel('Envelope Amplitude');
xlabel('Spindown frequency or speed (Hz or RPS)');

figure(33)
plot(ff1,abs(data_w1(:,2))./(ff1.^2),
ff4,abs(data_w4(:,2))./(ff4.^2),ff6,abs(data_w6(:,2))./(ff6.^2),
ff7,abs(data_w7(:,2))./(ff7.^2))
title('Baseline vs Loose vs Wire Wrapped (NormalizedSpindown Whiskers)-
Y Direction');
legend('Baseline', 'All Four Mounts Loose','Baseline', 'Wire Wrapped
Around Blade');
ylabel('Envelope Amplitude');
xlabel('Spindown frequency or speed (Hz or RPS)');

figure(34)
plot(ff1,abs(data_w1(:,3))./(ff1.^2),
ff4,abs(data_w4(:,3))./(ff4.^2),ff6,abs(data_w6(:,3))./(ff6.^2),
ff7,abs(data_w7(:,3))./(ff7.^2))
title('Baseline vs Loose vs Wire Wrapped (NormalizedSpindown Whiskers)-
Z Direction');
legend('Baseline', 'All Four Mounts Loose','Baseline', 'Wire Wrapped
Around Blade');
ylabel('Envelope Amplitude');
xlabel('Spindown frequency or speed (Hz or RPS)');

```

9.2.5 USGC SENECA MATLAB Code

```

clc
clear
close all

%% USGC SENECA- two visits, loose mounts, clamped mounts, wire wrapped
around the rotor blade, and baselines
% Written by Katie Gerhard

load('SENECA29MARVISIT.mat')

load('CAPTCHA0308.mat')           % Terminal Box
load('CAPTCHA0411.mat')          % Base of Fan
load('CAPTCHA0D0B.mat')          % Side Structure of Fan

fs= 3200;
nom_rpm= 3450;

% friction = friction = [-0.0202,   -0.0030]; % just a quick fit to TB1.

% Baseline on 29 MAR 2013
[data_w1, pre_w1, post_w1, ff1, friction1, stop_time1, stop_index1] =
spindown_fitter(TB1, fs, nom_rpm);
% the outputs are form the pre (magenta), post (green), and "data"
(black)
% whiskers.
%
% One Loose Mount
[data_w2, pre_w2, post_w2, ff2, friction2, stop_time2, stop_index2] =
spindown_fitter(TB2, fs, nom_rpm);

```

```

% Two Loose Mounts
[data_w3, pre_w3, post_w3, ff3, friction3, stop_time3, stop_index3] =
spindown_fitter(TB3, fs, nom_rpm);

% All Four Loose Mounts
[data_w4, pre_w4, post_w4, ff4, friction4, stop_time4, stop_index4] =
spindown_fitter(TB4, fs, nom_rpm);

% Baseline Recalibration
[data_w6, pre_w6, post_w6, ff6, friction6, stop_time6, stop_index6] =
spindown_fitter(TB6, fs, nom_rpm);

% All Four Mounts Clamped
[data_w7, pre_w7, post_w7, ff7, friction7, stop_time7, stop_index7] =
spindown_fitter(TB7, fs, nom_rpm);

Baseline 20 MARCH 2013

[data_w8, pre_w8, post_w8, ff8, friction8, stop_time8, stop_index8] =
spindown_fitter(TERMBOX1, fs, nom_rpm);

% Wire wrapped around the rotor blade
[data_w9, pre_w9, post_w9, ff9, friction9, stop_time9, stop_index9] =
spindown_fitter(TERMBOX11, fs, nom_rpm);

% basic plot: does X,Y,Z
% If you only want one of those guys, then data_W is :,1= x, :,2= Y,
% :,3=Z

%% X,Y, and Z Baseline compared to Sequential Loosening

% Baseline compared to sequential Loosing of All Mounts
figure (2)
plot(ff1,abs(data_w1(:,1)), ff2,abs(data_w2(:,1)),
ff3,abs(data_w3(:,1)), ff4,abs(data_w4(:,1)))
title('Baseline Compared to Sequential Loosening of Mounts on SENECA- X
Direction')
legend('Baseline', '1 Mount Loose', '2 Mounts Loose', 'All Four Mounts
Loose');
ylabel('envelope amplitude');
xlabel('spindown frequency or speed (Hz or rps)');

% Baseline compared to sequential Loosing of All Mounts
figure (3)
plot(ff1,abs(data_w1(:,2)), ff2,abs(data_w2(:,2)),
ff3,abs(data_w3(:,2)), ff4,abs(data_w4(:,2)))
title('Baseline Compared to Sequential Loosening of Mounts on SENECA- Y
Direction')
legend('Baseline', '1 Mount Loose', '2 Mounts Loose', 'All Four Mounts
Loose');
ylabel('envelope amplitude');
xlabel('spindown frequency or speed (Hz or rps)');

% Baseline compared to sequential Loosing of All Mounts

```

```

figure (4)
plot(ff1,abs(data_w1(:,3)), ff2,abs(data_w2(:,3)),
ff3,abs(data_w3(:,3)), ff4,abs(data_w4(:,3)))
title('Baseline Compared to Sequential Loosening of Mounts on SENECA- Z
Direction')
legend('Baseline', '1 Mount Loose', '2 Mounts Loose', 'All Four Mounts
Loose');
ylabel('envelope amplitude');
xlabel('spindown frequency or speed (Hz or rps)');

%% Baseline- Loose- Baseline- All Clamped

% Baseline- All Loose- Baseline- All Clamped
figure (5)
plot(ff1,abs(data_w1(:,1)), ff4,abs(data_w4(:,1)),
ff6,abs(data_w6(:,1)), ff7,abs(data_w7(:,1)))
title('29 MAR 2013 Baseline Vs Loose and Clamped on SENECA- X
Direction')
legend('Baseline', 'All Four Mounts Loose', 'Baseline Recalibration',
'All Mounts Clamped');
ylabel('envelope amplitude');
xlabel('spindown frequency or speed (Hz or rps)');

% Baseline- All Loose- Baseline- All Clamped
figure (6)
plot(ff1,abs(data_w1(:,2)), ff4,abs(data_w4(:,2)),
ff6,abs(data_w6(:,2)), ff7,abs(data_w7(:,2)))
title('29 MAR 2013 Baseline Vs Loose and Clamped on SENECA- Y
Direction')
legend('Baseline', 'All Four Mounts Loose', 'Baseline Recalibration',
'All Mounts Clamped');
ylabel('envelope amplitude');
xlabel('spindown frequency or speed (Hz or rps)');

% Baseline- All Loose- Baseline- All Clamped
figure (7)
plot(ff1,abs(data_w1(:,1)), ff4,abs(data_w4(:,3)),
ff6,abs(data_w6(:,3)), ff7,abs(data_w7(:,3)))
title('29 MAR 2013 Baseline Vs Loose and Clamped on SENECA- Z
Direction')
legend('Baseline', 'All Four Mounts Loose', 'Baseline Recalibration',
'All Mounts Clamped');
ylabel('envelope amplitude');
xlabel('spindown frequency or speed (Hz or rps)');

%% Baseline Comparison

% Baseline- Baseline
figure (8)
plot(ff1,abs(data_w1(:,1)),
ff6,abs(data_w6(:,1)),ff8,abs(data_w8(:,1)) )
title('Baseline Comparison on USCGC SENECA- X Direction')
legend('Baseline', 'Baseline Recalibration', 'Baseline from 20 March
2013 tests');
ylabel('envelope amplitude');
xlabel('Spindown frequency or speed (Hz or RPS)');

```

```

% Baseline- Baseline
figure (9)
plot(ff1,abs(data_w1(:,2)),
ff6,abs(data_w6(:,2)),ff8,abs(data_w8(:,2)) )
title('Baseline Comparison on USCGC SENECA- Y Direction')
legend('Baseline', 'Baseline Recalibration', 'Baseline from 20 March
2013 tests');
ylabel('envelope amplitude');
xlabel('Spindown frequency or speed (Hz or RPS)');

% Baseline- Baseline
figure (10)
plot(ff1,abs(data_w1(:,3)),
ff6,abs(data_w6(:,3)),ff8,abs(data_w8(:,3)) )
title('Baseline Comparison on USCGC SENECA- Z Direction')
legend('Baseline', 'Baseline Recalibration', 'Baseline from 20 March
2013 tests');
ylabel('envelope amplitude');
xlabel('Spindown frequency or speed (Hz or RPS)');

%% Baseline Loose Clamped Wired

% Baseline- Loose-Clamped-Wired
figure (11)
plot(ff1,abs(data_w1(:,1)), ff4,abs(data_w4(:,1)),
ff7,abs(data_w7(:,1)),ff9,abs(data_w9(:,1)) )
title('Baseline Compared to Loose Mounts, Clamped Mounts, and Wire on
Rotor on SENECA- X Direction')
legend('Baseline', 'All Mounts Loose', 'All Mounts Clamped', 'Wire
Wrapped Around Blade');
ylabel('envelope amplitude');
xlabel('Spindown frequency or speed (Hz or RPS)');

% Baseline- Loose-Clamped-Wired
figure (12)
plot(ff1,abs(data_w1(:,2)), ff4,abs(data_w4(:,2)),
ff7,abs(data_w7(:,2)),ff9,abs(data_w9(:,2)) )
title('Baseline Compared to Loose Mounts, Clamped Mounts, and Wire on
Rotor on SENECA- Y Direction')
legend('Baseline', 'All Mounts Loose', 'All Mounts Clamped', 'Wire
Wrapped Around Blade');
ylabel('envelope amplitude');
xlabel('Spindown frequency or speed (Hz or RPS)');

% Baseline- Loose-Clamped-Wired
figure (13)
plot(ff1,abs(data_w1(:,3)), ff4,abs(data_w4(:,3)),
ff7,abs(data_w7(:,3)),ff9,abs(data_w9(:,3)) )
title('Baseline Compared to Loose Mounts, Clamped Mounts, and Wire on
Rotor on SENECA- Z Direction')
legend('Baseline', 'All Mounts Loose', 'All Mounts Clamped', 'Wire
Wrapped Around Blade');
ylabel('envelope amplitude');
xlabel('Spindown frequency or speed (Hz or RPS)');

% Baseline- Loose- Wired
figure (14)

```



```

plot(ff1,abs(data_w1(:,1)),
ff4,abs(data_w4(:,1)),ff9,abs(data_w9(:,1)) )
title('Loose Mounts Compared to Wire Wraped around Rotor Blade on
SENECA- X Direction')
legend('Baseline', 'All Mounts Loose', 'Wire Wrapped Around Blade');
ylabel('envelope amplitude');
xlabel('Spindown frequency or speed (Hz or RPS)');

% Baseline- Loose- Wired
figure (15)
plot(ff1,abs(data_w1(:,2)),
ff4,abs(data_w4(:,2)),ff9,abs(data_w9(:,2)) )
title('Loose Mounts Compared to Wire Wraped around Rotor Blade on
SENECA- Y Direction')
legend('Baseline', 'All Mounts Loose', 'Wire Wrapped Around Blade');
ylabel('envelope amplitude');
xlabel('Spindown frequency or speed (Hz or RPS)');

% Baseline- Loose- Wired
figure (16)
plot(ff1,abs(data_w1(:,3)),
ff4,abs(data_w4(:,3)),ff9,abs(data_w9(:,3)))
title('Loose Mounts Compared to Wire Wraped around Rotor Blade on
SENECA- Z Direction')
legend('Baseline', 'All Mounts Loose', 'Wire Wrapped Around Blade');
ylabel('envelope amplitude');
xlabel('Spindown frequency or speed (Hz or RPS)');

%% Loose Clamped Wired- Tests John's Theory or Steve's comparison

% Loose- Wired- Clamped
figure (17)
plot(ff4,abs(data_w4(:,1)),ff7,abs(data_w7(:,1)),ff9,abs(data_w9(:,1)))
title('Clamped Mounts- Loose Mounts- Wire Wrapped Around Rotor Blade on
SENECA- X Direction')
legend('Clamped', 'All Mounts Loose', 'Wire Wrapped Around Blade');
ylabel('Envelope Amplitude');
xlabel('Spindown frequency or speed (Hz or RPS)');

% Loose- Wired- Clamped
figure (18)
plot(ff4,abs(data_w4(:,2)),ff7,abs(data_w7(:,2)),ff9,abs(data_w9(:,2)))
title('Clamped Mounts- Loose Mounts- Wire Wrapped Around Rotor Blade on
SENECA- Y Direction')
legend('Clamped', 'All Mounts Loose', 'Wire Wrapped Around Blade');
ylabel('Envelope Amplitude');
xlabel('Spindown frequency or speed (Hz or RPS)');

% Loose- Wired- Clamped
figure (19)
plot(ff4,abs(data_w4(:,3)),ff7,abs(data_w7(:,3)),ff9,abs(data_w9(:,3)))
title('Clamped Mounts- Loose Mounts- Wire Wrapped Around Rotor Blade on
SENECA- Z Direction')
legend('Clamped', 'All Mounts Loose', 'Wire Wrapped Around Blade');
ylabel('Envelope Amplitude');
xlabel('Spindown frequency or speed (Hz or RPS)');

```

```
%% Normalized Graphs
```

```
% Baseline vs Sequential Loosening of the Mounts
```

```
figure(20)
plot(ff1,abs(data_w1(:,1))./(ff1.^2), ff2,abs(data_w2(:,1))./(ff2.^2),
ff3,abs(data_w3(:,1))./(ff3.^2), ff4,abs(data_w4(:,1))./(ff4.^2))
title('Baseline vs Sequential Loosening of the Mounts (Normalized Spin-
down)- X Direction');
legend('Baseline', '1 Mount Loose', '2 Mounts Loose', 'All Four Mounts
Loose');
ylabel('envelope amplitude');
xlabel('Spindown frequency or speed (Hz or RPS)');
```

```
figure(21)
plot(ff1,abs(data_w1(:,2))./(ff1.^2), ff2,abs(data_w2(:,2))./(ff2.^2),
ff3,abs(data_w3(:,2))./(ff3.^2), ff4,abs(data_w4(:,2))./(ff4.^2))
title('Baseline vs Sequential Loosening of the Mounts (Normalized Spin-
down)- Y Direction');
legend('Baseline', '1 Mount Loose', '2 Mounts Loose', 'All Four Mounts
Loose');
ylabel('envelope amplitude');
xlabel('Spindown frequency or speed (Hz or RPS)');
```

```
figure(22)
plot(ff1,abs(data_w1(:,3))./(ff1.^2), ff2,abs(data_w2(:,3))./(ff2.^2),
ff3,abs(data_w3(:,3))./(ff3.^2), ff4,abs(data_w4(:,3))./(ff4.^2))
title('Baseline vs Sequential Loosening of the Mounts (Normalized Spin-
down)- Z Direction');
legend('Baseline', '1 Mount Loose', '2 Mounts Loose', 'All Four Mounts
Loose');
ylabel('envelope amplitude');
xlabel('Spindown frequency or speed (Hz or RPS)');
```

```
% Baseline vs loose and clamped
```

```
figure(23)
plot(ff1,abs(data_w1(:,1))./(ff1.^2), ff4,abs(data_w4(:,1))./(ff4.^2),
ff6,abs(data_w6(:,1))./(ff6.^2), ff7,abs(data_w7(:,1))./(ff7.^2))
title('Baselines vs Loose Mounts and Clamped Mounts (Normalized Spin-
down)- X Direction');
legend('Baseline', 'All Four Mounts Loose', 'Baseline Recalibration',
'All Mounts Clamped');
ylabel('Envelope Amplitude');
xlabel('Spindown frequency or speed (Hz or RPS)');
```

```
figure(24)
plot(ff1,abs(data_w1(:,2))./(ff1.^2), ff4,abs(data_w4(:,2))./(ff4.^2),
ff6,abs(data_w6(:,2))./(ff6.^2), ff7,abs(data_w7(:,2))./(ff7.^2))
title('Baselines vs Loose Mounts and Clamped Mounts (Normalized Spin-
down)- Y Direction');
legend('Baseline', 'All Four Mounts Loose', 'Baseline Recalibration',
'All Mounts Clamped');
ylabel('Envelope Amplitude');
xlabel('Spindown frequency or speed (Hz or RPS)');
```

```
figure(25)
```

```

plot(ff1,abs(data_w1(:,3))./(ff1.^2), ff4,abs(data_w4(:,3))./(ff4.^2),
ff6,abs(data_w6(:,3))./(ff6.^2), ff7,abs(data_w7(:,3))./(ff7.^2))
title('Baselines vs Loose Mounts and Clamped Mounts (Normalized Spin-
down)- Z Direction');
legend('Baseline', 'All Four Mounts Loose', 'Baseline Recalibration',
'All Mounts Clamped');
ylabel('Envelope Amplitude');
xlabel('Spindown frequency or speed (Hz or RPS)');

```

```

% Baseline Comparisons

```

```

figure(26)
plot(ff1,abs(data_w1(:,1))./(ff1.^2), ff6,abs(data_w6(:,1))./(ff6.^2),
ff8,abs(data_w8(:,1))./(ff8.^2))
title('Baseline Comparisons (Normalized Spin-down)- X Direction');
legend('Baseline', 'Baseline Recalibration', 'Baseline from 20 March
Visit');
ylabel('Envelope Amplitude');
xlabel('Spindown frequency or speed (Hz or rps)');

```

```

figure(27)
plot(ff1,abs(data_w1(:,2))./(ff1.^2), ff6,abs(data_w6(:,2))./(ff6.^2),
ff8,abs(data_w8(:,2))./(ff8.^2))
title('Baseline Comparisons (Normalized Spin-down)- Y Direction');
legend('Baseline', 'Baseline Recalibration', 'Baseline from 20 March
Visit');
ylabel('Envelope Amplitude');
xlabel('Spindown frequency or speed (Hz or rps)');

```

```

figure(28)
plot(ff1,abs(data_w1(:,3))./(ff1.^2), ff6,abs(data_w6(:,3))./(ff6.^2),
ff8,abs(data_w8(:,3))./(ff8.^2))
title('Baseline Comparisons (Normalized Spin-down)- Z Direction');
legend('Baseline', 'Baseline Recalibration', 'Baseline from 20 March
Visit');
ylabel('Envelope Amplitude');
xlabel('Spindown frequency or speed (Hz or rps)');

```

```

% Baseline vs Loose/Clamped/Wired

```

```

figure(29)
plot(ff1,abs(data_w1(:,1))./(ff1.^2),ff4,abs(data_w4(:,1))./(ff4.^2),
ff7,abs(data_w7(:,1))./(ff7.^2), ff9,abs(data_w9(:,1))./(ff9.^2))
title('Baseline vs Loose Mounts, Clamped Mounts, and Wire Wrapped
Around Rotor Blade (Normalized Spin-down)- X Direction');
legend('Baseline', 'All Mounts Loose', 'All Mounts Clamped', 'Wire
Wrapped Around Rotor Blade');
ylabel('Envelope Amplitude');
xlabel('Spindown frequency or speed (Hz or RPS)');

```

```

figure(30)
plot(ff1,abs(data_w1(:,2))./(ff1.^2),ff4,abs(data_w4(:,2))./(ff4.^2),
ff7,abs(data_w7(:,2))./(ff7.^2), ff9,abs(data_w9(:,2))./(ff9.^2))
title('Baseline vs Loose Mounts, Clamped Mounts, and Wire Wrapped
Around Rotor Blade (Normalized Spin-down)- Y Direction');
legend('Baseline', 'All Mounts Loose', 'All Mounts Clamped', 'Wire
Wrapped Around Rotor Blade');

```

```

ylabel('Envelope Amplitude');
xlabel('Spindown frequency or speed (Hz or RPS)');

figure(31)
plot(ff1,abs(data_w1(:,3))./(ff1.^2),ff4,abs(data_w4(:,3))./(ff4.^2),
ff7,abs(data_w7(:,3))./(ff7.^2), ff9,abs(data_w9(:,3))./(ff9.^2))
title('Baseline vs Loose Mounts, Clamped Mounts, and Wire Wrapped
Around Rotor Blade (Normalized Spin-down)- Z Direction');
legend('Baseline', 'All Mounts Loose', 'All Mounts Clamped', 'Wire
Wrapped Around Rotor Blade');
ylabel('Envelope Amplitude');
xlabel('Spindown frequency or speed (Hz or RPS)');

% Loose/Clamped/Wired Only

figure(32)
plot(ff4,abs(data_w4(:,1))./(ff4.^2), ff7,abs(data_w7(:,1))./(ff7.^2),
ff9,abs(data_w9(:,1))./(ff9.^2))
title('Loose Mounts, Clamped Mounts, and Wire Wrapped Around Rotor
Blade (Normalized Spin-down)- X Direction');
legend('All Mounts Loose', 'All Mounts Clamped', 'Wire Wrapped Around
Rotor Blade');
ylabel('Envelope Amplitude');
xlabel('Spindown frequency or speed (Hz or RPS)');

figure(33)
plot(ff4,abs(data_w4(:,2))./(ff4.^2), ff7,abs(data_w7(:,2))./(ff7.^2),
ff9,abs(data_w9(:,2))./(ff9.^2))
title('Loose Mounts, Clamped Mounts, and Wire Wrapped Around Rotor
Blade (Normalized Spin-down)- Y Direction');
legend('All Mounts Loose', 'All Mounts Clamped', 'Wire Wrapped Around
Rotor Blade');
ylabel('Envelope Amplitude');
xlabel('Spindown frequency or speed (Hz or RPS)');

figure(34)
plot(ff4,abs(data_w4(:,3))./(ff4.^2), ff7,abs(data_w7(:,3))./(ff7.^2),
ff9,abs(data_w9(:,3))./(ff9.^2))
title('Loose Mounts, Clamped Mounts, and Wire Wrapped Around Rotor
Blade (Normalized Spin-down)- Z Direction');
legend('All Mounts Loose', 'All Mounts Clamped', 'Wire Wrapped Around
Rotor Blade');
ylabel('Envelope Amplitude');
xlabel('Spindown frequency or speed (Hz or RPS)');

```

9.2.6 National Security Cutters MATLAB Code

```

clear
close all

%% Looking at the BERHTOLF and STRATTON Fans

load('NSCWhiskers.mat')

TopFanBERT= TopFanBERT(1.8*10^6:2.6*10^6,:); % Data for

```

```

1-42-4 in FWD Fan Rm
BottomFanBERT=BottomFanBERT(1.7*10^6:2.7*10^6,:); %Data
for 1-42-2 in FWD Fan RM- BAD FAN
%
%
%
% load('STRATTON DATA.mat')
%
TopFanSTRATTON= TopFanSTRATTON(4.5*10^5:8.2*10^5,:); %
Data for 1-42-4 in FWD Fan Rm
BottomFanSTRATTON=
BottomFanSTRATTON(1.0*10^6:1.3*10^6,:); %Data for 1-42-2
in FWD Fan RM- BAD FAN

fs= 3200;
nom_rpm= 3450;

% friction = friction = [-0.0202, -0.0030]; % just a quick fit to TB1.

% BERTHOLF Top Fan
[data_w1, pre_w1, post_w1, ff1,friction1, stop_time1, stop_index1] =
spindown_fitter(TopFanBERT, fs, nom_rpm);
% the outputs are form the pre (magenta), post (green), and "data"
(black)
% whiskers.

% BERTHOLF Bottom Fan
[data_w2, pre_w2, post_w2, ff2, friction2, stop_time2, stop_index2] =
spindown_fitter(BottomFanBERT, fs, nom_rpm);

% STRATTON TOP FAN
[data_w3, pre_w3, post_w3, ff3, friction3, stop_time3, stop_index3] =
spindown_fitter(TopFanSTRATTON, fs, nom_rpm);

% Stratton Bottom Fan
[data_w4, pre_w4, post_w4, ff4, friction4, stop_time4, stop_index4] =
spindown_fitter(BottomFanSTRATTON, fs, nom_rpm);

% basic plot: does X,Y,Z
% If you only want one of those guys, then data_W is :, 1= x, :,2= Y, :,
3=
% Z

%% Top Fan on BERTHOLF compared to Top Fan on the STRATTON
figure (2)
plot(ff1,abs(data_w1(:,1)), ff3,abs(data_w3(:,1)))
title('(1-42-4) Ventilation Fan Spin-down: BERTHOLF vs STRATTON - X
Direction')
legend('BERTHOLF Top (1-42-4) Ventilation Fan', 'STRATTON Top (1-42-4)
Ventilation Fan');

```

```

ylabel('Envelope Amplitude');
xlabel('Spindown frequency or speed (Hz or RPS)');

% Top Fan on BERTHOLF compared to Top Fan on the STRATTON
figure (3)
plot(ff1,abs(data_w1(:,2)), ff3,abs(data_w3(:,2)))
title('(1-42-4) Ventilation Fan Spin-down: BERTHOLF vs STRATTON - Y
Direction')
legend('BERTHOLF Top (1-42-4) Ventilation Fan', 'STRATTON Top (1-42-4)
Ventilation Fan');
ylabel('Envelope Amplitude');
xlabel('Spindown frequency or speed (Hz or RPS)');

% Top Fan on BERTHOLF compared to Top Fan on the STRATTON
figure (4)
plot(ff1,abs(data_w1(:,3)), ff3,abs(data_w3(:,3)))
title('(1-42-4) Ventilation Fan Spin-down: BERTHOLF vs STRATTON - Z
Direction')
legend('BERTHOLF Top (1-42-4) Ventilation Fan', 'STRATTON Top (1-42-4)
Ventilation Fan');
ylabel('Envelope Amplitude');
xlabel('Spindown frequency or speed (Hz or RPS)');

%% Bottom Fans Compared
figure (5)
plot(ff2,abs(data_w2(:,1)), ff4,abs(data_w4(:,1)))
title('(1-42-2) Ventilation Fan Spin-down: BERTHOLF vs STRATTON - X
Direction')
legend('BERTHOLF Bottom (1-42-2) Ventilation Fan', 'STRATTON Bottom (1-
42-2) Ventilation Fan');
ylabel('Envelope Amplitude');
xlabel('Spindown frequency or speed (Hz or RPS)');

% Bottom Fans Compared
figure (6)
plot(ff2,abs(data_w2(:,2)), ff4,abs(data_w4(:,2)))
title('(1-42-2) Ventilation Fan Spin-down: BERTHOLF vs STRATTON - Y
Direction')
legend('BERTHOLF Bottom (1-42-2) Ventilation Fan', 'STRATTON Bottom (1-
42-2) Ventilation Fan');
ylabel('Envelope Amplitude');
xlabel('Spindown frequency or speed (Hz or RPS)');

% Bottom Fans Compared
figure (7)
plot(ff2,abs(data_w2(:,3)), ff4,abs(data_w4(:,3)))
title('(1-42-2) Ventilation Fan Spin-down: BERTHOLF vs STRATTON - Z
Direction')
legend('BERTHOLF Bottom (1-42-2) Ventilation Fan', 'STRATTON Bottom (1-
42-2) Ventilation Fan');
ylabel('Envelope Amplitude');
xlabel('Spindown frequency or speed (Hz or RPS)');

%% All Fans on One Graph
figure (8)

```

```

plot(ff1,abs(data_w1(:,1)), ff2, abs(data_w2(:,1)), ff3,
abs(data_w3(:,1)), ff4,abs(data_w4(:,1)) )
title('Ventilation Fan Comparison- X Direction')
legend('BERTHOLF Top (1-42-4) Ventilation Fan', 'BERTHOLF Bottom (1-42-
2) Ventilation Fan', 'STRATTON Top (1-42-4) Ventilation Fan', 'STRATTON
Bottom (1-42-2) Ventilation Fan');
ylabel('Envelope Amplitude');
xlabel('Spindown frequency or speed (Hz or RPS)');

```

```

figure (9)
plot(ff1,abs(data_w1(:,2)), ff2, abs(data_w2(:,2)), ff3,
abs(data_w3(:,2)), ff4,abs(data_w4(:,2)) )
title('Ventilation Fan Comparison- Y Direction')
legend('BERTHOLF Top (1-42-4) Ventilation Fan', 'BERTHOLF Bottom (1-42-
2) Ventilation Fan', 'STRATTON Top (1-42-4) Ventilation Fan', 'STRATTON
Bottom (1-42-2) Ventilation Fan');
ylabel('Envelope Amplitude');
xlabel('Spindown frequency or speed (Hz or RPS)');

```

```

figure (10)
plot(ff1,abs(data_w1(:,3)), ff2, abs(data_w2(:,3)), ff3,
abs(data_w3(:,3)), ff4,abs(data_w4(:,3)) )
title('Ventilation Fan Comparison- Z Direction')
legend('BERTHOLF Top (1-42-4) Ventilation Fan', 'BERTHOLF Bottom (1-42-
2) Ventilation Fan', 'STRATTON Top (1-42-4) Ventilation Fan', 'STRATTON
Bottom (1-42-2) Ventilation Fan');
ylabel('Envelope Amplitude');
xlabel('Spindown frequency or speed (Hz or RPS)');

```

```

%% Normalized

```

```

%
figure(11)
plot(ff1,abs(data_w1(:,1))./(ff1.^2), ff2,abs(data_w2(:,1))./(ff2.^2),
ff3,abs(data_w3(:,1))./(ff3.^2), ff4,abs(data_w4(:,1))./(ff4.^2))
title('Fan Comparison (Normalized Spindown Whiskers)- X Direction');
legend('BERTHOLF Top Fan', 'BERTHOLF Bottom Fan', 'STRATTON Top Fan',
'STRATTON Bottom Fan');
ylabel('Envelope Amplitude');
xlabel('Spindown frequency or speed (Hz or RPS)');

```

```

figure(12)
plot(ff1,abs(data_w1(:,2))./(ff1.^2), ff2,abs(data_w2(:,2))./(ff2.^2),
ff3,abs(data_w3(:,1))./(ff3.^2), ff4,abs(data_w4(:,1))./(ff4.^2))
title('Fan Comparison (Normalized Spindown Whiskers)- Y Direction');
legend('BERTHOLF Top Fan', 'BERTHOLF Bottom Fan', 'STRATTON Top Fan',
'STRATTON Bottom Fan');
ylabel('Envelope Amplitude');
xlabel('Spindown frequency or speed (Hz or RPS)');

```

```

figure(13)
plot(ff1,abs(data_w1(:,3))./(ff1.^2), ff2,abs(data_w2(:,3))./(ff2.^2),
ff3,abs(data_w3(:,1))./(ff3.^2), ff4,abs(data_w4(:,1))./(ff4.^2))
title('Fan Comparison (Normalized Spindown Whiskers)- Z Direction');
legend('BERTHOLF Top Fan', 'BERTHOLF Bottom Fan', 'STRATTON Top Fan',
'STRATTON Bottom Fan');
ylabel('Envelope Amplitude');
xlabel('Spindown frequency or speed (Hz or RPS)');

```

```

% "excitation normalized plot:

figure(14)
plot(ff1,abs(data_w1(:,1))./(ff1.^2), ff3,abs(data_w3(:,1))./(ff3.^2))
title('(1-42-4)Ventilation Fan Spin-down: BERTHOLF vs STRATTON
(Normalized) - X Direction');
legend('BERTHOLF Top Fan', 'STRATTON Top Fan');
ylabel('Envelope Amplitude');
xlabel('Spindown frequency or speed (Hz or RPS)');

figure(15)
plot(ff1,abs(data_w1(:,2))./(ff1.^2), ff3,abs(data_w3(:,2))./(ff3.^2))
title('(1-42-4)Ventilation Fan Spin-down: BERTHOLF vs STRATTON
(Normalized) - Y Direction');
legend('BERTHOLF Top Fan', 'STRATTON Top Fan');
ylabel('Envelope Amplitude');
xlabel('Spindown frequency or speed (Hz or RPS)');

figure(16)
plot(ff1,abs(data_w1(:,3))./(ff1.^2), ff3,abs(data_w3(:,3))./(ff3.^2))
title('(1-42-4)Ventilation Fan Spin-down: BERTHOLF vs STRATTON
(Normalized) - Z Direction');
legend('BERTHOLF Top Fan', 'STRATTON Top Fan');
ylabel('Envelope Amplitude');
xlabel('Spindown frequency or speed (Hz or RPS)');

% Bottom fan

figure(17)
plot(ff1,abs(data_w2(:,1))./(ff2.^2), ff4,abs(data_w4(:,1))./(ff4.^2))
title('(1-42-2)Ventilation Fan Spin-down: BERTHOLF vs STRATTON
(Normalized) - X Direction');
legend('BERTHOLF Bottom Fan', 'STRATTON Bottom Fan');
ylabel('envelope amplitude');
xlabel('spindown frequency or speed (Hz or rps)');

figure(18)
plot(ff1,abs(data_w2(:,2))./(ff2.^2), ff4,abs(data_w4(:,2))./(ff4.^2))
title('(1-42-2)Ventilation Fan Spin-down: BERTHOLF vs STRATTON
(Normalized) - Y Direction');
legend('BERTHOLF Bottom Fan', 'STRATTON Bottom Fan');
ylabel('envelope amplitude');
xlabel('spindown frequency or speed (Hz or rps)');

figure(19)
plot(ff1,abs(data_w2(:,3))./(ff2.^2), ff4,abs(data_w4(:,3))./(ff4.^2))
title('(1-42-2)Ventilation Fan Spin-down: BERTHOLF vs STRATTON
(Normalized) - Z Direction');
legend('BERTHOLF Bottom Fan', 'STRATTON Bottom Fan');
ylabel('envelope amplitude');
xlabel('spindown frequency or speed (Hz or rps)');

```

9.2.7 USS MICHAEL MURPHY MATLAB Code

```

clear
clc

```



```

close all

%% DDG 112 Fire Pumps 2, 3 and 5

% Unfortunately, the CAPTCHA's were only placed on FP 2, 3, and 5 even
% though the Gulf Coast showed problems on FP 4...
% GCDC2322,FP1 Terminal Box
% GCDC2054,FP1 Upper Foundation
% GCDC2065,FP1 Lower Foundation
% CAPTCHA0308,FP2 Terminal Box (C)
% GCDC2438,FP2 Terminal Box
% CAPTCHA0D0B,FP3 Terminal Box (C)
% GCDC2069,FP3 Terminal Box
% GCDC2436,FP4 Terminal Box
% CAPTCHA0411,FP5 Terminal Box (C)
% GCDC2060,FP5 Terminal Box
% GCDC2057,FP5 Pump End
% GCDC2079,FP6 Terminal Box

load('DDGdata.mat')

FP2= FP2(1.7*10^6:1.75*10^6,:);
FP3= FP3(5.5*10^5: 6.5*10^5,:);
FP5= FP5(1.5*10^6:1.63*10^6,:);
fs= 3200;
nom_rpm= 3600;

% friction = friction = [-0.0202,   -0.0030]; % just a quick fit to TB1.
%
% Fire Pump 2 on DDG 112
[data_w1, pre_w1, post_w1, ff1, friction1, stop_time1, stop_index1] =
spindown_fitter(FP2, fs, nom_rpm);
% the outputs are form the pre (magenta), post (green), and "data"
(black)
% whiskers.

% Fire Pump 3 on DDG 112
[data_w2, pre_w2, post_w2, ff2, friction2, stop_time2, stop_index2] =
spindown_fitter(FP3, fs, nom_rpm);

% Fire Pump 4 on DDG 112
[data_w3, pre_w3, post_w3, ff3, friction3, stop_time3, stop_index3] =
spindown_fitter(FP5, fs, nom_rpm);

% basic plot: does X,Y,Z
% If you only want one of those guys, then data_W is :, 1= x, :,2= Y, :,
3=
% Z

% % Fire Pumps 2, 3, and 4 Spin-down
figure (2)
plot(ff1,abs(data_w1(:,1)), ff2,abs(data_w2(:,1)),
ff3,abs(data_w3(:,1)))
title('Fire Pumps 2, 3, and 4 Spin-down on DDG 112- X Direction')
legend('FP2', 'FP3', 'FP5');

```

```

ylabel('Envelope Amplitude');
xlabel('Spindown frequency or speed (Hz or RPS)');

figure (3)
plot(ff1,abs(data_w1(:,2)), ff2,abs(data_w2(:,2)),
ff3,abs(data_w3(:,2)))
title('Fire Pumps 2, 3, and 4 Spin-down on DDG 112- Y Direction')
legend('FP2', 'FP3', 'FP5');
ylabel('Envelope Amplitude');
xlabel('Spindown frequency or speed (Hz or RPS)');

figure (4)
plot(ff1,abs(data_w1(:,3)), ff2,abs(data_w2(:,3)),
ff3,abs(data_w3(:,3)))
title('Fire Pumps 2, 3, and 4 Spin-down on DDG 112- Z Direction')
legend('FP2', 'FP3', 'FP5');
ylabel('Envelope Amplitude');
xlabel('Spindown frequency or speed (Hz or RPS)');

% Fire Pump 2 vs Fire Pump 3
figure (5)
plot(ff1,abs(data_w1(:,1)), ff2,abs(data_w2(:,1)))
title('Fire Pump 2 vs Fire Pump 3 on DDG 112- X Direction')
legend('FP2', 'FP3');
ylabel('Envelope Amplitude');
xlabel('Spindown frequency or speed (Hz or RPS)');

figure (6)
plot(ff1,abs(data_w1(:,2)), ff2,abs(data_w2(:,2)))
title('Fire Pump 2 vs Fire Pump 3 on DDG 112- Y Direction')
legend('FP2', 'FP3');
ylabel('Envelope Amplitude');
xlabel('Spindown frequency or speed (Hz or RPS)');

figure (7)
plot(ff1,abs(data_w1(:,3)), ff2,abs(data_w2(:,3)))
title('Fire Pump 2 vs Fire Pump 3 on DDG 112- Z Direction')
legend('FP2', 'FP3');
ylabel('Envelope Amplitude');
xlabel('Spindown frequency or speed (Hz or RPS)');

% Fire Pump 3 vs Fire Pump 5
figure (8)
plot(ff2,abs(data_w2(:,1)), ff3,abs(data_w3(:,1)))
title('Fire Pump 3 vs Fire Pump 5 on DDG 112- X Direction')
legend('FP3', 'FP5');
ylabel('Envelope Amplitude');
xlabel('Spindown frequency or speed (Hz or RPS)');

figure (9)
plot(ff2,abs(data_w2(:,2)), ff3,abs(data_w3(:,2)))
title('Fire Pump 3 vs Fire Pump 5 on DDG 112- Y Direction')
legend('FP3', 'FP5');
ylabel('Envelope Amplitude');

```

```

xlabel('Spindown frequency or speed (Hz or RPS)');

figure (10)
plot(ff2,abs(data_w2(:,3)), ff3,abs(data_w3(:,3)))
title('Fire Pump 3 vs Fire Pump 5 on DDG 112- Z Direction')
legend('FP3', 'FP5');
ylabel('Envelope Amplitude');
xlabel('Spindown frequency or speed (Hz or RPS)');

% Fire Pump 2 vs Fire Pump 5
figure (11)
plot(ff1,abs(data_w1(:,1)), ff3,abs(data_w3(:,1)))
title('Fire Pump 2 vs Fire Pump 5 on DDG 112- X Direction')
legend('FP2', 'FP5');
ylabel('Envelope Amplitude');
xlabel('Spindown frequency or speed (Hz or RPS)');

figure (12)
plot(ff1,abs(data_w1(:,2)), ff3,abs(data_w3(:,2)))
title('Fire Pump 2 vs Fire Pump 5 on DDG 112- Y Direction')
legend('FP2', 'FP5');
ylabel('Envelope Amplitude');
xlabel('Spindown frequency or speed (Hz or RPS)');

figure (13)
plot(ff1,abs(data_w1(:,3)), ff3,abs(data_w3(:,3)))
title('Fire Pump 2 vs Fire Pump 5 on DDG 112- Z Direction')
legend('FP2', 'FP5');
ylabel('Envelope Amplitude');
xlabel('Spindown frequency or speed (Hz or RPS)');

%% Normalized Graphs for DDG 112
% "excitation normalized plot:
% Comparison Between Fire Pumps
figure(14)
plot(ff1,abs(data_w1(:,1))./(ff1.^2), ff2,abs(data_w2(:,1))./(ff2.^2),
ff3,abs(data_w3(:,1))./(ff3.^2))
title('Comparison Between Fire Pumps (Normalized Spindown Whiskers) on
DDG 112- X Direction');
legend('Fire Pump 2', 'Fire Pump 3', 'Fire Pump 5');
ylabel('Envelope Amplitude');
xlabel('Spindown frequency or speed (Hz or RPS)');

figure(15)
plot(ff1,abs(data_w1(:,2))./(ff1.^2), ff2,abs(data_w2(:,2))./(ff2.^2),
ff3,abs(data_w3(:,2))./(ff3.^2))
title('Comparison Between Fire Pumps (Normalized Spindown Whiskers) on
DDG 112- Y Direction');
legend('Fire Pump 2', 'Fire Pump 3', 'Fire Pump 5');
ylabel('Envelope Amplitude');
xlabel('Spindown frequency or speed (Hz or RPS)');

```

```

figure(16)
plot(ff1,abs(data_w1(:,3))./(ff1.^2), ff2,abs(data_w2(:,3))./(ff2.^2),
ff3,abs(data_w3(:,3))./(ff3.^2))
title('Comparison Between Fire Pumps (Normalized Spindown Whiskers) on
DDG 112- Z Direction');
legend('Fire Pump 2', 'Fire Pump 3', 'Fire Pump 5');
ylabel('Envelope Amplitude');
xlabel('Spindown frequency or speed (Hz or RPS)');

% 2 v 3
figure(17)
plot(ff1,abs(data_w1(:,1))./(ff1.^2), ff2,abs(data_w2(:,1))./(ff2.^2))
title('Fire Pump 2 vs Fire Pump 3 (Normalized Spindown Whiskers) on DDG
112- X Direction');
legend('Fire Pump 2', 'Fire Pump 3');
ylabel('Envelope Amplitude');
xlabel('Spindown frequency or speed (Hz or RPS)');

figure(18)
plot(ff1,abs(data_w1(:,2))./(ff1.^2), ff2,abs(data_w2(:,2))./(ff2.^2))
title('Fire Pump 2 vs Fire Pump 3 (Normalized Spindown Whiskers) on DDG
112- Y Direction');
legend('Fire Pump 2', 'Fire Pump 3');
ylabel('Envelope Amplitude');
xlabel('Spindown frequency or speed (Hz or RPS)');

figure(19)
plot(ff1,abs(data_w1(:,3))./(ff1.^2), ff2,abs(data_w2(:,3))./(ff2.^2))
title('Fire Pump 2 vs Fire Pump 3 (Normalized Spindown Whiskers) on DDG
112- Z Direction');
legend('Fire Pump 2', 'Fire Pump 3');
ylabel('Envelope Amplitude');
xlabel('Spindown frequency or speed (Hz or RPS)');

% 3 v 5
figure(20)
plot(ff2,abs(data_w2(:,1))./(ff2.^2), ff3,abs(data_w3(:,1))./(ff3.^2))
title('Fire Pump 3 vs Fire Pump 5 (Normalized Spindown Whiskers) on DDG
112- X Direction');
legend('Fire Pump 3', 'Fire Pump 5');
ylabel('Envelope Amplitude');
xlabel('Spindown frequency or speed (Hz or RPS)');

figure(21)
plot(ff2,abs(data_w2(:,2))./(ff2.^2), ff3,abs(data_w3(:,2))./(ff3.^2))
title('Fire Pump 3 vs Fire Pump 5 (Normalized Spindown Whiskers) on DDG
112- Y Direction');
legend('Fire Pump 3', 'Fire Pump 5');
ylabel('Envelope Amplitude');
xlabel('Spindown frequency or speed (Hz or RPS)');

figure(22)
plot(ff2,abs(data_w2(:,3))./(ff2.^2), ff3,abs(data_w3(:,3))./(ff3.^2))
title('Fire Pump 3 vs Fire Pump 5 (Normalized Spindown Whiskers) on DDG
112- Z Direction');

```

```

legend('Fire Pump 3', 'Fire Pump 5');
ylabel('Envelope Amplitude');
xlabel('Spindown frequency or speed (Hz or RPS)');

% 2 v 5
figure(23)
plot(ff1,abs(data_w1(:,1))./(ff1.^2), ff3,abs(data_w3(:,1))./(ff3.^2))
title('Fire Pump 2 vs Fire Pump 5 (Normalized Spindown Whiskers) on DDG
112- X Direction');
legend('Fire Pump 2', 'Fire Pump 5');
ylabel('Envelope Amplitude');
xlabel('Spindown frequency or speed (Hz or RPS)');

figure(24)
plot(ff1,abs(data_w1(:,2))./(ff1.^2), ff3,abs(data_w3(:,2))./(ff3.^2))
title('Fire Pump 2 vs Fire Pump 5 (Normalized Spindown Whiskers) on DDG
112- Y Direction');
legend('Fire Pump 2', 'Fire Pump 5');
ylabel('Envelope Amplitude');
xlabel('Spindown frequency or speed (Hz or RPS)');

figure(25)
plot(ff1,abs(data_w1(:,3))./(ff1.^2), ff3,abs(data_w3(:,3))./(ff3.^2))
title('Fire Pump 2 vs Fire Pump 5 (Normalized Spindown Whiskers) on DDG
112- Z Direction');
legend('Fire Pump 2', 'Fire Pump 5');
ylabel('Envelope Amplitude');
xlabel('Spindown frequency or speed (Hz or RPS)');

```

9.2.8 LCS MATLAB Code

```

clear
clc

%% LCS Fire Pumps #1 and #3

load('temps.mat')

figure(1)
[P1,W]=pwelch(temp1-mean(temp1),3200,1600,3200,3200);
[P2,W]=pwelch(temp2-mean(temp2),3200,1600,3200,3200);
semilogy(W,[P1 P2])
xlabel('Frequency(Hz)')
ylabel('Amplitude')
title('LCS 2- Fire Pump #1 vs Fire Pump #3')
legend('Fire Pump #1', 'Fire Pump #3')

```

9.3 Gulf Coast Instructions

GULF COAST DATA CONCEPTS, LLC

Thank you for your purchase! These simple instructions describe how to quickly configure and operate your new GCDC accelerometer.

Quick Start Guide

- 1a Plug the X6-2 or X250-2 device into a computer USB port to charge the internal rechargeable lithium-polymer battery. One hour will charge a depleted battery to 80%. The computer will mount the device as a local drive.
- 1b Open the X6-1A enclosure and install an 'AA' sized alkaline, lithium, or NiMH battery. Plug the device into a computer USB port and the computer will mount the device as a local drive.
- 2 Start XLR8R by clicking *xlr8r.jar* in the *xlr8r* directory located on the device (requires Java 6). Select the *Utilities>Configuration File Editor* tab and make appropriate changes to the configuration settings (see reverse side of this guide for details).*
- 3 Select the *Utilities>Set Device Time* tab. Click "Write File" to automatically create a file on the device containing the current host time.**
- 4 Remove the device from the host computer. Activate the device by pressing the start button with a pen, pencil, or stylus. Upon start up, the device will initialize the clock with the time file.** You may turn off the unit by pressing and holding the button for 2 seconds.
- 5 Attach the device to the target object and turn the device on. See *Tips & Tricks* for mounting suggestions.
- 6 When data collection is complete, return the device to a computer USB port. The device will mount as a new drive containing the data files located in the *GCDC* directory.
- 7 Start XLR8R. Select a data file or directory containing data files. XLR8R will display the time series data in the *Plotted Data* tab. XLR8R allows copy-paste operations to import data into other applications.

Notes:

- * GCDC products use text files to configure system settings and store data. Only a text editor and spreadsheet are needed to fully utilize a device. XLR8R is a Java based application provided on each device to allow easy configuration and quick viewing of data.
- ** When the X6-1A device is powered off, the clock time is maintained using the on-board backup battery. This backup battery lasts for several hours. The X6-2 and X250-2 maintain the clock time continuously using the main lithium-polymer battery even when the device is powered off.

<http://www.gcdconcepts.com>

Tips & Tricks:

- Most types of motions, such as running, walking, and roller coasters, can be captured with 20 hertz sample rate.
- Slower sample rates and the use of the deadband feature will conserve battery life.
- Attach the accelerometer device using double stick tape, zip-ties, hook-and-loop fabric, a small amount of cyanoacrylate glue (super glue), or use a long #6-32 screw for a more permanent attachment.
- Lithium batteries provide about 30% more capacity than alkaline, which helps extend the operating life of the X6-1A.

9.4 Acronyms

DDG- Missile Guided Destroyer of the DDG 51 ARLEIGH BURKE Class; USS MICHAEL MURPHY (DDG 112) was visited.

LCS- Littoral Combat Ship; USS INDEPENDENC (LCS 2) was visited.

LPD- Landing Platform Dock; USS SAN DIEGO (LPD 22) was visited.

RADM- Rear Admiral Upper Half (2 stars)

RDML- Rear Admiral Lower Half (1 star)

WMSL- Legend class maritime security cutter for the US Coast Guard

WMEC- USCG medium endurance cutter

10.0 Bibliography

- [1] E. F. Noonan, G. . Antonide, and W. A. Wood, "Practical Guide for Shipboard Vibration Control and Attenuation," Ship Structural Committee, Washington, DC, SR-1293, Mar. 1984.
- [2] Y. Shin, J. Robinson, and G. Rossano, "Submarine-Installed Machinery Monitoring and Diagnostics: A State-Of-The-Art Review," Naval Postgraduate School, Monterey, California, DARPA, Nov. 1991.
- [3] V. Insinna, "Navy Surface Fleet Faces Rough Waters Trying to Maintain Ships," *National Defense*, vol. 97, no. 712, Mar-2013.
- [4] R. Burgess, "Stress Test," *SEAPOWER*, vol. 56, no. 3, Mar-2013.
- [5] W. D. Strunk, "Considerations for the Establishment of a Machinery Monitoring and Analysis Program for Surface Ships of the U.S. Navy," presented at the Proceedings of the 6th International Modal Analysis Conference, 1988, vol. II, pp. 914-920.
- [6] Department of the Navy, "Joint Fleet Maintenance Manual-COMUSFLTFORCOMINST 4790.3 REVISION C." SUBMEPP Portsmouth Naval Shipyard, 2012.
- [7] D. Morales, "Condition Based Maintenance." DoD, 25-Oct-2002.
- [8] R. Lyon, *Machinery Noise and Diagnostics*. Stoneham, MA: Butterworth Publishers, 1987.
- [9] C. Babb, "Acoustic Mine- Gosport," *Geograph: Photograph every grid square!*, 11-Jan-2009. [Online]. Available: <http://www.geograph.org.uk/photo/1115817>.
- [10] R. Steinhour, "Haiti. USS BATAAN Sailors Rebuilt, Bring Relief to Grande Goave.," *BYM Marine and Maritime News*, 29-Jan-2010.
- [11] C. Hooper, "USS Bataan: Is High OPTEMPO Taking a Toll?," *Next Navy: Future Maritime Security*, 10-Mar-2010.
- [12] B. Oceau and P. Hardin, "Analysis of the Impact of OPTEMPO on Navy O&S Cost," Arlington, VA.
- [13] G. Ziezulewicz, "2 Navy Ships Getting New Lease on Life Courtesy of Budget Concerns," *Stars and Stripes*, 23-Sep-2011. [Online]. Available: <http://www.stripes.com/news/2-navy-ships-getting-new-lease-on-life-courtesy-of-budget-concerns-1.155948>. [Accessed: 14-Mar-2013].
- [14] "DoD Budget: Fiscal 2013-17 Highlights, Numbers & Unfolding Events," *Defense Industry Daily*. [Online]. Available: <http://www.defenseindustrydaily.com/departement-defense-2013-budget-07304/>. [Accessed: 12-Feb-2013].
- [15] S. Nikiforov, "Acoustic Design of Naval Structures," NSWC Carderock, NSWCCD-70-TR-2005/149, Dec. 2005.
- [16] E. F. Noonan, "Shipboard Vibration Research In the USA," Defense Documentation Center for Scientific and Technical Information, Cameron Station, Alexandria, VA, 435058, Jul. 1964.
- [17] G. White, *Machine Vibration*, 2.2 ed. Bainbridge Island, WA: DLI Engineering Corp., 1997.

- [18] J. Donnal, U. Orji, C. Schantz, J. Moon, S. Leeb, J. Paris, A. Goshorn, K. Thomas, J. Dubinsky, and R. Cox, "VAMPIRE: Accessing the Life-Blood of Information for Maintenance and Damage Assessment," MIT, 2011.
- [19] M. Tranquilli and M. Watts, "Vibration Analysis Report on USCGC BERTHOLF (WMSL-750)," EG&G Technical Services, Inc., Sep. 2009.
- [20] J. Utterback, *Mastering the Dynamics of Innovation*. Harvard Business School Press, 1994.
- [21] M. DiUlio, "Enterprise Remote Monitoring CBM+ AG," Washington, DC, 02-Sep-2009.
- [22] M. G. Walker, R. Kapadia, B. Sammulu, and M. Venkatesh, "A Model-based Reasoning Framework For Condition Based Maintenance and Distance Support," *Proceedings*, p. 18, 2007.
- [23] MELS, "USS GETTYSBURG RDS IPAR Summary Report: System Status Summary." DoD, 08-Sep-2009.
- [24] S. Sullivan, "CBM in the Navy Surface Fleet," 02-Feb-2013.
- [25] COMNAVSURFPAC, "USS SAN DIEGO (LPD 22) 'Semper Vigilans'," *America's Navy*, 20-May-2012. [Online]. Available: <http://www.san-diego.navy.mil/>. [Accessed: 02-Jan-2013].
- [26] webster@scisland.org, "Navy Training and the SCI Environment," *San Clemente Island*, 2010. [Online]. Available: <http://www.scisland.org/aboutsci/aboutsci.php>. [Accessed: 11-Jan-2013].
- [27] "USS MICHAEL MURPHY," *Destroyer History Home Page*, 2013. [Online]. Available: http://www.destroyerhistory.org/arleighburkeclass/ddg112michaelmurphy_01.html. [Accessed: 03-Jan-2013].
- [28] K. O'Brien, "SECNAV Names New Guided-Missile Destroyer USS MICHAEL MURPHY," *America's Navy*, 07-May-2008. [Online]. Available: http://www.navy.mil/submit/display.asp?story_id=36931. [Accessed: 03-Jan-2013].
- [29] C. Terrell, "Coast Guard Cutter SENECA," *United States Coast Guard: Visual Information Gallery*, 16-May-2008. [Online]. Available: http://cgvi.uscg.mil/media/main.php?g2_itemId=285484&g2_imageViewsIndex=1. [Accessed: 15-Mar-2013].
- [30] GC Data Concepts, "USB Accelerometer Model X6-1A." GC Data Concepts, Nov-2010.